PHOSPHATE REMOVAL AND RECOVERY USING IRON NANOPARTICLES AND IRON CROSS-LINKED BIOPOLYMER

A Dissertation
Submitted to the Graduate Faculty
of the
North Dakota State University
of Agriculture and Applied Science

By

Talal Bakheet Almeelbi

In Partial Fulfillment
for the Degree of
DOCTOR OF PHILOSOPHY

Major Program:
Environmental and Conservation Science

November 2012

Fargo, North Dakota

North Dakota State University
Graduate School

Title

PHOSPHATE REMOVAL AND RECOVERY USING IRON NANOPARTICLES AND IRON CROSS-LINKED BIOPOLYMER

By

TALAL BAKHEET ALMEELBI

The Supervisory Committee certifies that this ***disquisition*** complies with North Dakota State University's regulations and meets the accepted standards for the degree of

DOCTOR OF PHILOSOPHY

SUPERVISORY COMMITTEE:

Dr. Achintya Bazbaruah
Chair

Dr. G. Padmanabhan

Dr. Senay Simsek

Dr. Xinnan Wang

Approved:

11/07/2012
Date

Craig Stockwell
Department Chair

ABSTRACT

Nanoscale zero-valent iron (NZVI) particles and iron cross-linked alginate (FCA) beads were successfully used for the first time for phosphate removal and recovery. NZVI was successfully used for phosphate removal and recovery. Batch studies indicated a removal of ~96 to 100% phosphate in 30 min (1, 5, and 10 mg PO_4^{3-}-P/L with 400 mg NZVI/L). Phosphate removal efficiency by NZVI was 13.9 times higher compared to Microscale ZVI (MZVI) particles. The successful rapid removal of phosphate by NZVI from aqueous solution is expected to have great ramification for cleaning up nutrient rich waters. The presence of sulfate, nitrate, and humic substances and the change in ionic strength in the water marginally affected phosphate removal by NZVI. A maximum phosphate recovery of ~78% was achieved in 30 min at pH 12.

Novel iron cross-linked alginate (FCA) beads were synthesized, characterized and used for phosphate removal. The beads removed up to 37-100% phosphate from aqueous solution in 24 h. Freundlich isotherm was found to most closely fit with experimental data and the maximum adsorption capacity was found to be 14.77 mg/g of dry beads. The presence of chloride, bicarbonate, sulfate, nitrate, and natural organic matters in aqueous solution did not interfere in phosphate removal by FCA beads. The phosphate removal efficacy FCA beads was not affected due to change in pH (4-9).

Nanosacle zero-valent iron (NZVI) and iron cross-linked alginate beads were also tested for phosphate removal using actual wastewater treatment plant effluent and animal feedlot runoff. The FCA beads could remove ~63% and ~77% phosphate from wastewater and feedlot runoff in 15 min, respectively.

Bioavailability of phosphate was examined using algae and higher plants. Phosphate and iron bioavailability of the NZVI sorbed phosphate was examined by supplying spent particles (NZVI with sorbed phosphate) to Tyee Spinach (*Spinacia oleracea*) and algae (*Selenastrum capricornutum*). Results revealed that the phosphate was bioavailable for both the algae and spinach. Also, presence of the nanoparticles enhanced the algae growth and plant growth and increases in biomass and plant length were observed. Iron (from spent NZVI) was found to be bioavailable for spinach.

ACKNOWLEDGEMENTS

I sincerely thank Allah, my God, the Most Gracious, the Most Merciful for enlightening my mind, making me understand, giving me confidence to pursue my doctoral studies at North Dakota State University (NDSU), and introducing me to so many good people who helped me on my journey.

I would like to express my sincere thanks, gratitude and deep appreciation for Dr. Achintya Bezbaruah, my advisor, for his excellent guidance, caring, patience, assistance in every step I went through and providing me with an excellent atmosphere for doing research. He is a real mentor, always available, and very inspirational. Throughout my studies, he provided encouragement, sound advice, good teaching, good company, and lots of good ideas.

I would like to thank the members of my dissertation committee, Drs. G. Padmanabhan Senay Simsek, and Xinnan Wang for generously offering their precious time, valuable suggestions, support, guidance and good will throughout my doctoral tenure at NDSU. I would also like to extend my gratitude to Dr. Donna Jacob for her assistance and guidance. I cannot forget to mention my wonderful colleagues and friends; they not only gave me a lot of support but also made my long journey much more pleasant. My thanks go to all members of Nanoenvirology Research Group and Environmental Engineering Laboratory at the Department of Civil Engineering. Special thanks to Harjyoti Kalita, Michael Quamme, and Adel Said. I would also like to thank my special friends Navaratnam Leelaruban, Mamdouh Alenezi, and Shadi Banitaan.

My tenure at NDSU was supported through a fellowship by the Saudi Arabian Cultural Mission to the United States. Major part of my research is supported by a grant from National Science Foundation (Grant: CMMI- 1125674). I would also like to acknowledge my gratitude to the Civil Engineering Department and Environmental Conservation Sciences Program at NDSU.

My special and deepest appreciations go out to my family members to whom I owe so much. I thank my parents for their love, prayers, and unconditional support not only throughout the three years of my doctoral program but throughout my entire life.

TABLE OF CONTENTS

LIST OF TABLES

LIST OF FIGURES

LIST OF APPENDIX TABLES

LIST OF APPENDIX FIGURES

CHAPTER 1. INTRODUCTION

1.1. Background

Phosphorus (P) exists in water in both particulate and dissolved forms. The usual forms of P in aqueous solutions are orthophosphates, polyphosphates and organic phosphates (Mezenner and Bensmaili 2009). Phosphorus is a necessary macronutrient for the growth of organisms and aquatic plants and is an excellent indicator of surface water quality. Excess P in waterbodies leads to deterioration of its overall health. The major point sources that contribute to phosphate (or phosphorus) built up in aquatic environment include municipal and industrial wastewaters while the run-offs from agriculture, including animal agriculture, are the major non-point sources. Phosphates have become pollutants due to their over application as both synthetic and animal-based fertilizers. They are also used as a major constituent in many detergents and pigments (Smith et al., 1999). Excessive P present in natural waters is known to cause eutrophication (Penn and Warren 2009). Eutrophication is one of the most serious environmental problems affecting the quality and sustainability of enclosed water bodies worldwide. In addition to the very apparent excessive plant growth problem, eutrophication depletes dissolved oxygen in natural waters which eventually leads to fish death and adversely affects other aquatic life forms. The amount of P compounds originating from the sources and/or arriving at the receiving waters should be controlled to prevent eutrophication. Accelerated eutrophication not only affects the aquatic life but impairs the economic advancement of communities that depend on aquatic food and other resources (Cleary et al., 2009). Dissolved phosphate of ~ 0.02 mg/L is considered to have potential to lead to profuse algal growth in waters which will in turn deplete the oxygen further leading to poor water quality (USEPA 1995).

Phosphate is recognized as one of the resources that will be in short supply in the near future. An assessment of future consumption of phosphorus fertilizers indicates that natural phosphate (PO_4^{3-}) deposits will last for approximately 60-240 years (Cornel and Schaum 2009), the phosphorus production rate is predicted to decline starting sometime in the year 2035 (Figure 1.1) while the demand for P-based fertilizers is on the rise (Cordell et al., 2011). Phosphorus is one of the most essential nutrients for plants and its projected decline in production is a major concern. P-based fertilizers are extensively used in food crops all over the world and they are intricately related to global food security. The possible short supply of P-fertilizers is a threat to global food security.

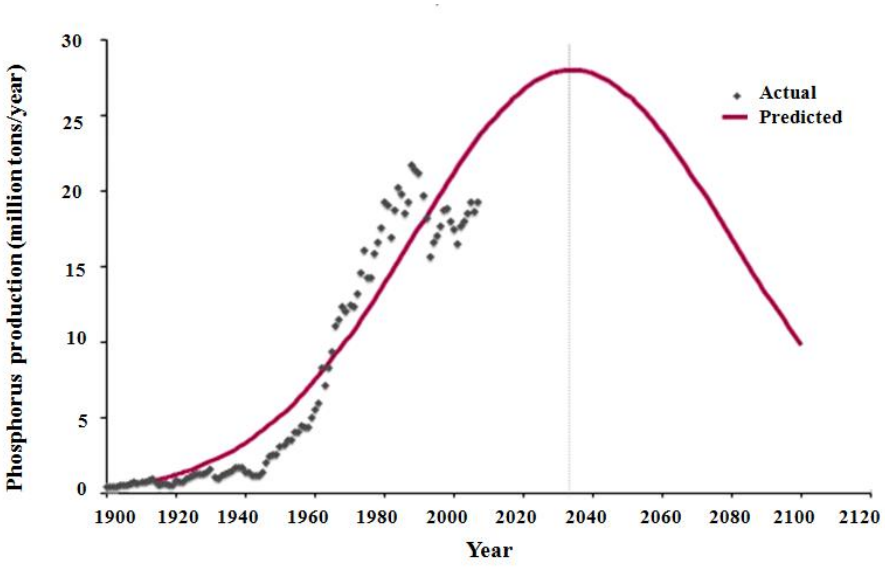

Figure 1.1: Global phosphorus production rate (modified after Cordell et al., 2009)

Being a nonrenewable resource, it is, therefore, essential to recover P from nonconventional sources. Municipal wastewater contains adequate amount (5 -15 mg/L) of P which can possibly be recovered and used in agriculture (Blackall et al., 2002). A total of 118 billion L/day of municipal wastewater is generated in the United States alone and total recovery of P from these wastewaters will amount to 1415 tons of P per year (USDD 2004). Further, there

are estimated 24773 eutrophic lakes (50% US lakes, 20% are hypereutrophic lakes) in the United States (USEPA, 2009). To top them all a huge amount of P-based fertilizers used in the United is wasted as run-off from agricultural fields. In addition, there is enough phosphorus generated in animal feedlot that can possibly be recovered with the appropriate technology. Recovery, however, involves a major challenge as most of these phosphorous exist in the water environment in diluted forms. While there are technologies to remove P (present as phosphate) from waters with varied degree of success and recovery of phosphate has not been a priority area. Enhanced removal and subsequent recovery of phosphate from waters are of considerable significance prior to their discharge into natural waters. By adopting the approach of 'remove and recover' two battles can be won together. Firstly, natural waters will be protected from phosphate pollution, and secondly, an important resource will be recovered.

Various technologies have been used to remove phosphate from waters are discussed in Section 1.2.2. Extensive work has been done on using adsorption for phosphate removal. Adsorption is attractive because of its operational simplicity and low cost, especially when phosphate is low in concentration (Saha et al., 2009). The effectiveness of adsorption-based methods mainly depends on the type of adsorbent. Recently, several iron-based materials have been developed and used for phosphate removal (Almeelbi and Bezbaruah, 2012; Biswas et al., 2007; Huang et al., 2009; Ogata et al., 2011; Zhang et al., 2011). Among them nanoscale zero-valent iron (NZVI) particles stand out as they are very effective in phosphate removal (Almeelbi and Bezbaruah, 2012). NZVI particles are known to have much higher reactive surface area (25-52 m^2/g) when compared to micro scale iron particles (1-2 m^2/g), iron filings or other iron based adsorbents, and have been previously used to remediate a wide range of environmental contaminants (Bezbaruah et. al., 2011; Zhang, 2003).

1.2. Literature Review

1.2.1. Importance of phosphate

Phosphorus (P) is a nonrenewable yet essential nutrient for plants and there is no substitute for it. Up in the food chain P is required to maintain important human body functions such as transporting energy to the brain and building cell walls (Cordell et al., 2012). The human consumption of P is estimated to be 1.2 g/person/day (Cordell et al., 2009) which are approximately 8300 tons of phosphorus for the global population annually. The phosphorus for human consumption typically comes from plants and animals.

With an expanding world population the demand of P fertilizers for agricultural uses is on the rise. The P fertilizers come from phosphate rocks present on the Earth's crust. Eighty percent (80%) of P extracted from the global reserves is used for agriculture (Smil, 2000). Fertilizer use in food crops is intricately related to global food security. However, the world reserves of phosphate rocks are becoming increasingly scarce and it is estimated that that natural phosphate (PO_4^{3-}) deposits will last for approximately 60-240 years (Cornel and Schaum, 2009). P production rate is predicted to decline sometime in year 2035 while the demand for P-based fertilizers is on the rise (Cordell et al., 2011). Phosphorous for fertilizer production comes predominantly from select mines from Morocco, Western Saharan region, and China (Fig. 1.2, Cordell et al., 2009; USGS, 2012). The price of phosphate rock has risen many folds over time and sudden jumps in price have seen whenever there is a food crisis (Cordell, 2008). Short supply of P-fertilizer and the vulnerability in the global phosphate rock market are the major concern in food security area (Elser, 2012; Neset and Cordel, 2012). It is, therefore, essential to recover P from 'wastes' for possible reuse in agriculture.

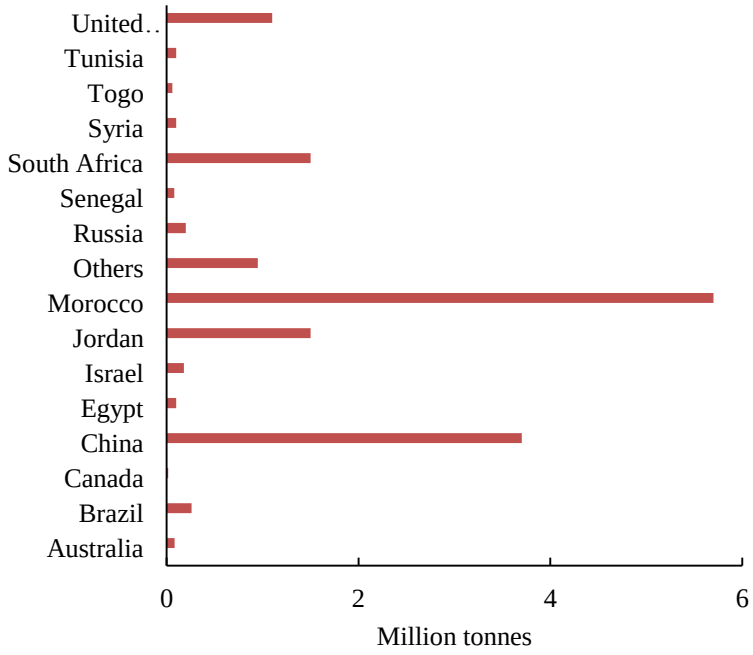

Figure 1.2: Global phosphate reserves (data source: USGS, 2012)

1.2.2. Phosphorus removal processes

Phosphorus removal from wastewater can be achieved via biological uptake by microorganisms and via chemical precipitation with metal cations. Both processes may be applied in wastewater treatment plants to achieve the desired effluent concentration. A biological process is used to remove the bulk of the phosphorus, and chemical process follows to achieve the target effluent concentration.

1.2.2.1. Biological phosphorus removal

Biological process removes phosphorus using phosphate-accumulating organisms (PAOs). PAOs go through anaerobic conditions first and followed by aerobic conditions. Under anaerobic conditions, phosphate (PO_4^{3-}) accumulated in their body is released by microorganisms as they break the bonds in the polyphosphate (the form in which phosphate is stored in biomass) while the microorganisms consume biodegradable organic compounds, mainly volatile fatty

acids (VFAs). The internal polyphosphate molecules are formed again under aerobic conditions where microbes take up the phosphate in a process called luxury uptake. In this process more phosphate is being taken up by the microbes than they release under the anaerobic conditions. Total phosphate concentration in water is being reduced as a result of the accumulation in the microbial biomass (Kang et al., 2008; Mulkerrins et al., 2004; Tchobanoglous et al., 2003).

VFAs are readily biodegradable and expressed as readily biodegradable chemical oxygen demand (rbCOD, a part of total COD). A sufficiently high ratio of VFAs or rbCOD to ortho-phosphorus is needed in the aenaerobic phase to maintain a healthy bacterial population. The minimum ratios of COD to total phosphorous (TP) and biochemical oxygen demand (BOD) to TP, VFA to TP are 45, 20 and 4, respectively, to achieve 1 mg/L of total phosphorus in the effluent (Kang et al., 2008). Sufficient generation of VFAs is affected by temperature. Phosphorus uptake is reduced under temperatures higher than 30 °C and PAOs show serious inhabitation at 40 °C (Panswad et al. 2003; Rabinowitz et al. 2004).

1.2.2.2. Chemical phosphorus removal

Multivalent metal cations are used in chemical precipitation process. As the first step in this process, phosphate species (e.g., $H_2PO_4^{1-}$, HPO_4^{2-}) are converted to PO_4^{3-} (Eq. 1.1).The most common multivalent ions used in the chemical precipitate process are calcium (Ca^{2+}), ferric ion (Fe^{3+}), and aluminum (Al^{3+}) (Kang et al., 2008).

$$H_nPO_4^{(3-n)-} + nOH^- \rightarrow PO_4^{3-} + n\,H_2O \qquad \text{(Eq. 1.1)}$$

Calcium is commonly added in the form of lime [$Ca(OH)_2$] which increases the pH as it reacts with natural bicarbonate alkalinity and precipitates out as $CaCO_3$.The excess of Ca^{2+} then reacts with the phosphate as the pH of wastewater is increased above 10 (Eq. 1.2). The quantity

of the required lime depends on the alkalinity of the water being treated (Tchobanoglous et al., 2003).

$$10Ca^{2+} + 6PO_4^{3-} + 2OH^- \leftrightarrow Ca_{10}(PO_4)_6(OH)_2 \quad \text{(Eq. 1.2)}$$

The mechanism of phosphate precipitation by ferric ion (Fe^{3+}) and aluminum ions (Al^{3+}) is different than the precipitation using Ca^{2+}. Trivalent ions interact with the orthophosphate to form a metal-phosphate precipitate (Eqs. 1.3 and 1.4). Although the reaction seems simple, other competing reactions might take place and interfere with the precipitation process. The typically Fe^{3+} and Al^{3+} are supplied as ferric chloride ($FeCl_3$) and alum (aluminum sulfate), respectively (Galarneau and Gehr, 1997; Tchobanoglous et al., 2003).

$$Al^{3+} + H_nPO_4^{3-n} \leftrightarrow AlPO_4 + nH^+ \quad \text{(Eq. 1.3)}$$

$$Fe^{3+} + H_nPO_4^{3-n} \leftrightarrow FePO_4 + nH^+ \quad \text{(Eq. 1.4)}$$

In this process a phosphate containing floc is formed which can then be filtered or settled to be removed. As the applied ion concentrations increase the P concentration in the effluent decreases (Kang et al., 2008).

1.2.3. Phosphate removal and recovery technologies

Major research on phosphate removal and recovery has been done with wastewaters. There are a number of existing technologies that have been accepted for the removal of phosphate from wastewater. The most used methods include chemical precipitation, biological methods, ion-exchange, and adsorption (Mezenner and Bensmail, 2009; Morse et al., 1998). Chemical methods for the removal of phosphate are very effective but they need high chemical inputs and generate sludge which needs additional treatment (Table 1.1). Chemical precipitation

of phosphate is achieved by adding of a coagulant to the wastewater. Calcium, aluminum and iron based coagulants are the commonly used. When lime $Ca(OH)_2$ is used, phosphate removal is achieved by direct precipitation of calcium phosphate in form of hydroxyapatite $Ca_5(PO_4)_3OH$ (de-Bashan and Bashan, 2004). Precipitation with Fe or Al is a relatively complex process that is influenced by pH of the wastewater and the presence of other ions as well as organic matters. Different metal-P complexes and metal hydroxyl complexes are formed with Fe and Al (Aguilar et al., 2002) that precipitate out.

The biological methods have been widely used by many because of the advantages they offer (Xiong et al., 2008). Biological treatment for phosphate removal from wastewater is achieved by stoichiometric coupling to microbial growth or enhanced storage of P as polyphosphate (poly-P in the biomass). This is the key mechanism in the enhanced biological phosphate removal (EBPR) process (Levin and Shapiro, 1965). In the EBPR process, a multiple-stage reactor (anaerobic and aerobic phases) is used to circulate activated sludge where influent wastewater is introduced into the anaerobic phase first (Barnard, 1975, Tchobanoglous et al., 2003). EBRP has potential to remove P from wastewater to low levels (<0.1 mg/L) at modest costs and with minimal additional sludge production (Barnard, 2006). Biological methods have a number of advantages over chemical methods. The advantages over chemical treatment include more effective treatment, less chemical usage, less energy consumption and less sludge production (Mulkerrins et al., 2003). However, some biological processes (e.g., EBPR) are reported to have high potential for process upsets, performance deterioration, and even failures (Blackalled et al., 2002).

Crystallization or struvite ($NH_4MgPO_4•6H_2O$) formation is one of the most practiced techniques for P recovery from municipal sludge (Parsons and Doyle, 2004, Parsons et al.,

2010). It occurs spontaneously in wastewater treatment plants as stable white orthorhombic crystals in 1:1:1 Mg:N:P molar ratio (Corre et al 2009). Struvite is a directly usable P source for plants.

In recent years phosphate recovery using adsorbent technologies is gaining momentum. The most commonly used low cost adsorbents are iron based adsorbents, red mud, natural ores and alum slag (Huang et al., 2011). The biggest concern associated with these adsorbents is their low adsorption capacity. Natural ores like calcite is reported to have a sorption capacity of 0.1 mM PO_4^{3-}/g (i.e., 3.1 mg PO_4^{3-}-P/g, Karageorgiou et al., 2007). Goethite (FeOOH, 17.3 mg PO_4^{3-}-P/g, Chitrakar et al., 2006), active red mud (9.8 PO_4^{3-}-P/g, Yue et al., 2010), and activated carbon (3.02 mg PO_4^{3-}-P/g, Hussain et al., 2011) are the most effective sorbents so far used for the removal of phosphate.

Iron-based adsorbents are gaining popularity for the removal of phosphate from wastewater. Iron is a non-toxic metal with the capability of adsorbing phosphate efficiently (Mezenner and Bensmail, 2009; Xiong, et al 2008). It is reported that the adsorbed phosphate can be recovered at certain conditions of temperature and pH (Huang et al., 2011). The iron-based adsorbents so far used include iron fillings, iron oxides, and micro-sized iron particles. Although iron is a preferred adsorbent for the removal of phosphate, the adsorption capacity of the iron based adsorbents is less [11.2 (Yan et al., 2010a) to 19.02 mg PO_4^{3-}-P/g (Cordray 2008)]. Binary-oxide sorbents such as iron-zirconia (adsorption capacity = 33.4 mg PO_4^{3-}-P/g) have been reported to be effective in phosphate removal from aqueous solutions but the possible adverse effects of zirconia have not been completely understood (Ren et al., 2012).

Table 1.1: Summary of phosphate removal and recovery technologies (adopted from Morse et al. 1998)

Removal Technology	Recovery value		Advantages	Disadvantages
	Industrial	Agriculture		
Chemical precipitation	Low: metal bound P makes recycling difficult	Moderate: P availability variable	Established low technology Easy to install and operate P removal can be high	Requires chemicals Sludge production increases P recyclability variable
Biological phosphorus removal	Moderate: biologically-bound P more recyclable	Moderate: biologically-bound P more Available	Establishing technology No need for chemicals N and P removal possible P more recyclable	More complex technology to install and operate Sludge handling may be more difficult
Crystallisation	Very high: easily recycled by industry	Moderate: P availability Variable	Demonstrated technology recyclable	Requires chemicals and operation skills
Advanced chemical precipitation (HYPO)	Low: metal-bound P makes recycling Difficult	Moderate: P availability Variable	Proven (pilot) technology Enhanced P and N removal. Part of a complete recycling concept	Requires chemicals Complex technology P may not be in a convenient form
Ion exchange (RIM-NUT)	Moderate: would require modifications	High: struvite is a good slow- release fertilizer	High P removal Struvite produced has high recycling potential for agriculture	for recycling Requires chemicals Complex technology Waste eluate
Magnetic (Smit-Nymegen)	Moderate: would require modifications	Low: agricultural suitability unknown	High P removal	Unnecessarily complex Requires chemicals
Phosphorus adsorbents	Moderate: Recent developments are very promising.	Limited resources available	High removal and recovery efficiency of ~ 98% Low Cost	By-products generation for adsorbents doped with certain metals
Tertiary filtration	None: no potential	None: no potential	Established technology Easy to retrofit and use	Not a recovery technology (no useful product)
Sludge treatments	Low: difficult to re-cycle	High: P re-use high	Increases sludge value	More complex technology Chemicals required
Recovery from sludge ash	High: P readily leached	Moderate: P re-use possible	Potential for recovering P at high concentrations	Undeveloped technology Only possible if incineration is the usual disposal route

1.2.4. Nanoscale zero-valent iron (NZVI)

The most basic and known form of NZVI is spherical $Fe^{(0)}$, which has dimensions less than 100 nm. Iron nanoparticles used for environmental remediation have particle sizes in the range of 12.5- 80 nm (Bezbaruah et al., 2009; Bezbaruah et al., 2011; Cullen et al., 2011; Li et al., 2006). NZVI particles have much higher reactive surface areas when compared to other larger iron particles, micro particles and iron fillings which make them more sought after for environmental remediation. (Macé et al., 2006; Zhang, 2003). The BET surface areas of NZVI reported in literature range between 20- 30 m^2g^{-1} (Bezbaruah et al., 2011; Zhang, 2003) compared to 1-2 m^2g^{-1} for micro iron particles (Sigma-Aldrich, 2008).

Nanoscale zero-valent Iron (NZVI) particles have been used to remediate a wide range of environmental contaminants including chlorinated compounds (Bezbaruah et al., 2011; Kim et al., 2010; Lien and Zhang 1999; Liu and Lowry 2006; Liu et al., 2005; Lowry and Johnson, 2004; Song and Carraway, 2005; Wang and Zhang, 1997), heavy metals (Alowitz and Scherer 2002; Kanel et al., 2005, Klimkova et al., 2011), pesticides (Bezbaruah et al., 2009; Joo and Zhao 2008) and explosives (Gregory et al., 2004).

NZVI particles are known to be very good adsorbents and have been successfully utilized for the removal of numberous environmental contaminants such as arsenic (Tanboonchuy et al.,2011), methyl orange (Cheng et al., 2011), cadmium (Boparai et. al., 2011) and lead (Liu et. al., 2009). NZVI has been found to be a favorable adsorbent for the aqueous phosphate (Almeelbi and Bezbaruah 2012).

1.2.5. Polymers for entrapment of NZVI

The use of a number of biopolymers like alginate, Poly(methyl methacrylate) (PMMA), chitosan, and carrageenan have been explored for environmental remediation applications

(Bezbaruah et al., 2009; Bezbaruah et al., 2011; Crini 2005; Krajangpan et al., 2008; Krajewska 2005; Ngila 2011; Vieira et al., 2011; Youssef et al., 2010).

Alginate is a biopolymer derived from seaweeds, and it has been used for entrapment for microbial cells (Adinarayana et al., 2005; Hill and Khan, 2008; Lee and Heo, 2002) and NZVI (Bezbaruah et al., 2009, Kim et al., 2010). The entrapped NZVI was found to work very efficiently for contaminants like trichloroethylene (TCE). The entrapment process does not require sophisticated instrumentation and can be performed at ambient temperature and pressure. Ca-alginate is non-toxic, biodegradable, and sparsely soluble in water making it an ideal polymer for use in environmental applications (Bezbaruah et al., 2009a; Chan et al., 2010; Lai et al., 2008). The porous nature of Ca-alginate allows solutes to diffuse and come in contact with the entrapped NZVI (Bezbaruah et al., 2009).

Ionic cross-linking refers to the ion exchange process between the monovalent ion on the water soluble alginate (e.g., sodium or potassium ions) and the multivalent ion (e.g., Ca^{2+}) to give a sol/gel transition (Draget et al., 1998). The characteristic chelate-type ion-binding properties of alginates can be explained by 'egg-box' model in which electronegative cavities are formed by polyguluronic chains in alginate to host divalent cations (Grant et al., 1973; Morris et al., 1978). In this model, guluronate sequences are responsible for creating cavities where the multivalent ions coordinate along the alginate chains (Mehrotra, 1983). The coordination of metal–carboxylate can occur in different ways: (a) an ionic or uncoordinated form, (b) unidentate coordination, (c) bidentate chelating coordination, and (d) bidentate bridging coordination (Fig. 1.3, Papageorgiou et al., 2010).

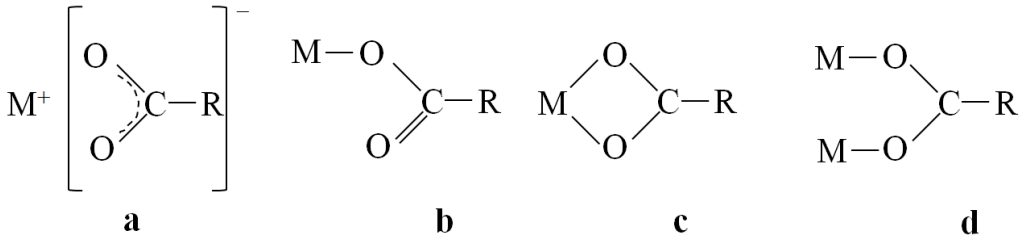

Figure 1.3: Types of metal–carboxylate coordination (After Papageorgiou et al., 2010). (**a**) an ionic or uncoordinated form, (**b**) unidentate coordination, (**c**) bidentate chelating coordination, and (**d**) bidentate bridging coordination.

Sodium alginate is the salt of alginic acid which consists of two uronic acids, b-D-mannuronic acid and a-L-guluronic acid. Ca^{2+} is typically used to replace Na^{+} in alginate to produce Ca-alginate. This stable gels is formed as Ca^{2+} interact ionically with blocks of uronic acid residues to form a three-dimensional network that is usually described by the 'egg-box' model (Papageorgiou et al., 2010). Other di-valent ions such as Fe^{+2} can also be used to cross-link with alginate. Fe^{+2} has been cross-linked with alginate and used in the biomedical research (Machida-Sano et al., 2009).

1.2.6. Plant nanoparticles interaction

Nanoparticles (size <100 nm) fall under the transitional zone between atom or molecules and bulk materials and are known to have different and unique physicochemical properties probably due to the small size (Taylor and Walton, 1993). Nanoparticles can affect components of our ecosystem including plants (Nel et al., Science, 2006)

Nanoparticle-plant interactions have been explored in the past to understand how nanoparticles affect plants. The ubiquitous nature of nanoparticles has resulted in their presence everywhere including contaminated water which finally reaches plants and wetlands. Jacob et.al. (2013) studied the effects of TiO_2 nanoparticles on two important plant species (*Phaseolus vulgaris* and *Triticum aestivum*). The results of this study revealed that titanium was bioavailable

for plants uptake, and significant concentrations of titanium was detected in the roots and shoots. A number of other researchers have reported increased photosynthesis and nitrogen metabolism in spinach (*Spinacea oleracea*) in the presence of TiO_2 nanoparticles (Hong et al., 2005a; Hong et al., 2005b; Zheng et al., 2005; Yang et al., 2006). On the other hand TiO_2 and ZnO nanoparticles have been found to reduce biomass in wheat (Triticum *spp.*) and bring about changes in soil enzyme activities (Du et al., 2011). Du et al., (2011) reported the presence of nanoparticles within primary root tips of wheat when the particles were introduced in bulk growth solution. Silver (Ag) and copper (Cu) nanoparticles in growth solution also caused decrease in plant biomass (Stampoulis et al., 2009).

1.3. Need Statement

Novel and inexpensive technologies are needed to manage phosphate in waters. All forms of phosphorus from waste streams and run-offs need to be removed as they are directly or indirectly related to eutrophication of surface water bodies. However, given that phosphorus is a nonrenewable and essential resource, recovery of phosphorus and subsequent agricultural application are important. There is no proven cost effective technology at present to remove phosphorus from water and recover it for application in agriculture. It is, therefore, felt necessary to develop a technology or technologies to address this need.

1.4. Research Objectives

The main objectives of this study are the development of efficient and cost effective techniques for the removal and recovery of phosphate from waters, and study of bioavailability of the recovered phosphate.

The specific objectives of this study are:

- Phosphate removal using NZVI and biopolymers.
- Phosphate recovery from used NZVI (i.e., NZVI used for phosphate removal).
- Study the bioavailability of phosphate from used NZVI.
- Application of the new technologies for phosphate removal from actual wastewaters.

1.5. Hypotheses

- Iron has high affinity for phosphate and the adsorption onto iron is known to be surface area dependent reaction. Therefore, nanoscale zero-valent iron (NZVI) particles with high reactive surface area (25-54 m^2/g) will be able to remove phosphate very efficiently.
- Calcium (Ca) cross-linked alginate is a porous biopolymer and entrapping NZVI in Ca-alginate matrix would help in retaining the particles within the matrix and the particles will be able to remove phosphate from aqueous solution.
- Iron (Fe^{2+}) can be used to cross-link alginate instead of calcium (Ca^{2+}) and the new iron cross-linked alginate will be able to adsorb phosphate very efficiently because of the presence of iron within it.
- The phosphate adsorbed by different adsorbents will be bioavailable for uptake by plants.

1.6. Expectations from This Study

- NZVI will be used for the first time for the removal and recovery of phosphate from aqueous solution.

- The mechanism associated with the removal of phosphate by NZVI will be elucidated.
- Iron cross-linked alginate beads will be synthesized for the first time to remove phosphate from wastewaters.

1.7. Dissertation Organization

Chapter 1 is an overview of the research problem and includes literature review, need statement and objectives of this research. It also enlists the expectations from this study. The rest of the chapters in the dissertation are presented in journal paper formats, and each chapter has already been published or will be submitted for publication to a peer reviewed journal. A paper on aqueous phosphate removal using NZVI published in the *Journal of Nanoparticle Research* (Almeelbi and Bezbaruah, 2012) is presented as Chapter 2**.** Chapter 3 describes the novel iron cross-linked alginate and its application to remove aqueous phosphate**.** The bioavailability of NZVI-sorbed phosphate has been discussed in Chapter 4. Phosphate availability to hydroponic *Spinacia oleracea* and *Selenastrum capricornutum* have been described in details in that chapter. While all results presented in Chapters 1 through 6 were based on experiments done with synthetic phosphate solution, Chapter 5 presents the data obtained from experiments done with actual wastewaters (municipal wastewater and animal feedlot runoff) and NZVI and iron cross-linked alginate were used for removal of phosphate from the wastewaters**.** Conclusions and future directions are summarized in Chapter 6. The dissertation also contains appendices dedicated to each chapter.

1.8. References

Adinarayana K, Jyothi B, Ellaiah P (2005). Production of akaline protease with immobilized cells of Bacillus subtilis PE-11 in various matrices by entrapment technique. AAPS Pharm. SciTech., 6: E391-E397.

Aguilar MI, Saez J, Llorens AM, Soler JF, Ortuno (2002) Nutrient removal and sludge production in the coagulation–flocculation process. Water Res., 36, 2910–2919

Alowitz, M.J., and M.M. Scherer. 2002. Kinetics of nitrate, nitrite, and Cr(VI) reduction by iron metal. Environmental Science & Technology 36: 299-306.

Bahmanyar MA (2008) Effects of long-term irrigation using industrial wastewater on soil properties and elemental contents of rice, spinach, clover, and grass. Communications in Soil Science and Plant Analysis 39(11-12):1620-1629.

Bahmanyar MA. (2008) Effects of long-term irrigation using industrial wastewater on soil properties and elemental contents of rice, spinach, clover, and grass. Communications in Soil Science and Plant Analysis 39(11-12):1620-1629.

Bezbaruah, A.N., S. Krajangpan, B.J. Chisholm, E. Khan and J.J.E. Bermudez. 2009. Entrapment of iron nanoparticles in calcium alginate beads for groundwater remediation applications. Journal of Hazardous Materials 166: 1339-1343.

Bezbaruah, A.N., S.S. Shanbhogue, S. Simsek and E.E. Khan. 2011. Encapsulation of iron nanoparticles in alginate biopolymer for trichloroethylene remediation. Journal of Nanoparticle 13:(12), 6673-6681.

Blackall LL, Crocetti G, Saunders AM, Bond PL (2002) A review and update of the microbiology of enhanced biological phosphorus removal in wastewater treatment plants. Antonie Van Leeuwenhoek International Journal of General and Molecular Microbiology 81(1-4):681-691.

Boparai HK, Joseph M, O'Carroll DM (2011) Kinetics and thermodynamics of cadmium ion removal by adsorption onto nano zerovalent iron particles. Journal of Hazardous Materials 186(1):458-465.

Chan, E.S., B.B. Lee, P. Ravindra and D. Poncelet. 2009. Prediction models for shape and size of ca-alginate macrobeads produced through extrusion-dripping method. Journal of Colloid and Interface Science 338: 63-72.

Chen ZX, Jin XY, Chen ZL, Megharaj M, Naidu R (2011) Removal of methyl orange from aqueous solution using bentonite-supported nanoscale zero-valent iron. Journal of Colloid and Interface Science 363(2):601-607.

Chen, S.S., Y.C. Huang, and T.Y. Kuo. 2010. The remediation of perchloroethylene contaminated groundwater by nanoscale iron reactive barrier integrated with surfactant and electrokinetics. Groundwater Monitoring and Remediation 30: 90-98.

Cornel P, Schaum C. (2009) Phosphorus recovery from wastewater: needs, technologies and costs. Water Science and Technology 59(6):1069-1076.

Crini, G. 2005. Recent developments in polysaccharide-based materials used as adsorbents in wastewater treatment. Progress in Polymer Science 30: 38-70.

Cullen, L.G., E.L. Tilston, G.R. Mitchell, C.D. Collins, and L.J. Shaw. 2011. Assessing the impact of nano- and micro-scale zerovalent iron particles on soil microbial activities: particle reactivity interferes with assay conditions and interpretation of genuine microbial effects. Chemosphere 82: 1675-1682.

Daniel TC, Sharpley AN, Lemunyon JL (1998) Agricultural phosphorus and eutrophication: A symposium overview. Journal of Environmental Quality 27(2):251-257.

De-Bashan LE, Bashan Y (2004) Recent advances in removing phosphorus from wastewater and its future use as fertilizer (1997–2003).Water Research, 38:(19), 4222-4246.

Deladino, L., P.S. Anbinder, A.S. Navarro and M.N. Martino. 2008. Encapsulation of natural antioxidants extracted from Ilex paraguariensis. Carbohydrate Polymers 71: 126-134.

Doyle JD, Parsons SA. (2002) Struvite formation, control and recovery. Water Research 36(16):3925-3940.

Draget KI, Steinsva GK, Onsoyen E, Smidsrod O (1998) Na- and K-alginate; effect on Ca2+ gelation. Carbohydr Polym, 35 1–6.

Du WC, Sun YY, Ji R, Zhu JG, Wu JC, Guo HY (2011) TiO2 and ZnO nanoparticles negatively affect wheat growth and soil enzyme activities in agricultural soil. Journal of Environmental Monitoring 13(4):822-828.

Fang Y, Al-Assaf S, Phillips GO, Nishinari K, Funami T, Williams PA, Li L (2007) Multiple steps and critical behaviors of the binding of calcium to alginate. The Journal of Physical Chemistry B, 111:(10), 2456-2462.

Gillham, R.W., and S.F. Ohannesin. 1994. Enhanced Degredation of halogenated aliphatics by zeo-valent iron. Ground Water 32: 958-967.

Grant GT, Morris ER, Rees DA, Smith PJ, Thom D (1973) Biological interactions between polysaccharides and divalent cations: the egg- box model. FEBS Lett. 32: 195- 198

Grieger, K.D., A. Fjordboge, N.B. Hartmann, E. Eriksson, P.L. Bjerg, and A. Baun. 2010. Environmental benefits and risks of zero-valent iron nanoparticles (nZVI) for in situ remediation: Risk mitigation or trade-off? Journal of Contaminant Hydrology 118: 165-183.

Hong F, Yang P, Gao F, Liu C, Zheng L, Yang F, Zhou J. (2005a) Effect of nano-anatase TiO2 on spectral characterization of photosystem II particles from spinach. Chemical Research in Chinese Universities:196-200.

Hong FH, Yang F, Liu C, Gao Q, Wan ZG, Gu FG, Wu C, Ma ZN, Zhou J, Yang P (2005b) Influences of nano-TiO2 on the chloroplast aging of spinach under light. Biological Trace Element Research 104(3):249-260.

Huang YH, Shih YJ, Chang CC, Chuang SH (2011) A comparative study of phosphate removal technologies using adsorption and fluidized bed crystallization process. Desalination and Water Treatment 32(1-3):351-356.

Idris, A., and W. Suzana. 2006. Effect of sodium alginate concentration, bead diameter, initial pH and temperature on lactic acid production from pineapple waste using immobilized Lactobacillus delbrueckii. Process Biochemistry 41: 1117-1123.

Iizuka A, Sasaki T, Hongo T, Honma M, Hayakawa Y, Yarnasaki A, Yanagisawa Y (2012) Phosphorus Adsorbent Derived from Concrete Sludge (PAdeCS) and its Phosphorus Recovery Performance. Industrial & Engineering Chemistry Research 51(34):11266-11273.

Jacob DL, Borchardt JD, Navaratnam L, Marinus LO, Bezbaruah AN (2013) Uptake and translocation of Ti from nanoparticles in crops and wetland plants. International Journal of Phytoremediation, 15:2,142-153

Joo, S.H., and D. Zhao. 2008. Destruction of lindane and atrazine using stabilized iron nanoparticles under aerobic and anaerobic conditions: Effects of catalyst and stabilizer. Chemosphere 70: 418-425.

Kanel, S.R., B. Manning, L. Charlet, and H. Choi. 2005. Removal of arsenic(III) from groundwater by nanoscale zero-valent iron. Environmental Science & Technology 39: 1291-1298.

Kim H, Hong H, Jung J, Kim S, Yang J. (2010) Degradation of trichloroethylene (TCE) by nanoscale zero-valent iron (nZVI) immobilized in alginate bead. Journal of Hazardous Materials 176(1-3):1038-1043.

Kim, H., H.J. Hong, J. Jung, S.H. Kim, and J.W. Yang. 2010a. Degradation of trichloroethylene (TCE) by nanoscale zero-valent iron (nZVI) immobilized in alginate bead. Journal of Hazardous Materials 176: 1038-1043.

Klimkova, S., M. Cernik, L. Lacinova, J. Filip, D. Jancik and R. Zboril. 2011. Zero-valent iron nanoparticles in treatment of acid mine water from in situ uranium leaching. Chemosphere 82: 1178-1184

Kosaraju, S.L., L. D'Ath and A. Lawrence. 2006. Preparation and characterisation of chitosan microspheres for antioxidant delivery. Carbohydrate Polymers 64: 163-167.

Krajangpan, S., L. Jarabek, J. Jepperson, B. Chisholm and A. Bezbaruah. 2008. A. Polymer modified iron nanoparticles for environmental remediation. Polymer preprints 49.

Krajewska, B. 2005. Membrane-based processes performed with use of chitin/chitosan materials. Separation and Purification Technology 41: 305-312.

Kulkarni, A.R., K.S. Soppimath, T.M. Aminabhavi, A.M. Dave and M.H. Mehta. 2000. Glutaraldehyde crosslinked sodium alginate beads containing liquid pesticide for soil application. Journal of Controlled Release 63: 97-105.

Lee KY, Heo TR (2000) Survival of Bifidobacterium longum immobilized in calcium alginate beads in simulated gastric juices and bile salt solution. Applied and Environmental Microbiology 66(2):869-873.

Levin GV, Shapiro J (1965) metabolic uptake of phosphorus by wastewater organisms. J. Water Pollut. Cont. 37 pp. 800–821

Li, X.Q., D.W. Elliott, and W.X. Zhang. 2006. Zero-valent iron nanoparticles for abatement of environmental pollutants: Materials and engineering aspects. Critical Reviews in Solid State and Materials Sciences 31: 111-122.

Lien, H.L., and W.X. Zhang. 1999. Transformation of chlorinated methanes by nanoscale iron particles. Journal of Environmental Engineering-ASCE 125: 1042-1047.

Lin DH, Xing BS (2007) Phytotoxicity of nanoparticles: Inhibition of seed germination and root growth. Environmental Pollution 150(2):243-250.

Liu QY, Bei YL, Zhou F (2009) Removal of lead(II) from aqueous solution with amino-functionalized nanoscale zero-valent iron. Central European Journal of Chemistry 7(1):79-82.

Liu, Y.Q., S.A. Majetich, R.D. Tilton, D.S. Sholl, and G.V. Lowry. 2005. TCE dechlorination rates, pathways, and efficiency of nanoscale iron particles with different properties. Environmental Science & Technology 39: 1338-1345.

Lowry, G.V., and K.M. Johnson. 2004. Congener-specific dechlorination of dissolved PCBs by microscale and nanoscale zerovalent iron in a water/methanol solution. Environmental Science & Technology 38: 5208-5216.

Lu CM, Zhang CY, Wen JQ, Wu GR, Tao MX (2002) Research of the effect of nanometer materials on germination and growth enhancement of Glycine max and its mechanism. Soybean Science 21.

Machida-Sano I, Matsuda Y, Namiki H (2009) In vitro adhesion of human dermal fibroblasts on iron cross-linked alginate films. Biomedical Materials 4(2).

Mehrotra, R. C.; Bohra, R. In Metal Carboxylates. Academic Press: London, UK, 1983.

Morris ER, Rees DA, Thom D, Boyd J (1978) Chiroptical and stoichiometric evidence of a specific, primary dimerisation process in alginate gelation. Carbohydrate research, 66:(1), 145-154.

Morse, G.K., Brett, S.W., Guy, J.A., Lester, J.N., 1998. Review: Phosphorus removal and recovery technologies. The Science of The Total Environment 212, 69-81.

Mulkerrins D, Dobson ADW, Colleran E (2004) Parameters affecting biological phosphate removal from wastewaters. Environment International 30(2):249-259.

Nel A, Xia T, Madler L, Li N (2006) Toxic potential of materials at the nanolevel. Science 311(5761):622-627.

Neset T, Cordell D. (2012) Global phosphorus scarcity: identifying synergies for a sustainable future. Journal of the Science of Food and Agriculture 92(1):2-6.

Ngila, J.C. 2011. Comparative studies of metal removal from surface water and wastewater using polymers. Abstracts of Papers of the American Chemical Society 241.

Ngole VM, Ekosse GE (2009) Zinc uptake by vegetables: Effects of soil type and sewage sludge. African Journal of Biotechnology 8(22):6258-6266.

Papageorgiou SK, Kouvelos EP, Favvas EP, Sapalidis AA, Romanos GE, Katsaros FK (2010) Metal-carboxylate interactions in metal-alginate complexes studied with FTIR spectroscopy. Carbohydrate Research 345(4):469-473.

Papageorgiou SK, Kouvelos EP, Favvas EP, Sapalidis AA, Romanos GE, Katsaros FK (2010) Metal–carboxylate interactions in metal–alginate complexes studied with FTIR spectroscopy. Carbohydrate research, 345:(4), 469-473.

Pichtel J, Bradway DJ (200) Conventional crops and organic amendments for Pb, Cd and Zn treatment at a severely contaminated site. Bioresource Technology 99(5):1242-1251.

Ren ZM, Shao LN, Zhang GS (2012) Adsorption of Phosphate from Aqueous Solution Using an Iron-Zirconium Binary Oxide Sorbent. Water Air and Soil Pollution 223(7):4221-4231.

Saha B, Chakraborty S, Das G (2009) A mechanistic insight into enhanced and selective phosphate adsorption on a coated carboxylated surface. Journal of Colloid and Interface Science, 331:(1) 21-26.

Saha B, Chakraborty S, Das G (2009) A mechanistic insight into enhanced and selective phosphate adsorption on a coated carboxylated surface. Journal of Colloid and Interface Science 331(1):21-26.

Seviour RJ, McIlroy S (2008) The microbiology of phosphorus removal in activated sludge processes - the current state of play. Journal of Microbiology 46(2):115-124.

Sharpley AN, Daniel T, Sims T, Lemunyon J, Stevens R, Parry R (2003)Agricultural Phosphorus and Eutrophication (second ed.) United States Department of Agriculture, Agricultural Research Service

Sigma-Aldrich, I. 2007. Specification Sheet # 267953.

Smil V(2000) Phosphorus in the environment: Natural flows and human interferences. Annu Rev Energy Environ 25, 25–53.

Song, H., and E.R. Carraway. 2005. Reduction of chlorinated ethanes by nanosized zero-valent iron: Kinetics, pathways, and effects of reaction conditions. Environmental Science & Technology 39: 6237-6245.

Stampoulis D, Sinha SK, White JC (2009) Assay-Dependent Phytotoxicity of Nanoparticles to Plants. Environmental Science & Technology 43(24):9473-9479.

Suh S, Yee S (2011) Phosphorus use-efficiency of agriculture and food system in the US. Chemosphere 84(6):806-813.

Tanboonchuy V, Hsu JC, Grisdanurak N, Liao CH (2011) Impact of selected solution factors on arsenate and arsenite removal by nanoiron particles. Environmental Science and Pollution Research 18(6):857-864.

Taylor R, Walton DRM (1993) THE CHEMISTRY OF FULLERENES. Nature 363(6431):685-693.

Tchobanoglous G, Burton FL, Stensel HD (2003). Wastewater Engineering Treatment and Reuse, 4th Edn. Metcalf and Eddy. Inc. McGraw-Hill Company.

U.S. Environmental Protection Agency (USEPA). 2009. National Lakes Assessment: A Collaborative Survey of the Nation's Lakes. EPA 841-R-09-001. U.S.Office of Water and Office of Research and Development, Washington, D.C. Available at http://www.epa.gov/owow/LAKES/lakessurvey/pdf/nla_report_low_res.pdf (retrieved October, 25, 2012)

USDD (2004) Unified Facilities Criteria (UFC) - Domestic Wastewater Treatment. U.S. Department of Defense, UFC 3-240-09A, January 2004.

USGS (1999) Phosphorus in a Ground-Water Contaminant Plume Discharging to Ashumet Pond, Cape Cod, Massachusetts, Northborough, MA.

Wang, C.B., and W.X. Zhang. 1997. Synthesizing nanoscale iron particles for rapid and complete dechlorination of TCE and PCBs. Environmental Science & Technology 31: 2154-2156.

Yang F, Hong F, You W, Liu C, Gao F, Wu C, Yang P (2006) Influences of nano-anatase TiO2 on the nitrogen metabolism of growing spinach. Biological Trace Element Research:179-190.

Youssef, M.E., E.A. Soliman, M.A. Abu-Saied, M.S.M. Eldin, S.S. Al-Deyab, E.R. Kenawy and A.A. Elzatahry. 2010. Laboratory Studies and Numerical Modeling of using Natural Micro beads for Environmental Applications. International Journal of Electrochemical Science 5: 1887-1897.

Zhang, W.X. 2003. Nanoscale iron particles for environmental remediation: An overview. Journal of Nanoparticle Research 5: 323-332.

Zheng L, Hong F, Lu S, Liu C (2005) Effect of nano-TiO_2 on strength of naturally and growth aged seeds of spinach. Biological Trace Element Research: 83-91.

CHAPTER 2. AQUEOUS PHOSPHATE REMOVAL USING NANOSCALE ZERO-VALENT IRON[1]

2.1. Abstract

Nanoscale zero-valent iron (NZVI) particles have been used for the remediation of a wide variety of contaminants. NZVI particles have high reactivity because of high reactive surface area. In this study, NZVI slurry was successfully used for phosphate removal and recovery. Batch studies conducted using different concentrations of phosphate (1, 5, and 10 mg PO_4^{3-}-P/L with 400 mg NZVI/L) removed ~96 to 100% phosphate in 30 minutes. Efficacy of the NZVI in phosphate removal was found to 13.9 times higher than micro-ZVI particles (MZVI) with same NZVI and MZVI surface area concentrations used in batch reactors. Ionic strength, sulfate, nitrate, and humic substances present in the water affected in phosphate removal by NZVI but they may not have any practical significance in phosphate removal in the field. Phosphate recovery batch study indicated that better recovery is achieved at higher pH and it decreased with lowering of the pH of the aqueous solution. Maximum phosphate recovery of ~78% was achieved in 30 minutes at pH 12. The successful rapid removal of phosphate by NZVI from aqueous solution is expected to have great ramification for cleaning up nutrient rich waters.

This chapter was published as an article in JNPR (Almeelbi T, Bezbaruah AN (2012) Aqueous phosphate removal using nanoscale zero-valent iron. Journal of Nanoparticle Research, 14(7), 1-14.

[1] The material in this chapter was co-authored by Talal Almeelbi and Dr. Achintya Bezbaruah. Talal Almeelbi had primary responsibility for conducting laboratory experiments. Talal Almeelbi was the primary developer of the conclusions that are advanced here. Talal Almeelbi also drafted and revised all versions of this chapter. Dr. Bezbaruah served as proofreader and checked the math in the statistical analysis conducted by Talal Almeelbi.

2.2. Introduction

Phosphorus (P) exists in water in both particulate and dissolved forms. The usual forms of P in aqueous solutions are orthophosphates, polyphosphates and organic phosphates (Mezenner and Bensmaili 2009). Phosphorus is necessary for the growth of organisms and plants and is an indicator of surface water quality. Excessive P present in natural waters is known to cause eutrophication (Penn and Warren 2009). Eutrophication results in the depletion of oxygen that leads to fish death and affects other aquatic life forms adversely. The major point sources that contribute to P built up in aquatic environment include municipal and industrial wastewaters. Run-offs from agriculture, including animal agriculture, are the major non-point sources. The amount of P compounds in these sources should be controlled to prevent eutrophication in lakes and other surface waters. Accelerated eutophication not only affects the aquatic life but indirectly hinders the economic progress of communities that depend on aquatic food and other resources (Cleary et al., 2009). Dissolved phosphate of ~ 0.02 mg/L is considered to have potential that lead to profuse algal growth in waters (USEPA 1995).

On the other hand, phosphorus is one of the required nutrients for plants. P-based fertilizers are extensively used in food crops and it is intricately related to global food security. Phosphorous for fertilizer production comes predominantly from select mines from Morocco, Western Saharan region, and China (Cordell et al., 2009). Phosphorus is a nonrenewable resource. While an assessment of future consumption of phosphorus fertilizers indicates that natural phosphate (PO_4^{3-}) deposits will last for approximately 60-240 years (Cornel and Schaum 2009), P production rate is predicted to decline sometime in year 2035 while the demand for P-based fertilizers is on the rise(Cordell et al., 2011). Short supply of P-fertilizer is a major concern

in food security area. It is, therefore, essential recover P from 'wastes' for possible reuse in agriculture.

Chemical precipitation (de-Bashan and Bashan 2004), physico-chemical processes (Mishra et al., 2010), and enhanced biological phosphate removal (Gouider et al., 2011) are the frequently used techniques to remove aqueous phosphate. Among them chemical treatment methods for aqueous phosphate removal are widely practiced using chemicals like lime (Ahn and Speece 2006), alum (Babatunde and Zhao 2010), and ferric chloride (Caravelli et al., 2010). However, the high cost of chemicals and problems associated with sludge management make these methods unattractive for waters containing high amounts of phosphate (for example, wastewater with a typical total P of 4–14 mg/L, Tchobanoglous et al., 2003).

Sorption has emerged as a viable option for phosphate removal from aqueous media. In the recent years considerable amount of emphasis has been put on the use of low cost (ad)sorbents. Cost effectiveness is identified as the prime criterion in the selection of a sorption technology whether it uses synthetic or natural sorbents (Mishra et al., 2010). Phosphate can be removed from water using sorbents such as oxides of iron, natural ores like calcite, and goethite (FeOOH), active red mud, and activated carbon. One of the problems encountered with these sorbents is that they have very low sorption capacities. For example, sorption capacities of iron oxides are 11.2 mg PO_4^{3-}/g (Yan et al., 2010a) and 19.02 mg PO_4^{3-}-P/g (Cordray 2008). Similarly, natural ores like calcite was reported to have a sorption capacity of 0.1 mM PO_4^{3-}/g (i.e., 3.1 mg PO_4^{3-}-P/g, Karageorgiou et al., 2007). Goethite (FeOOH, 17.3 mg PO_4^{3-}-P/g, Chitrakar et al., 2006), active red mud (9.8 PO_4^{3-}-P/g, Yue et al., 2010), and activated carbon (3.02 mg PO_4^{3-}-P/g, Hussain et al., 2011) are so far tried for P removal.

In the last two decades nanoscale zero-valent iron (NZVI) particles have received a lot of attention because of their unique reactive and sorbtive characteristics (Bezbaruah et al., 2009 and 2011; Li et al., 2006). N ZVI particles show good sorbtive characteristics owing to their high surface to volume ratio (Yan et al., 2010b). However, most of the reported work on sorption by NZVI has been on metalloids and heavy metals including some actinides (Giasuddin et al., 2007; Kanel et al., 2005; Klimkova et al., 2011; Scott et al., 2011) and, to the best of authors' knowledge, there is no literature on phosphate removal and subsequent recovery using NZVI.

The objective of this study is to investigate the efficacy of NZVI particles for phosphate removal and recovery from aqueous solutions. Phosphate removal was tried under different environmental conditions (temperature, ionic strength), and in the presence of interfering ions and organic compounds. Effect of particle size on phosphate removal was studied. Batch experiments were conducted under different pH conditions to investigate the optimal pH conditions for phosphate recovery from NZVI.

2.3. Materials and Methods

2.3.1. Chemicals and reagents

Iron (III) chloride hexahydrate ($FeCl_3$**.**$6H_2O$, 98%, Alfa Aesar), sodium borohydride ($NaBH_4$, 98%, Aldrich), methanol (production grade, BDH), calcium chloride ($CaCl_2$, ACS grade, BDH), monopotassium phosphate (KH_2PO_4, 99%, EMD), potassium nitrate (KNO_3, 99%, Alfa Aesar), sodium hydroxide (5 N NaOH, Alfa Aesar), potassium sulfate (K_2SO_4, ACS grade, HACH), natural organic matter (Suwannee River NOM, RO isolation, IHSS), and humic acid (H1452, Spectrum) were used as received unless and otherwise specified.

2.3.2. Synthesis of NZVI

NZVI particles were synthesized using sodium borohydride reduction method (Eq. 2.1, Huang and Ehrman 2007).

$$2FeCl_3 + 6NaBH_4 + 18H_2O \rightarrow 2Fe^0 + 21H_2 + 6B(OH)_3 + 6NaCl \quad (2.1)$$

Ferric chloride hydrate (1.35 g) was dissolved in 40 mL of deoxygenated de-ionized (DI) water (solution A), and 0.95 g of sodium borohydride was dissolved in 10 mL of deoxygenated DI water in a separate beaker (solution B). Then solution A was added drop wise to solution B under vigorous stirring conditions (using a magnetic stirrer). The resultant black precipitates (NZVI) were centrifuged and washed with copious amount of deoxygenated DI water. The NZVI in slurry form was then stored in 20 mL vials in methanol to prevent oxidation, and used for experiments later. NZVI slurry in the vials was withdrawn using a pipette after vigorous stirring. The average weight of dry NZVI present in 1 mL well stirred slurry was measured to be 20 mg ± 0.6 mg (n = 25).

2.3.3. Phosphate removal batch studies

Batch experiments were conducted using (a) NZVI, and (b) microscale zero-valent iron (MZVI) particles. Phosphate solution (50 mL of 1, 5, and 10 mg PO_4^{3-}-P /L) with 20 mg of NZVI (i.e., 400 mg/L) in multiple 50 mL polypropylene plastic vials fitted plastic caps (reactors). The reactors were rotated end-over-end at 28 rpm in a custom-made shaker to reduce mass transfer resistance. One of the reactors was withdrawn at specific time interval (0, 10, 20, 30 and 60 min) and the content was centrifuged at 4000 rpm. Bulk solution was collected for phosphate analysis from this reactor and reactor was sacrificed or used for phosphate recovery study (see 'Phosphate recovery batch studies'). Ascorbic acid method (Eaton et al., 2005) was

used for phosphate analysis. This method depends on the formation phosphomolybdic acid during the reaction between orthophosphate and molybdate. Ascorbic acid reduces phosphomolybdic to form a blue complex. The color was measured in a UV-vis spectrophotometer (HACH, DR 5000) at wavelength of 880 nm. A five-point calibration was done routinely.

2.3.4. Effect of initial NZVI concentration

Batch studies were conducted with six different NZVI concentrations (80, 160, 240, 320, 400, 480, and 560 mg/L) for an initial bulk PO_4^{3-}-P concentration of 5 mg/L. The experimental procedure described earlier (see 'Phosphate removal batch studies') was followed. Samples were withdrawn for phosphate analysis at 30 min.

2.3.5. Interference studies

The effects ionic strength, presence of selected anions and cations, and humic substances were examined. Batch studies were conducted in room temperature (22±2 ^oC) using 400 mg NZVI/L and 40 mL of solution with an initial bulk phosphate concentration of 5 mg PO_4^{3-}-P /L. Sampling frequency was maintained as described earlier (see 'Phosphate removal batch studies').

The ionic strength was varied from 0 to 10 mM by adding specific amounts of $CaCl_2$ to the phosphate solution. The range of ionic strength was selected to represent groundwater conditions. The possible interference due to the presence of other important ions was also studied using two important anions (sulfate and nitrate). Potassium sulfate was used as the source of SO_4^{2-} (0, 100, 500, 900 mg/L). The effect of NO_3^- (0, 1, 5, 10 mg NO_3^--N /L) was studied by adding KNO_3. Humic substances present in water may affect phosphate removal by NZVI, and to evaluate such impacts Suwannee River (USA) natural organic matter (0, 1, 10, 50 mg/L) and

humic acids (0, 1, 10, 50 mg/L) were used in separate batch experiments. The batch experiments were conducted as described earlier (see 'Phosphate removal batch studies').

2.3.6. Effect of temperature

Experiments were conducted under deferent temperatures conditions (4, 22, and 60 ^{o}C) to find out the effect of temperature change on phosphate removal by NZVI. The temperature of phosphate solution was first adjusted to the desired temperature by keeping it in the specific environment for long enough periods (~24h). NZVI particles (400 mg/L) were added to phosphate solution (40 mL, 5 mg/L) once the specific temperature was reached. Samples were shaken at 100 rpm under temperature-controlled environment using an incubator-cum-orbital shaker (Thermo Scientific, MaxQ4000).

2.3.7. Effect of particle size

Effect of zero-valent iron (ZVI) particle size on phosphate removal was evaluated using NZVI particles synthesized within this research and microscale zero-valent iron (MZVI) particles purchased from a supplier (Aldrich, 99.9% purity, used as received). ZVI reactions are known to be surface mediated (Thompson et al., 2010), and as such it was ensured that the same surface area concentrations were used in the experiments conducted with NZVI and MZVI. The NZVI particles used in this experiment had a surface area of ~25 m^2/g (Bezbaruah et al., 2009) and MZVI had a surface area of ~2 m^2/g (reported by the manufacturer). NZVI and MZVI surface area concentration of 10 m^2/L (400 mg/L NZVI and 5 g/L MZVI) was used in the study.

2.3.8. Phosphate recovery batch studies

An initial batch study was conducted to find out the pattern of desorption (recovery) of phosphate into water from NZVI used for phosphate removal. Batch experiments were run first

in 50 mL plastic vials fitted a plastic cap (reactors) with 400 mg/L NZVI and 50 mL of 5 mg PO_4^{3-}-P/L to get the phosphate sorbed onto NZVI. The batch reactors were withdrawn after 60 min and centrifuged to separate the spent NZVI (i.e., NZVI particles with phosphate sorbed onto them). The bulk solution was decanted out and phosphate concentration was measured. A 50 mL DI water was added to the spent NZVI and the pH was manipulated (2-12) with either 0.1 N HCl or NaOH. The reactors were closed and rotated end-over-end for 30 min. The reactors with the samples were then centrifuged and concentration of phosphate was measured in the bulk solution. The optimal pH for phosphate recovery (i.e., when maximum phosphate recovery) was determined based on this initial batch study results, and the rest of the phosphate recovery experiments were conducted at that particular (optimal) pH.

Additional batch studies were conducted in sacrificial reactors at the optimal pH, and phosphate recovery was monitored over time (0, 10, 20, and 30 min). The data obtained from the removal experiments were normalized with respect to the original bulk phosphate concentration. For the data sets from the recovery studies, the initial phosphate concentration was calculated based on the mass of phosphate sorbed onto the NZVI and the data were normalized with respect to that.

2.3.9. NZVI characterization

X-ray diffraction (XRD) was done to find out NZVI composition. The samples were placed in stainless steel sample holders and XRD patterns were recorded using CuKα radiation (= 1.5418A˚) on a Philips X'Pert diffractometer operating at 40 kV and 40 mA between 5˚ and 90˚ (2θ) at a step size of 0.0167˚(Xi et al., 2010).

High-resolution transmission electron microscopy (HRTEM, JEOL JEM-2100-LaB6 TEM) was used to observe the shape of NZVI particles and determine their particle size. NZVI

particles were vacuum dried and the dry particles were placed in ethanol and sonicated for 5 min to achieve proper dispersion. Drops of the resulting solution were placed onto lacey carbon grids (Electron Microscopy Sciences, USA) and allowed to dry. Images were taken using a Gatan ORIUS large format CCD camera.

2.3.10. Quality control

All experiments were done in triplicates during this research and the average values are reported along with the standard deviations. Blanks with only phosphate (without NZVI/MZVI) were run along with the NZVI and MZVI experiments. The analytical instruments and tools were calibrated before the day's measurements. One-way ANOVA tests were performed to compare the variance between data sets as needed. Additionally, Dunnett Method was used to compare control with rest of the treatment data. Minitab 16 software (Minitab, USA) was used for all statistical analyses.

2.4. Results and Discussion

2.4.1. NZVI synthesis and characterization

NZVI synthesized (Fig. 2.1a) during this research were mostly spherical in shape and had particle size distribution from 10 nm to 30 nm with an average size of 16.24±4.05 nm (n = 109, Fig. 2.1b). Huang and Ehrman (2007) reported particle size of 20 nm using the same method. The XRD spectrum (Fig. 2.1c) for the particles synthesized during this study shows three peaks of zero-valent iron (Fe^0). A couple of iron oxide peaks were also observed which might be because of exposure of the particles to air during the XRD experiment. During the synthesis of NZVI, the particles were not bleed with air (as in Bezbaruah et al., 2009 and 2011) but there is still a possibility that a thin oxide layer around the particles was formed due to reaction with

atmospheric oxygen. A peak for iron chloride was also observed which might be from the left over reactants used for the synthesis of NZVI (see Eq. 2.1).

2.4.2. Phosphate removal

Batch experiments were conducted for phosphate removal using 400 mg/L NZVI and different phosphate concentrations (1, 5, 10 mg PO_4^{3-}-P/L). Rapid phosphate removal was observed in the first a few minutes of the experiment for all three concentrations. About 88-95% of phosphate was removed within the first 10 min and only minimal removal was observed beyond that (Fig. 2.2). Blanks didn't show any removal of phosphate. Three consecutive data points (20, 30, and 60 min) showed no major change (maximum 2.7% variation) in phosphate removal for the two higher concentrations (5 and 10 mg PO_4^{3-}-P/L). while a much larger variation (~7.8% from 20 to 60 min) was observed for 1 mg PO_4^{3-}-P/L. While complete (100%) phosphate removal was observed for 1 mg PO_4^{3-}-P/L solution, 96.29±0.13 and 97.53±0.16 percent removals were observed for 5 and 10 mg PO_4^{3-}-P/L, respectively. The sorption capacities at 60 min were found to be 2.27±0.00, 12.00±0.02, and 24.38±0.04 mg/g for 1, 5, and 10 mg PO_4^{3-}-P/L, respectively. The sorption capacity increased linearly (R^2 = 0.9999) with the increase in phosphate concentration.

For 5 mg PO_4^{3-}-P/L, 30 min was found to be long enough time to achieve equilibrium with 400 mg NZVI/L. As such all experimental data for 5 mg PO_4^{3-}-P/L and 400 mg NZVI/L were collected up to 30 min. Iron-based removal techniques are reported by others where 15-100% phosphate removal has been achieved (Table 2.1).

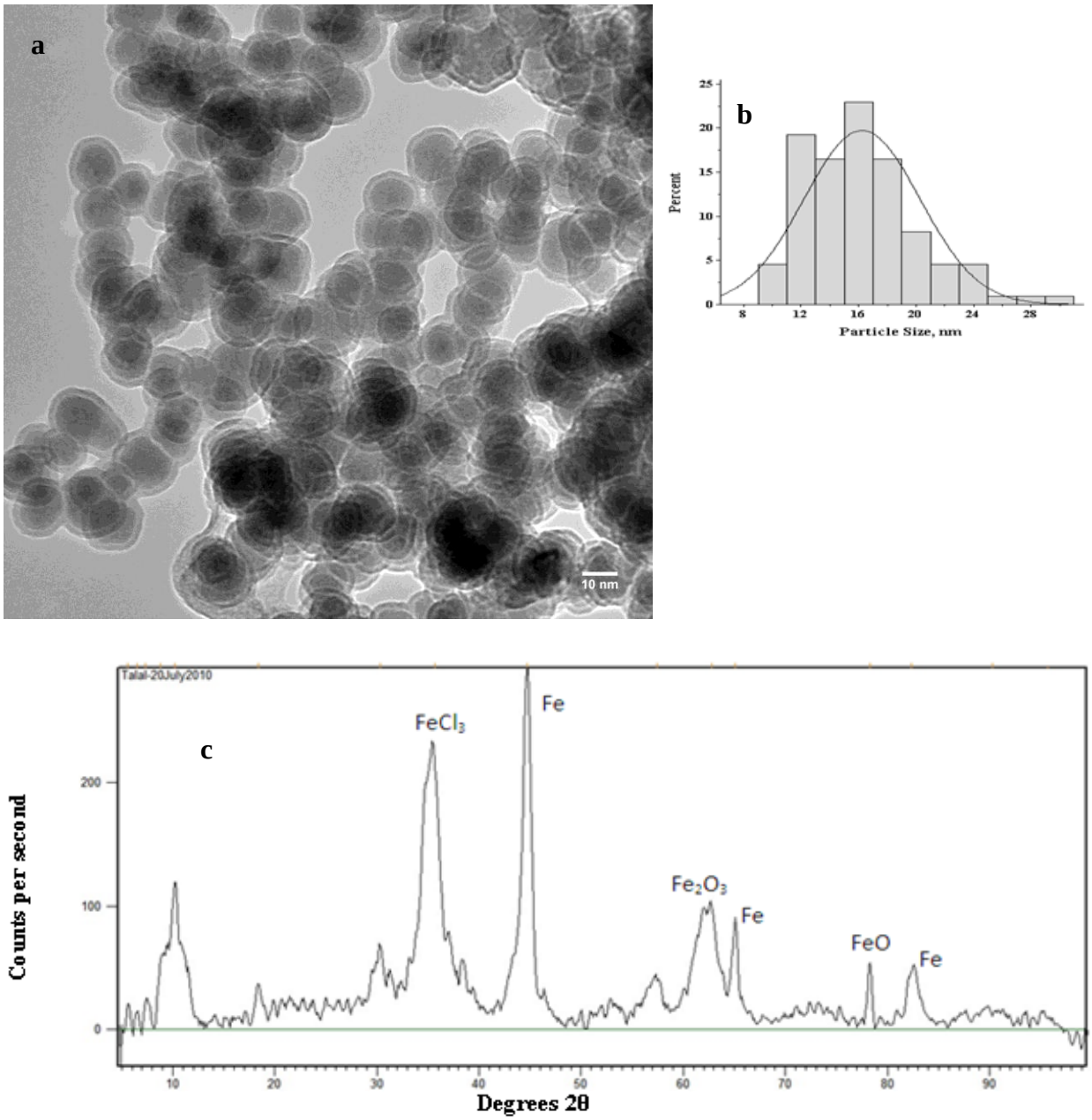

Figure 2.1: (a) High-resolution transmission electron microscopy (HRTEM) image of NZVI; **(b)** Particles size distribution of the nanoparticles synthesized was 10-30 nm with an average size of 16.24±4.05 nm (n = 109); **(c)** X-ray diffraction (XRD) spectrum of NZVI with prominent peaks for Fe^0. Peaks for oxides are from Fe-oxide layer on the NZVI, and the $FeCl_3$ peak is from residuals of raw materials used in NZVI synthesis

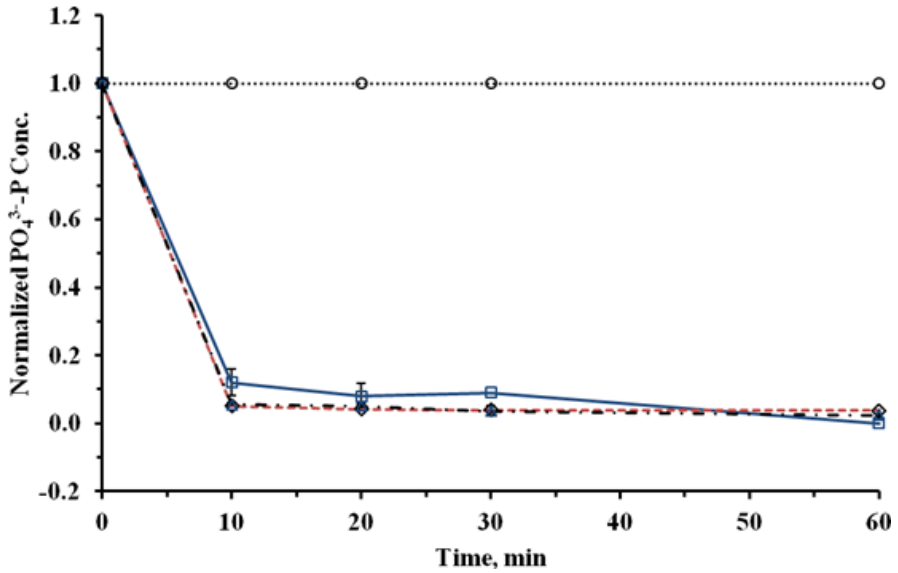

Figure 2.2: Phosphate removal by NZVI/L from bulk solutions with different initial phosphate concentrations (10 mg PO_4^{3-}-P/L, 5 mg PO_4^{3-}-P/L , 1 mg PO_4^{3-}-P/L, Blank). NZVI = 400 mg/L

Hydroxides of iron were found to be most effective in the removal process but a wide range of efficiency (15-100%) has been reported (Chitrakar et al., 2006; Cordray 2008; Mezenner 2009; Yan 2010a). Synthetic goethite (α-FeOOH) was found to remove up to 1 mg P/L completely (100%) from NaH_2PO_4 solution (Chitrakar et al., 2006). Again 100% phosphate removal was observed with akaganeite (β-FeOOH) up to 0.3 mg P/L. It took 2-8 h to reach equilibrium in most of the reported phosphate removal experiments done with DI/distilled/wastewater (Chitrakar et al., 2006; Mezenner and Bensmaili 2009; Xiong et al., 2008; Yan et al., 2010a) but took 24 h to reach equilibrium in seawater (Chitrakar et al., 2006). It is pertinent here to discuss treatment time in other sorption systems for comparison purposes. Hussain et al., (2011) reported 95% removal of phosphate with granular activated carbon over a 150-min period. Sorption of ~95% of phosphate on calcite in 45 min was reported by Karageorgiou et al., (2007).

In the present study, very fast removal of phosphate (88-95% in 10 min) was achieved, and that makes this research very relevant for continuously flowing (pumped) water (i.e., required contact time will be short). The sorption capacities of NZVI after 10-min interaction with the aqueous solution containing phosphate were found to be 2.20±0.06, 11.87±1.20, and 23.62±0.11 mg/g for 1, 5, and 10 mg PO_4^{3-}-P/L solutions, respectively. The sorption capacities of 3.02-19.02 mg PO_4^{3-}-P/g reported by others (Chitrakar et al., 2006; Cordray 2008; Hussain et al., 2011; Karageorgiou et al., 2007; Yan et al., 2010a and 2010b) are comparable to the sorption capacities achieved for the NZVI in this study. However, the reaction time is much shorter with NZVI.

Table 2.1: Different iron-based adsorbents used for phosphate removal and their performance data

Type of Iron	***Type of Water/ Phosphate***	***Removal (%, time)***	***% Recovery***	***Source***
Hydroxy-iron	DI/KH_2PO_4	90%, 5.83 h	-	Yan et al., (2010a)
Iron ore	wastewater	97%, 15 d	-	Guo et al., (2009)
Iron hydroxide-eggshell waste	Distilled water/KH_2PO_4	73%, 3.67h		Mezenner and Bensmaili (2009)
Steel slag	Distilled water/KH_2PO_4	71–82%, 2 h	-	Xiong et al., (2008)
Synthetic Goethite	NaH_2PO_4	40-100%, 2-8 h	~82%	Chitrakar et al., (2006)
Akaganeite	NaH_2PO_4	15-100%, 4-8 h	~90%	Chitrakar et al., (2006)
Synthetic Goethite	Sea water + NaH_2PO4	60%, 24h	-	Chitrakar et al., (2006)

The mechanism of phosphate removal by NZVI in the present study can be explained based on point of zero charge (PZC) and ligand exchange (Eq. 2.2, Karageorgiou et al., 2007, and Fig. 2.3). PZC for NZVI is around 7.7 (Giasuddin et al., 2007), and when pH is less than PZC the surface of NZVI is positively charged which makes the surface suitable for anion (PO_4^{3-}) sorption. The initial pH of the test solutions used in this study was ~4.0 and final pH after 60

min reaction was ~7.5 which was still lower than the PZC of NZVI. The pH environment maintained in the reactor was ideal for PO_4^{3-} sorption and that is why 97.53-100% removal was achieved in this study.

$$\equiv Fe-OH + X^- \xrightarrow{H^+} \equiv Fe-O\overset{H}{\underset{H}{\cdots}} X^- \ (pH < PZC) \qquad (2.2)$$

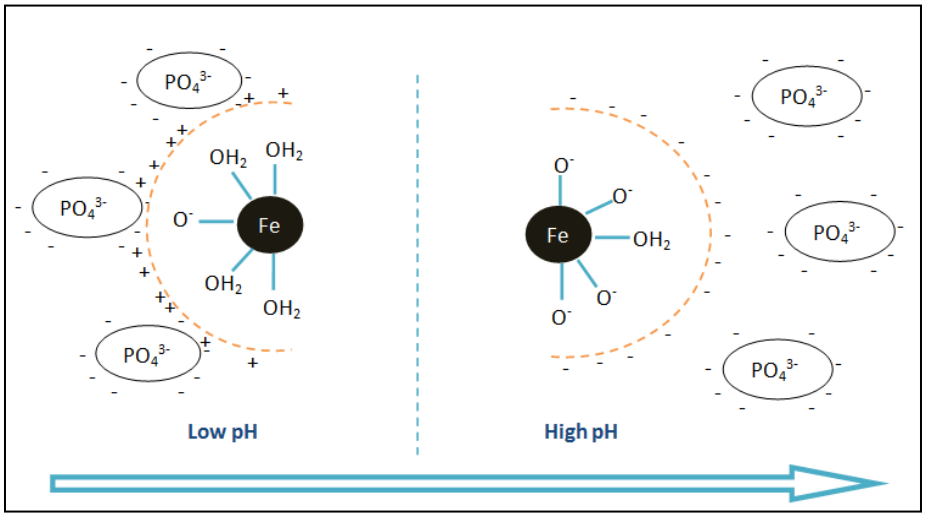

Figure 2.3: Phosphate sorption by NZVI under various pH conditions (after Cordray, 2008). Lower pH is more conducive for phosphate adsorption while desorption is the dominant phenomenon at higher pH

2.4.3. Effect of initial NZVI concentration

The removal of phosphate (C_0 = 5 mg/L) was found to increase with increase in the initial NZVI concentration (Fig. 2.4) and followed a linear trend (R^2 = 0.9539) as NZVI concentration increased from 0 to 560 mg/L. NZVI concentration beyond 400 mg/L didn't improve PO_4^{3-} removal significantly. Phosphate removal of 100% was obtained for using 560 mg NZVI/L. When the initial NZVI concentration was increased from 80 to 560 mg/L, the removal of phosphate increased by ~78%. The increase in phosphate removal efficiency with the increase in NZVI concentration was expected as the contaminant removal by NZVI is a surface area

mediated process. When NZVI concentration increased from 0 to 560 mg/L the reactive iron surface area in solution increased from 0 to 14 m^2/L (NZVI surface area = 25 m^2/g). The observations are consistent with findings by others with sorption media where surface area controls the sorption of phosphate (Mezenner and Bensmaili 2009).

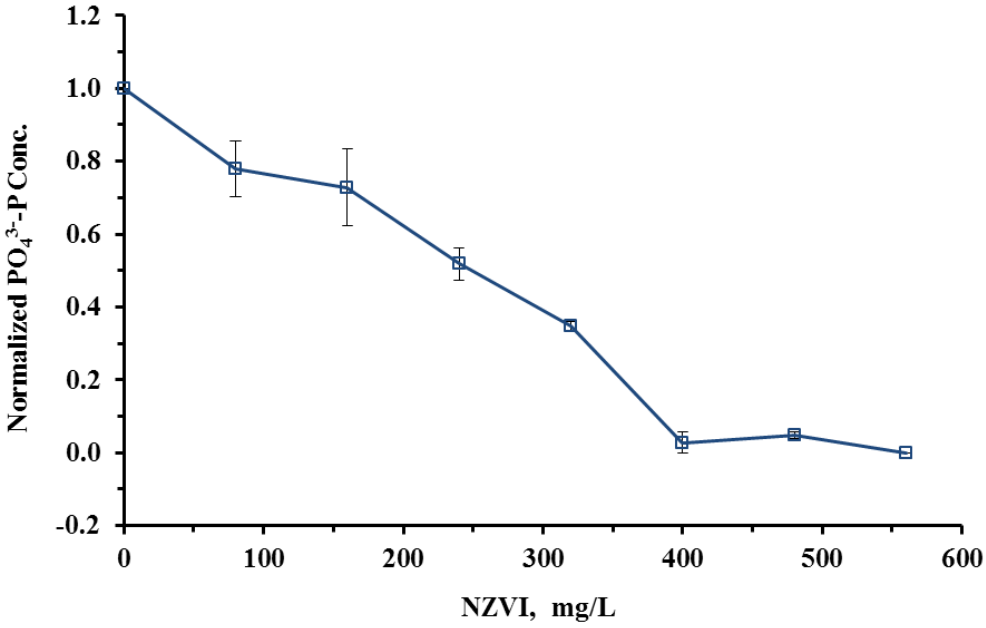

Figure 2.4: Effect of initial NZVI concentration on phosphate removal. Initial PO_4^{3-}-P = 5 mg/L

2.4.4. Interference studies

The interferences of various ions and organic matters on phosphate removal were studied with an objective to understand how NZVI is going to behave during real field applications. Ionic strength (varied from 0 to 10 mM) did not have any statistically significant effect on phosphate (C_0 = 5 mg/L) removal by NZVI (Fig. 2.5a, α =0.005, p = 0.225). However, analysis of variance (ANOVA) showed statistically significant differences in the treatment data for nitrate (α =0.005, p = 0.001), sulfate (0-900 mg/L, α =0.005, p = 0.00), humic acid (0-50 mg/L, α =0.005, p = 0.00), and NOM (0-50 mg/L, α =0.005, p = 0.00). Dunnett method was used to

further compare the control with rest of the treatment data. All nitrate concentrations (1, 5, 10 mg NO_3^--N/L, Fig 2.5b) were found to significantly interfere in phosphate removal from aqueous solution. However, this statistically significant increase in phosphate removal (1.40-2.77%) may not have any practical significance bring very marginal. Again, the treatment data were significantly different from the control for all sulfate concentrations (100, 500, 900 mg/L). Phosphate removal by NZVI decreased by 5.16-6.27% in the presence of sulfate in the solution (Fig. 2.5c). While the presence of NOM (1, 10, 50 mg/L, Fig. 2.5d) decreased phosphate removal by 6.01-11.03% (all statistically significant), the presence of humic acid showed mixed results. The presence of 1 mg/L humic acid (Fig. 2.5e) significantly reduced (13.86%) phosphate removal but interference was not statistically significant when humic acid concentration was increased (10 and 50 mg/L).

Liu et al., (2011) have reported interference due to ionic strength during phosphate removal with lanthanum-doped activated carbon fiber. They increased ionic strength from 0 to 10 mM and observed an 8.1% drop in phosphate removal (from 98.8 to 90.7%). Even 10 mM ionic strength did not affect the phosphate removal efficiency in the present study, and a removal of 96.0-98.5% was achieved in all cases (ionic strength varied from 0 to 10 mM). Introducing competing anions was expected to have negative effects on phosphate adsorption (Liu et al., 2011). Fe^0 was successfully used by others to remove nitrate from aqueous solution (Bezbaruah et al., 2009; Hwang et al., 2011) and so it was expected that nitrate will compete with phosphate for reactive/sorption sites on NZVI. Nitrate was found to interfere in phosphate removal in layered double hydroxides (Das et al., 2006) and ~12% reduction in phosphate removal in the presence of nitrate was reported. Xue et al., (2009), however, did not find any interference of NO_3^- during phosphate removal using basic oxygen furnace slag. In the present study slight

increase (1.40-2.77%) in phosphate removal (though not environmentally significant) was observed. Further research would be needed to find out the possible reason for this increase but the authors would like to hypothesis that nitrate reacted with NZVI to produce iron (hydr)oxides with a higher affinity for phosphate. Sulfate was also reported to interfere with phosphate and reduced phosphate removal by 24.5% in layered double hydroxides (Das et al., 2006). In this study, sulfate retarded the phosphate removal process and reduced removal efficiency as high 6.27%. The adsorption of phosphate in presence of humic acid was studied by Antelo et al., (2007) and found that phosphate adsorption onto the surface of goethite decreased by 45 and 25% in the presence of humic acid at pH of 4.5 and 7, respectively. This can be explained by the competition of the humic acids functional groups with phosphate for the sorption sites where the humic acid outcompeted the phosphate. Also, the sorption sites on the surface could be blocked by the relatively large size of humic acids (~15 Å in diameter, Simeoni et al., 2003), thus less sorption sites will be available for phosphate (~2.56 Å in diameter) (Antelo et al., 2007). Similar results were reported by others (Shuai and Zinati 2009). In the presently study only low concentration (1 mg/L) of humic acid affected phosphate removal while higher concentration did not. This happened possibly because of increased sorption of phosphate onto NZVI due to lowering of solution pH (see Fig. 2.3) at higher humic acid concentrations. Additional experiments are needed to investigate why the presence of the humic substances did not adversely affect phosphate removal by NZVI, the authors feel that NZVI reacts very fast with phosphate in the first 10 min or so the possible inferring compounds are not competitive enough. In this study, phosphate removal in the presence of Suwannee River NOM (1, 10, 50 mg/L) was found to be significantly different from the control (without NOM). Phosphate removal efficiency of NZVI reduced by 9.01-11.03% in the presence of NOM. This result was expected

as NOM negatively impacts NZVI reactivity. Li et al., (2010) reported the minimum concentration of NZVI that inhibited *E. coli* growth after 24 h exposure as 5 mg NZVI/L. However, in the presence of NOM, the NZVI concentration had to be increased to 100 mg/L to achieve the same degree of inhibition. This happened possibly because the NZVI particles' reactive surfaces were covered with NOM and, thus, reducing the overall reactivity of NZVI. Chen et al., (2011) also observed a 23% reduction in trichloroethylene (TCE) degradation by NZVI in the presence of Suwannee River NOM.

2.4.5. Effects of temperature

Experiments were conducted at 4, 22 and 60 ^{o}C during this study. The removal of phosphate at 4 and 22 °C was relatively slower than the removal at 60 ^{o}C. However, after 30 min, the removal was the more or less same (91.4-95.3%) for all temperatures (Fig. 2.6) and there was no significant differences between the values (one-way ANOVA: α =0.005, p = 0.144). This is in contrast to findings by others. Increasing the temperature from 25 to 45 °C increased the phosphate adsorption capacity of granular ferric hydroxide from 3.6 to 5.1 M P/g (i.e., 0.11-0.16 mg/g, Saha et al., 2010). Liu et al., (2011) also reported increase adsorption capacity in lanthanum-doped activated carbon fibers from 8.54 to 9.41 mg/g of with the increase of temperature from 20 to 50 °C. Mezenner and Bensmaili (2009) reported ~60% increase in phosphate adsorption onto iron hydroxide-eggshell waste when the temprature was increased from 20 to 45 ^{o}C. Fast phosphate removal that takes place within the first 10 min may be the reason why no distinction could be made between removal achieved in three different temperatures.

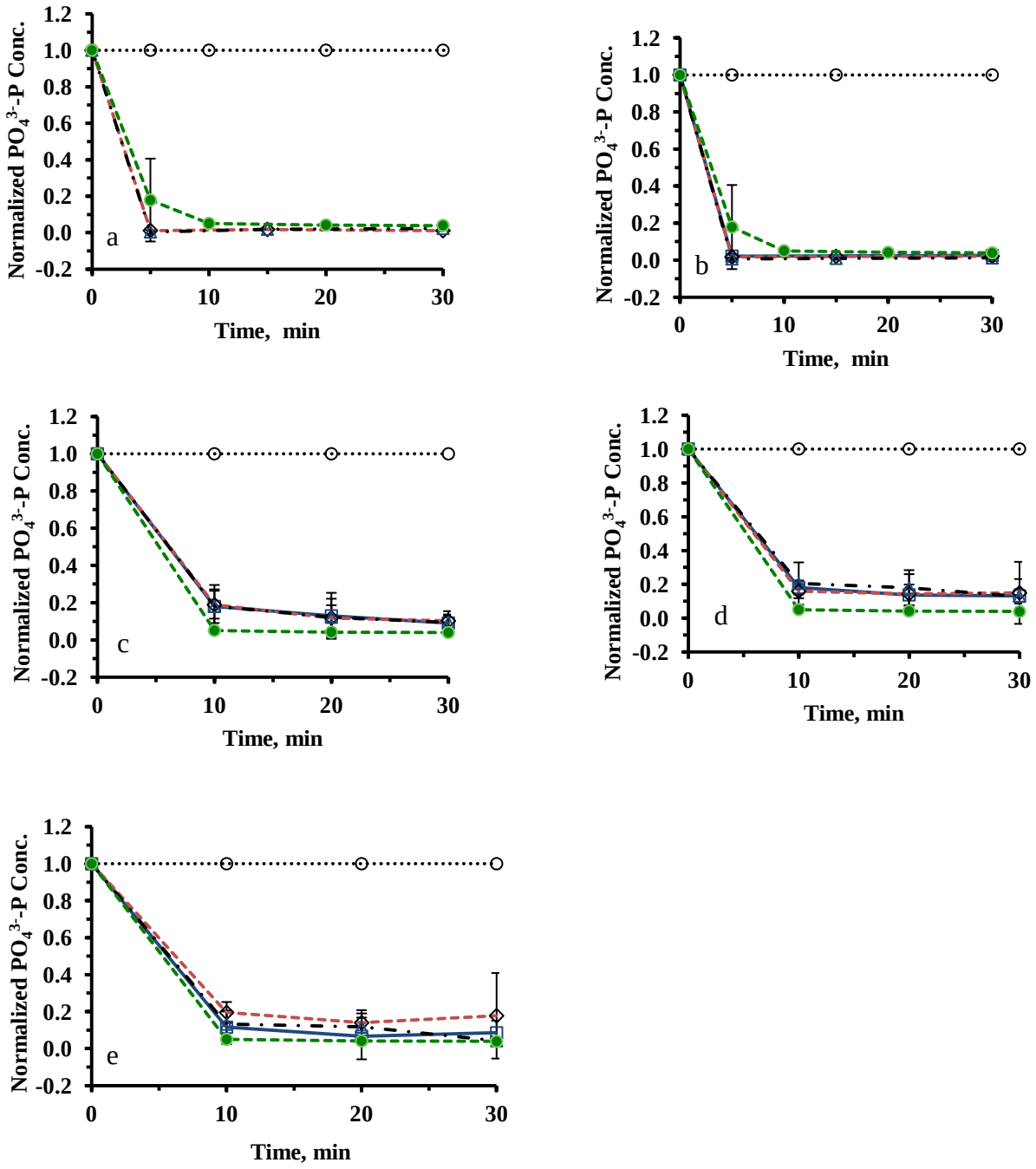

Figure 2.5: (a) Phosphate removal under different ionic strength conditions (0 mM ionic strength, 5 mM ionic strength, 10 mM ionic strength)**; (b)** Phosphate removal in the presence of nitrate (0 mg NO_3^--N/L, 1 mg NO_3^--N/L, 5 mg NO_3^--N/L, 10 mg NO_3^--N/L); **(c)** Phosphate removal in the presence of sulfate (0 mg SO_4^{2-}/L, 100 mg SO_4^{2-}/L, 500 mg SO_4^{2-}/L, 900 mg SO_4^{2-}/L); **(d)** Phosphate removal in the presence of natural organic matter (0 mg NOM/L, 1 mg NOM/L, 10 mg NOM/L, 50 mg NOM/L); **(e)** Phosphate removal in the presence of humic acids (0 mg/L, 1 mg/L, 10 mg/L, 50 mg/L). For all figures: Blank, NZVI = 400 mg/L, Initial PO_4^{3-}-P = 5 mg/L

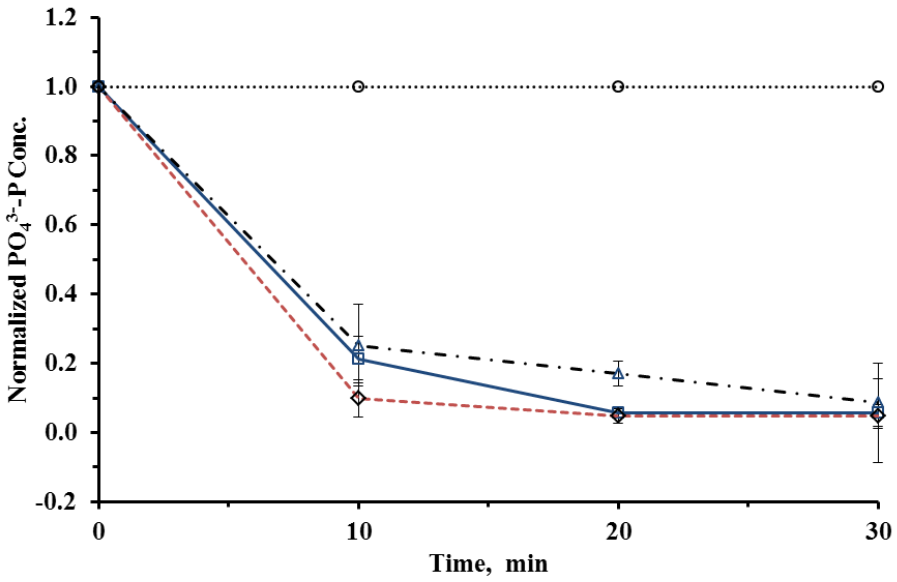

Figure 2.6: Effect of temperature on phosphate removal by NZVI, (4 °C, 22 °C, 60 °C, Blank with only PO_4^{3-} solution). NZVI = 400 mg/L, Initial PO_4^{3-}-P = 5 mg/L. Blank shown here is for 22 °C only. The blanks at other temperatures followed similar trends and not shown here to maintain clarity

2.4.6. Effect of particle size

Sorption is dependent on surface area and, hence, in this study the same surface area (10 m^2/L) was used for the comparison of phosphate removal by NZVI (particle size ~16 nm) and MZVI (<10 µm). MZVI removed only 23% of phosphate (C_0 = 5 mg PO_4^{3-}-P/L) in 30 min whereas NZVI removed ~96% of phosphate over the same time period (Fig. 2.7). NZVI was 13.9 times more efficient than MZVI in removing aqueous phosphate. Others reported similar observations with NZVI for other contaminants. Surface area normalized rate constant (k_{sa}) of NZVI (surface area ~ 30–35 m^2/g) for tetrachloromethane degradation was reported as over two orders of magnitude higher than that of MZVI (Li et al., 2006). Also, removal capacity of Cr(VI) using NZVI was more than 100 time that of the removal capacity using MZVI (Li et al., 2006). Kanel et al., (2005) reported that the k_{sa} for As(III) removal by NZVI was 1-3 orders of magnitude higher than MZVI. While using NZVI, k_{sa} of alachlor degradation was found to be

~10 times that with MZVI ($k_{sa\text{-}NZVI}$ = 38.5 × 10^{-5} and $k_{sa\text{-}MZVI}$ = 3.8–7.7 × 10^{-5} L $h^{-1}m^{-2}$, Thompson et al., 2010)

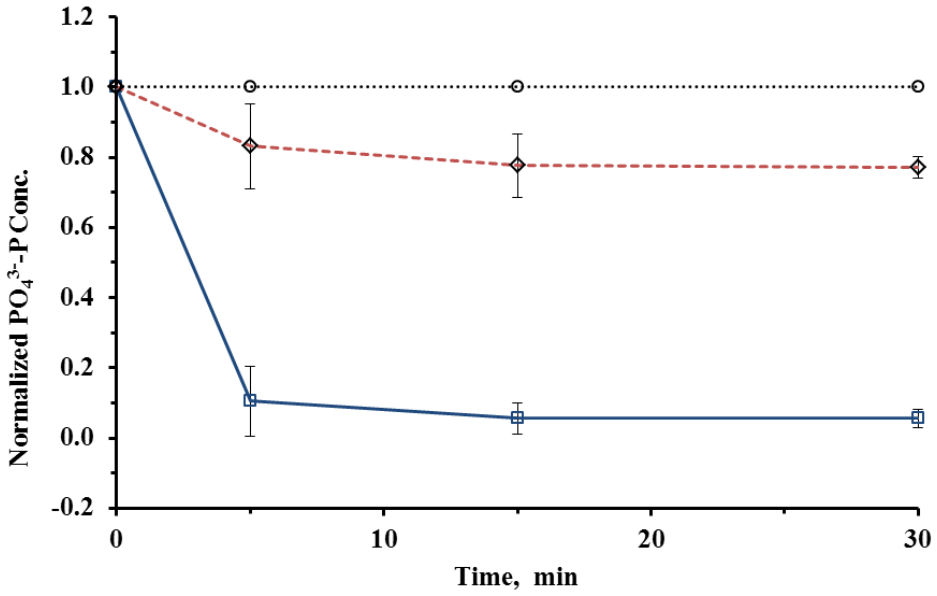

Figure 2.7: Effect of ZVI particles size on phosphate removal (Micro-ZVI, NZVI, Blank). MZVI = 5 g/L; NZVI = 400 mg/L; Equal ZVI surface area concentrations (10 m^2/L) were used for both MZVI and NZVI, Initial PO_4^{3-}-P = 5 mg/L

2.4.7. Phosphate recovery

In the initial batch study run to find out the optimal pH for phosphate recovery maximum phosphate recovery was achieved at pH 12, and the recovery was minimal at acidic pH (data not shown). In the follow up phosphate desorption (recovery) batch studies conducted at pH 12, 78.4% phosphate recovery was obtained (Fig. 2.8). The 78.4% recovery is based on the mass of phosphate sorbed onto NZVI during removal experiment. If the recovery is calculated based on the mass of the phosphate present in the original bulk solution from which removal was achieved than the phosphate removal is 74.5%. In terms of practical applications, if 5 mg/L phosphate is present in bulk solution 4.80 mg/L (96% removal, see 'Phosphate removal' under 'Results and discussion') will be removed by NZVI and 3.73 mg/L (74.5% recovery) can be recovered back from the NZVI. Better phosphate recovery at higher pH was achieved possibly because of the

abundantly present hydroxide ions at a higher pH. The presence of these hydroxide ions would result in a net negative surface charge to which few phosphate anions would be bound. The opposite phenomena would occur at a lower pH which would result in more sorption. Poor recovery of phosphate at pH 4 and 6 supports the previously proposed mechanism where an electrostatic attraction between the phosphate ions and the surface of NZVI occur resulting in phosphate sorption on the surface of NZVI. Also, pH 12 is higher than PZC of NZVI and particles are negatively charged resulting in desorption of phosphate (Eq. 2.3, Karageorgiou et al., 2007 and Fig. 2.3). Research indicate that phosphate can be recovered from sorptive media under high pH conditions (Babatunde and Zhao 2010; Cordray 2008; Karageorgiou et al., 2007; Liu et al., 2011). Similar results were reported by others using other forms of iron oxides (Yan et al., 2010a; Zeng et al., 2004).

$$\equiv Fe-OH + X^- \xrightarrow{OH^-} \equiv Fe-\bar{O} + X^- + H_2O \qquad (pH > PZC) \qquad (2.3)$$

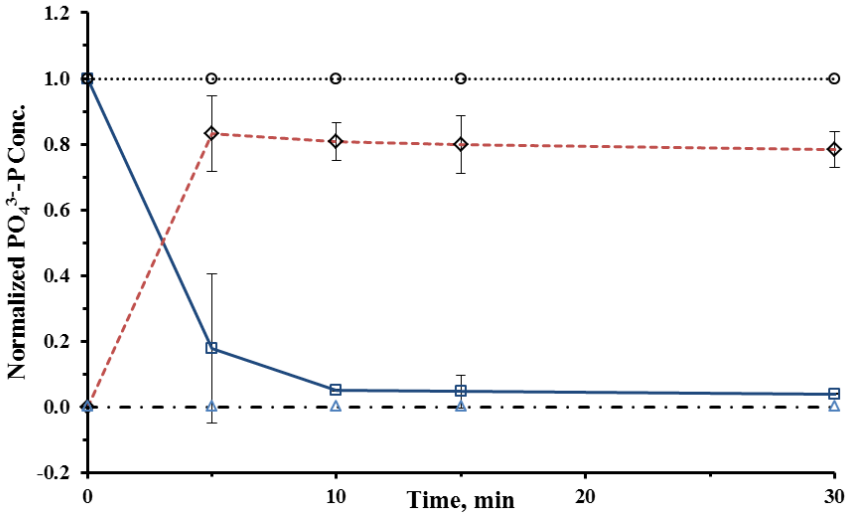

Figure 2.8: Phosphate removal and recovery using NZVI (Removal, Blank in removal experiment (PO_4^{3-} solution), Recovery, Control in recovery experiment (pH adjusted DI water + fresh NZVI)). NZVI = 400 mg/L, Initial PO_4^{3-}-P = 5 mg/L. Control for the removal experiment was DI water with NZVI; no phosphate was detected in the sample, and the data points coincided with the control for the recovery experiment

2.5. Environmental Significance

Phosphate removal using NZVI has potential applications in wastewater treatment plants, where phosphate removal is otherwise not very efficient. The speed of phosphate removal using NZVI (88-95% removal in the first 10 min) gives the nanoparticles an advantage over other sorbents. The high speed of phosphate removal by NZVI can be used to engineer a commercially viable treatment process with low detention time and minimal infrastructure. More research is needed to optimize the recovery of phosphate from NZVI as pH 12 may not be a practical value from economic and hazard perspectives.

2.6. Conclusions

Results from the batch studies conducted during this study demonstrate the effectiveness of NZVI for phosphate removal and recovery with different initial phosphate concentrations (1, 5, 10 mg PO_4^{3-}-P/L). Phosphate removal of 88-95% was achieved in the first 10 min itself and 96-100% removal was achieved after 30 min. Increase in phosphate removal efficiency improved with the increase in initial NZVI concentration use and followed a linear trend ($R^2 = 0.9539$). When the initial NZVI concentration was increased from 80 to 560 mg/L, the removal of phosphate increased by ~78% ($C_0 = 5$ mg/L). Little interference was observed in phosphate removal due to ionic strength and temperature change. Sulfate and natural organic matters had statistically significant negative impacts but nitrate marginally improved phosphate removal. The phosphate removal efficiency was also not affected by high concentrations of humic acid. Phosphate sorbed onto NZVI was successfully recovered (~78%). The phosphate recovery process was found to be pH dependent with maximum recovery achieved at pH 12.

2.7. References

Ahn YH, Speece RE (2006) Waste lime as a potential cation source in the phosphate crystallization process. Environ Technol 27:1225-1231.

Antelo J, Arce F, Avena M, Fiol S, Lopez R, Macias F (2007) Adsorption of a soil humic acid at the surface of goethite and its competitive interaction with phosphate. Geoderma 138:12-19.

Babatunde AO, Zhao YQ (2010) Equilibrium and kinetic analysis of phosphorus adsorption from aqueous solution using waste alum sludge. J Hazard Mater 184:746-752.

Bezbaruah AN, Krajangpan S, Chisholm BJ, Khan E, Bermudez JJE (2009) Entrapment of iron nanoparticles in calcium alginate beads for groundwater remediation applications. J Hazard Mater 166:1339-1343.

Bezbaruah AN, Shanbhogue SS, Simsek S, Khan EE (2011) Encapsulation of iron nanoparticles in alginate biopolymer for trichloroethylene remediation J Nanopart Res 13:6673–6681.

Caravelli AH, Contreras EM, Zaritzky NE (2010) Phosphorous removal in batch systems using ferric chloride in the presence of activated sludges. J Hazard Mater 177:199-208.

Chen JW, Xiu ZM, Lowry GV, Alvarez PJJ (2011) Effect of natural organic matter on toxicity and reactivity of nano-scale zero-valent iron. Water Res 45:1995-2001.

Chitrakar R, Tezuka S, Sonoda A, Sakane K, Ooi K, Hirotsu T (2006) Phosphate adsorption on synthetic goethite and akaganeite. J Colloid Interf Sci 298:602-608.

Cleary J, Slater C, Diamond D (2009) Analysis of Phosphate in Wastewater Using an Autonomous Microfluidics-Based Analyser. World Academy of Science, Engineering and Technology 52:196-199

Cordray A (2008) Phosphorus removal characteristics on biogenic ferrous iron oxides. Master's Thesis, Washington State University, USA

Cordell D, Drangert JO, White S (2009) The story of phosphorus: Global food security and food for thought. Glob Environ Change-Human Policy Dimens 19:292-305.

Cordell D, Rosemarin A, Schroder JJ, Smit AL (2011) Towards global phosphorus security: A systems framework for phosphorus recovery and reuse options. Chemosphere 84:747-758.

Cornel P, Schaum C (2009) Phosphorus recovery from wastewater: needs, technologies and costs. Water Sci Technol 59:1069-1076.

Das J, Patra BS, Baliarsingh N, Parida KM (2006) Adsorption of phosphate by layered double hydroxides in aqueous solutions. Appl Clay Sci 32:252-260. doi

de-Bashan LE, Bashan Y (2004) Recent advances in removing phosphorus from wastewater and its future use as fertilizer (1997-2003). Water Res 38:4222-4246.

Eaton AD, Franson MAH, Association AWW, Federation WE (2005) Standard methods for the :10.1016/j.clay.2006.02.005examination of water and wastewate. 21st ed. American Public Health Association, Washington, DC, USA

Giasuddin ABM, Kanel SR, Choi H (2007) Adsorption of humic acid onto nanoscale zerovalent iron and its effect on arsenic removal. Environ Sci Technol 41:2022-2027.

Gouider M, Mlaik N, Feki M, Sayadi S (2011) Integrated Physicochemical and Biological Treatment Process for Fluoride and Phosphorus Removal from Fertilizer Plant Wastewater. Water Environ Res 83:731-738.

Guo CH, Stabnikov V, Kuang SL, Ivanov V (2009) The removal of phosphate from wastewater using anoxic reduction of iron ore in the rotating reactor. Biochem Eng J 46:223-226.

Huang KC, Ehrman SH (2007) Synthesis of iron nanoparticles via chemical reduction with palladium ion seeds. Langmuir 23:1419-1426.

Hussain S, Aziz HA, Isa MH, Ahmad A, Van Leeuwen J, Zou L, Beecham S, Umar M (2011) Orthophosphate removal from domestic wastewater using limestone and granular activated carbon. Desalination 271:265-272.

Hwang YH, Kim DG, Shin HS (2011) Mechanism study of nitrate reduction by nano zero valent iron. J Hazard Mater 185:1513-1521.

Kanel SR, Manning B, Charlet L, Choi H (2005) Removal of arsenic(III) from groundwater by nanoscale zero-valent iron. Environ Sci Technol 39:1291-1298.

Karageorgiou K, Paschalis M, Anastassakis GN (2007) Removal of phosphate species from solution by adsorption onto calcite used as natural adsorbent. J Hazard Mater 139:447-452.

Klimkova S, Cernik M, Lacinova L, Filip J, Jancik D, Zboril R (2011) Zero-valent iron nanoparticles in treatment of acid mine water from in situ uranium leaching. Chemosphere 82:1178-1184.

Li XQ, Elliott DW, Zhang WX (2006) Zero-valent iron nanoparticles for abatement of environmental pollutants: Materials and engineering aspects. Crit Rev Solid State 31:111-122.

Li ZQ, Greden K, Alvarez PJJ, Gregory KB, Lowry GV (2010) Adsorbed Polymer and NOM Limits Adhesion and Toxicity of Nano Scale Zerovalent Iron to E. coli. Environ Sci Technol 44:3462-3467.

Liu J, Wan L, Zhang L, Zhou Q (2011) Effect of pH, ionic strength, temperature on the phosphate adsorption onto lanthanum-doped activated carbon fiber. J Colloid Interf Sci 364:490-496.

Mezenner NY, Bensmaili A (2009) Kinetics and thermodynamic study of phosphate adsorption on iron hydroxide-eggshell waste. Chem Eng J 147:87-96.

Mishra SP, Das M, Dash UN (2010) Review on adverse effects of water contaminants like arsenic, fluoride and phosphate and their remediation. J Sci Ind Res 69:249-253

Penn CJ, Warren JG (2009) Investigating Phosphorus Sorption onto Kaolinite Using Isothermal Titration Calorimetry. Soil Sci Soc Am J 73:560-568.

Saha B, Griffin L, Blunden H (2010) Adsorptive separation of phosphate oxyanion from aqueous solution using an inorganic adsorbent. Environ Geochem Hlth 32:341-347.

Scott TB, Popescu IC, Crane RA, Noubactep C (2011) Nano-scale metallic iron for the treatment of solutions containing multiple inorganic contaminants. J Hazard Mater 186:280:287.

Shuai XF, Zinati G (2009) Proton Charge and Adsorption of Humic Acid and Phosphate on Goethite. Sci Soc Am J 73:2013-2020.

Simeoni MA, Batts BD, McRae C (2003) Effect of groundwater fulvic acid on the adsorption of arsenate by ferrihydrite and gibbsite. Appl Geochem 18:1507-1515.

Tchobanoglous G, Burton FL, Stensel HD, Metcalf & Eddy (2003) Wastewater engineering: treatment and reuse. 4th ed. McGraw-Hill, New York, NY, USA

Thompson JM, Chisholm BJ, Bezbaruah AN (2010) Reductive Dechlorination of Chloroacetanilide Herbicide (Alachlor) Using Zero-Valent Iron Nanoparticles. Environ Eng Sci 27:227-232.

USEPA (1995) Ecological Restoration: A Tool to Manage Stream Quality, Report EPA 841-F-95-007, US EPA, Washington, DC, USA

Xi YF, Mallavarapu M, Naidu R (2010) Reduction and adsorption of Pb(2+) in aqueous solution by nano-zero-valent iron-A SEM, TEM and XPS study. Mater Res Bull 45:1361-1367.

Xiong JB, He ZL, Mahmood Q, Liu D, Yang X, Islam E (2008) Phosphate removal from solution using steel slag through magnetic separation. J Hazard Mater 152:211-215.

Xue YJ, Hou HB, Zhu SJ (2009) Characteristics and mechanisms of phosphate adsorption onto basic oxygen furnace slag. J Hazard Mater 162:973-980.

Yan LG, Xu YY, Yu HQ, Xin XD, Wei Q, Du B (2010) Adsorption of phosphate from aqueous solution by hydroxy-aluminum, hydroxy-iron and hydroxy-iron-aluminum pillared bentonites. J Hazard Mater 179:244-250.

Yan WL, Herzing AA, Kiely CJ, Zhang WX (2010) Nanoscale zero-valent iron (nZVI): Aspects of the core-shell structure and reactions with inorganic species in water. J Contam Hydrol 118:96-104.

Yue QY, Zhao YQ, Li Q, Li WH, Gao BY, Han SX, Qi YF, Yu H (2010) Research on the characteristics of red mud granular adsorbents (RMGA) for phosphate removal. J Hazard Mater 176:741-748.

Zeng L, Li XM, Liu JD (2004) Adsorptive removal of phosphate from aqueous solutions using iron oxide tailings. Water Res 38:1318-1326.

CHAPTER 3. AQUEOUS PHOSPHATE REMOVAL USING IRON CROSS-LINKED ALGINATE

3.1. Abstract

Iron (II) corss-linked alginate (FCA) biopolymer was synthesized and investigated for phosphate removal. Phosphate was completely removed from water using the FCA beads in 12 h (C_0 = 5 mg PO_4^{3-}–P/L). The second order reaction model fitted well for the reaction and reaction rate constants were found to be 0.771 and 2×10^{-4} per h for 5 and 100 mg PO_4^{3-}-P/L, respectively. Interference of Cl^-, HCO_3^-, SO_4^{2-}, NO_3^- and natural organic matter (NOM) were investigated and no change in the removal efficiency of phosphate was observed. Maximum adsorption capacity was calculated as 14.77 mg/g of dry beads, and the experimental data were found to most closely fit Freundlich isotherm (R^2 = 0.9078). On electron microscopic examination, nanoparticles with average size of 83.65±42.83 (n = 67) were observed inside the beads. For comparison purposes calcium cross-linked alginate entrapped NZVI (NCC) beads were also prepared. The NCC beads had a relatively very low phosphate removal rate and could completely remove PO_4^{3-} after ~24 h (C_0 = 5 mg PO_4^{3-}–P/L) while FCA beads removed 100% PO_4^{3-} in 12 h. Calcium cross-liked beads (CC) (with no form of iron) could also removed PO_4^{3-} to a great extent 88%, however they were saturated after ~8 h. The presence of iron increased the phosphate removal efficiency of NCC and FCA beads. Removal efficiency of PO_4^{3-} by FCA beads was not affected when pH was changed (4- 9). Column studies using 15 and 30 PO_4^{3-}-P/L showed sharp decrease of phosphate removal efficiency from 99 to 57% after 4 bed volume for the higher concentration. In the case of lower phosphate concentration (15 mg PO_4^{3-}–P/L), the removal decreased gradually (only about 5% in the first 6 bed volumes).

Keywords: Iron nanoparticles, Phosphate removal, Phosphate recovery, Adsorption, Alginate, Iron cross-link

3.2. Introduction

While phosphorus (P) is essential for plant growth, excess P concentration (>1.0 mg/L P) in water bodies causes eutrophication of aquatic ecosystems resulting in deterioration of water quality (Smith 2003). Therefore, it is important to reduce P concentrations in water to improve water quality. On the other hand, with an increasing world population the demand of P for food production is estimated to peak sometime between 2030 and 2040 (Ashley et al., 2011), and it is imperative that P demand is met. While there is no opportunity to increase P supply from conventional sources (i.e., mining), alternative sources are worth exploring. Municipal wastewater, runoff from animal feedlot, agricultural runoff, and eutrophic lakes rich in phosphates can serve as nonconventional 'mines' for P. The phosphates present in these aquatic sources are otherwise considered pollutants (causing eutrophication). Mining phosphates from these sources will, thus, offer viable solutions to both pollution and global food security issues.

The most common forms of P present in aqueous environments are orthophosphates, polyphosphates and organic phosphates (Mezenner and Bensmaili 2009). Orthophosphate is the most readily removable forms of phosphate. Physical, chemical, biological and combination of these methods have been utilized to remove phosphorus from water (de-Bashan and Bashan 2004; Gouider et al., 2011; Mishra et al., 2010). While most of the methods can remove phosphate to reasonable degree, adsorption is getting more attention in recent years as it is cost effective and the adsorbed phosphate can be recovered under the right environmental conditions. Different adsorbents have been used for aqueous phosphate removal which include oxides of iron, natural ores like calcite, and goethite (FeOOH), active red mud, and activated carbon

(Chitrakar et al., 2006, Cordary 2008, Hussain et al., 2011, Karageorgiou et al., 2007, Yan et al., 2010a-b).

Alginate is a natural polysaccharide extracted from brown seaweed and composed of (1→4)-linked-d-mannuronic acid (M units) and –L-guluronic acid (G units) monomers (Fig. 3.1). In the presence of multivalent cations (e.g., calcium, and iron) the polymer undergoes a sol-gel transition because of the reactive carboxylate groups (Kroll et al., 1996). When alginate react with metal ions it forms stable organic–inorganic hybrid composite. Alginate polymers are widely investigated for water remediation because they are inexpensive, non-toxic, porous, and biodegradable (Bezbaruah et al., 2009, 2011). It has been used as an immobilizing agent for nanoparticles used for water remediation (Bezbaruah et al., 2009, 2011).

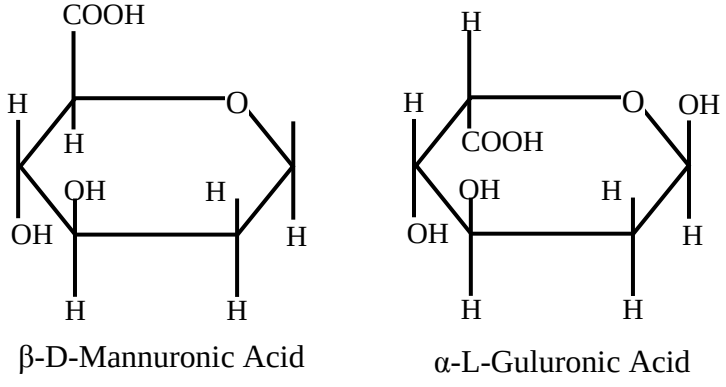

Figure 3.1: Chemical structures for the two monomers present in algiante

Iron [Fe(III)] cross-linked alginate has been used as source of Fe catalyst for Fenton-enhanced decoloration/degradation of Orange II (Fernandez et al., 2000) and azo dyes (Dong et al., 2011). Sreeram et al., (2004) studied the interaction between iron (III) and alginate and suggested 'site binding model' where Fe(III) ions are bound to the binding sites in the alginate forming spatially separated iron(III) centers on the alginate backbone.

The objective of this paper is to synthesize and utilize Fe-cross-linked alginate (FCA) beads for phosphate removal from aqueous solution. The effects of interfering ions on phosphate removal using Fe-cross-linked alginate beads would be investigated as well. The new beads were expected to have high sorption capacity.

3.3. Materials and Methods

3.3.1. Chemicals

Iron (II) chloride tetrahydrate ($FeCl_2 \bullet 4H_2O$, reagent grade, J.T. Baker), calcium chloride ($CaCl_2$, ACS grade, BDH), monopotassium phosphate (KH_2PO_4, 99% pure, EMD), sodium alginate (production grade, Pfaltz & Bauer), potassium nitrate (KNO_3, 99%, Alfa Aesar), sodium hydroxide (NaOH, ACS Grade, BDH), potassium sulfate (K_2SO_4, ACS grade, HACH), natural organic matter (Suwannee River NOM, RO isolation, IHSS), and humic acid (H1452, Spectrum) were used as received unless and otherwise specified.

3.3.2. Alginate beads synthesis

Sodium alginate (20 g) was dissolved in 1L of deionized (DI) water to form a 2% alginate solution. Fe-cross-linked alginate (FCA) beads were synthesized by adding the alginate solution to continuously stirred ferrous chloride ($FeCl_2$) solution (2% w/v) at room temperature (22 ± 2^oC). The alginate solution was added drop wise into $FeCl_2$ solution using a 10-mL disposable plastic syringe (Fig. 3.2). FCA beads were prepared in batches using 5 mL alginate solution in each batch. Alginate beads are formed immediately as the alginate come in contact with the ferrous chloride solution. The beads from each batch were kept separately in a polypropylene vial fitted with a plastic cap. Enough $FeCl_2$ solution was added to each vial to completely submerge the beads, and the beads in the vials were allowed to harden in $FeCl_2$ solution for an additional ~6 h.

Calcium cross-linked alginate (CCA) beads were also synthesized for use in control studies as per Bezbaruah et al., (2009). The hardened beads were then washed with DI water and the excess water is sorbed with tissue papers before using them in experiments. If necessary the beads were stored in $FeCl_2$ solution in 20 mL vials and used in experiments with 24 h.

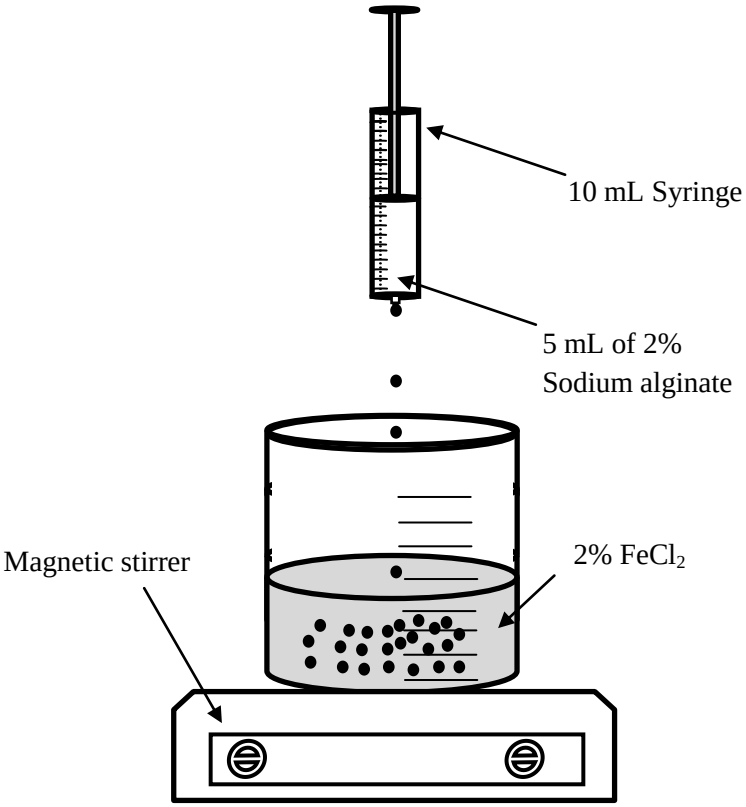

Figure 3.2: Schematic of FCA beads synthesis procedure

3.3.3. Entrapped NZVI beads synthesis

Entrapped NZVI was prepared using method described elsewhere (Bezbaruah et al., 2009), where 20 mg of NZVI was mixed with 5 mL of sodium alginate solution (2% w/v) in a 10 mL syringe. The content in the syringe was stirred vigorously for some time with a glass rod to ensure homogeneity. The NZVI-alginate mixture was then added drop wise into a 2% (w/v) deoxygenated solution of $CaCl_2$ at room temperature. NZVI-Ca-alginate (NCC) beads were

formed as soon as the alginate drops came in contact with the $CaCl_2$ solution. The beads were kept in deoxygenated 2% $CaCl_2$ solution for additional ~6 h for hardening. The beads were then washed with deoxygenated DI water and sorbed the excess water with tissue papers before using them in experiments. If necessary the beads were stored in deoxygenated $CaCl_2$ solution in 20 mL vials (with $CaCl_2$ solution filled in completely to avoid any oxygen transfer) and used in experiments with 24 h.

3.3.4. Batch studies

Kinetic Studies: (**a**) NCC beads: Batch experiments were conducted using NCC beads. Beads produced in a single batch (0.121 g dry alginate and 20 mg NZVI in 50 mL or 2.42 g dry alginate/L and 0.4 g NZVI/L) were added to 50 mL phosphate solution (5 mg PO_4^{3-}-P/L) in multiple polypropylene plastic vials fitted plastic caps (reactors). Controls were run using CCA beads. The reactors and controls were rotated end-over-end at 28 rpm in a custom-made shaker to reduce mass transfer resistance. A set of sacrificial reactors was withdrawn at specific time intervals (0, 0.5, 2, 4, 6, 8, 12, 18, and 24 h). The phosphate concentration in the bulk solution was measured and reported as average (with standard deviations) of readings from three replicates. Ascorbic acid method (Eaton et al., 2005) was used for phosphate analysis. (**b**) FCA beads: Batch experiments were conducted using Fe-cross-linked alginate (FCA) beads (2.42 g dry alginate/L) using the same procedure described above (kinetic studies with CC beads with entrapped NZVI). Blanks (no FCA or CCA beads but only PO_4^{3-} solution) were also run.

Interference Studies: Removal of phosphate in the presence of selected ions as well as natural organic matter (NOM) found in surface waters were tried in batch experiments. Interference studies were carried out with known concentrations of chloride (Cl^-, 50 to 500 mg/L), bicarbonate (HCO_3^-, 10 to 100 mg/L), sulfate (SO_4^{2-}, 50 to 1000 mg/L), nitrate (NO_3^-, 10

to 100 mg/L as NO_3^--N), and Suwanee River NOM (10 to 50 mg/L) using FCA and NCC beads with 5 mg/L of PO_4^{3-} solution. The specific ion or NOM was mixed with the PO_4^{3-} solution in a 50 mL plastic vial and one batch FCA beads was added to it. The reactors were then capped and placed in an end over end shaker (28 rpm) for 24 h. The batch studies were carried out at room temperature (22 ± 2 ˚C) and triplicate reactors were run for each study.

3.3.5. Column studies

Column studies were conducted to simulate a real world application of the FCA beads for PO_4^{3-} removal. Two concentrations of PO_4^{3-} were used in the column studies (15 and 30 mg PO_4^{3-}-P/L) to simulate extreme conditions. Glass columns (height 30 cm and internal diameter 1.5 cm) with an empty bed volume of 53 mL were used. Each column was filled with FCA beads (made with 1.2 grams alginate) and had a packed bed volume of 27 mL. PO_4^{3-} solution was fed in an up-flow mode using a peristaltic pump at a flow rate of ~0.1 mL/min. Samples were collected over time from the effluent point at the top of the column (Fig 3.3) and analyzed for PO_4^{3-} concentration.

3.3.6. Alginate beads characterization

Scanning electron microscopy along with energy dispersive spectroscopy (SEM/EDS, JEOL JSM-6300, JEOL Ltd.) was used to observe surface morphology and characterize the elemental composition of the beads. SEM analyses were performed in a wide beam current range to determine the microstructure of the dry FCA beads before (new FCA beads) and after using them for PO_4^{3-} removal (used FCA beads). New and used beads were dried overnight in a vacuum oven under nitrogen environment, and cross sectional samples of the dry beads were used for imaging and EDS analyses.

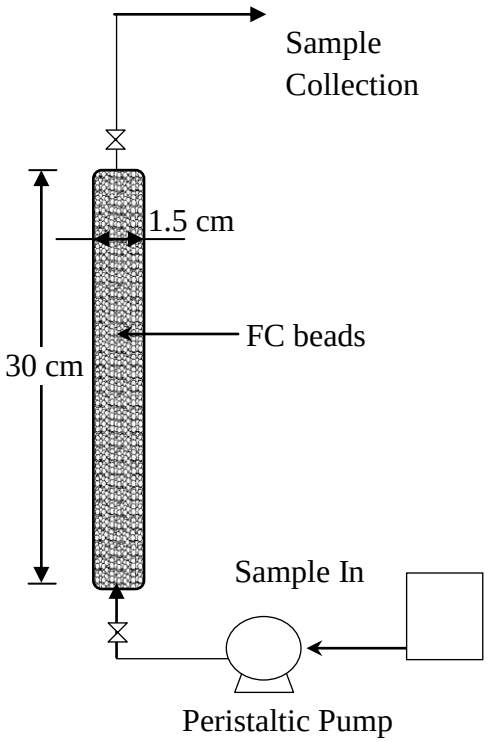

Figure 3.3: Schematic FCA beads column study set-up

3.4. Results and Discussion

3.4.1. Synthesis and characterization of alginate beads

FCA, CCA, and NCC beads were synthesized successfully (Fig. 3.4). All the beads were approximately spherical in shape with average diameters of 3.09±0.16 (FCA), 3.02±0.04 (CCA), and 4.55±0.88 mm (NCC). Similar bead size and shape was reported for NCC by Bezbaruah et al., (2009). Average number of beads produced per batch was 124±4 (n = 5) for FCA and CCA beads and 53±10 (n = 5) for NCC beads. For NCC beads, there was a possibility that some NZVI particles might have been left behind in the syringe and that would result in erroneous interpretations of the results. The loss of NZVI was accounted for by rinsing the syringe with copious amount of deoxygenated DI water and measuring the weight of iron particles in the rinse water as per Bezbaruah et al., (2009). The rinsed iron particles were dried overnight in a vacuum

oven in nitrogen environment. The average amount leftover iron (not entrapped) was found to be 0.0007 g (out of total 0.02 g) which corresponds to an error of 3.5%.

To know the dry weights of the beads, the beads were dried overnight in a vacuum oven in nitrogen environment. Each batch of dry FCA beads weighted 0.121±0.002 g, while dry CCA and NCC beads weighed 0.155±0.025 g and 0.224±0.016 g, respectively.

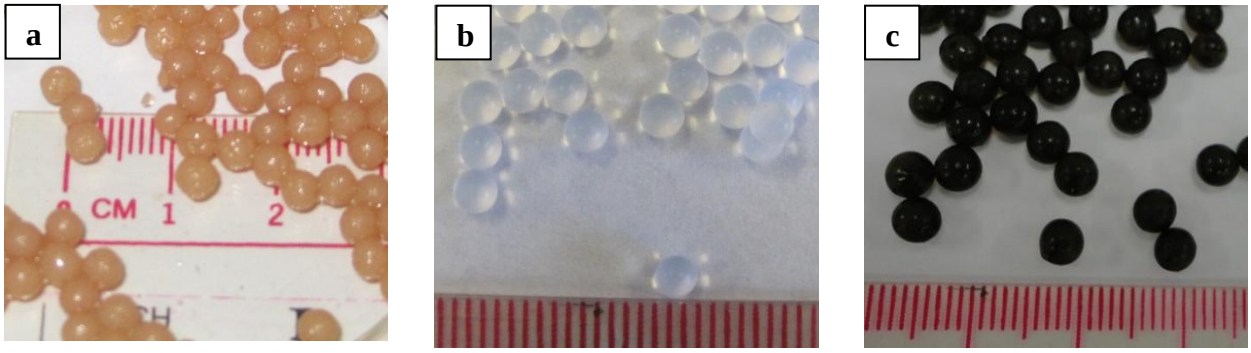

Figure 3.4: Images of the synthesized beads (**a**) Fe-cross-linked alginate (FCA) beads, (**b**) Ca-cross-linked alginate (CCA) beads, and (**c**) NZVI entrapped Calcium cross-linked alginate (NCC) beads

The size of the dry FCA beads was ~1 mm and the dry beads had a uniform hard texture (Fig. 3.5a and b). Nanoparticles with average size of 74.45±35.60 nm (n =97) were observed inside the fresh beads (Fig. 3.5e). The surface morphology of the beads changed completely once phosphate was adsorbed (fresh bead in Fig. 3.5c and used bead in Fig 3.5d). A fragile outer layer was formed around the hard core after phosphate was adsorbed (Fig. 3.5d). The size of nanoparticles increased marginally after phosphate adsorption. The average size of nanoparticles was 83.65±42.83 nm (n=67) inside the used beads (Fig. 3.5f). Nanoparticle size was measured using ImageJ software.

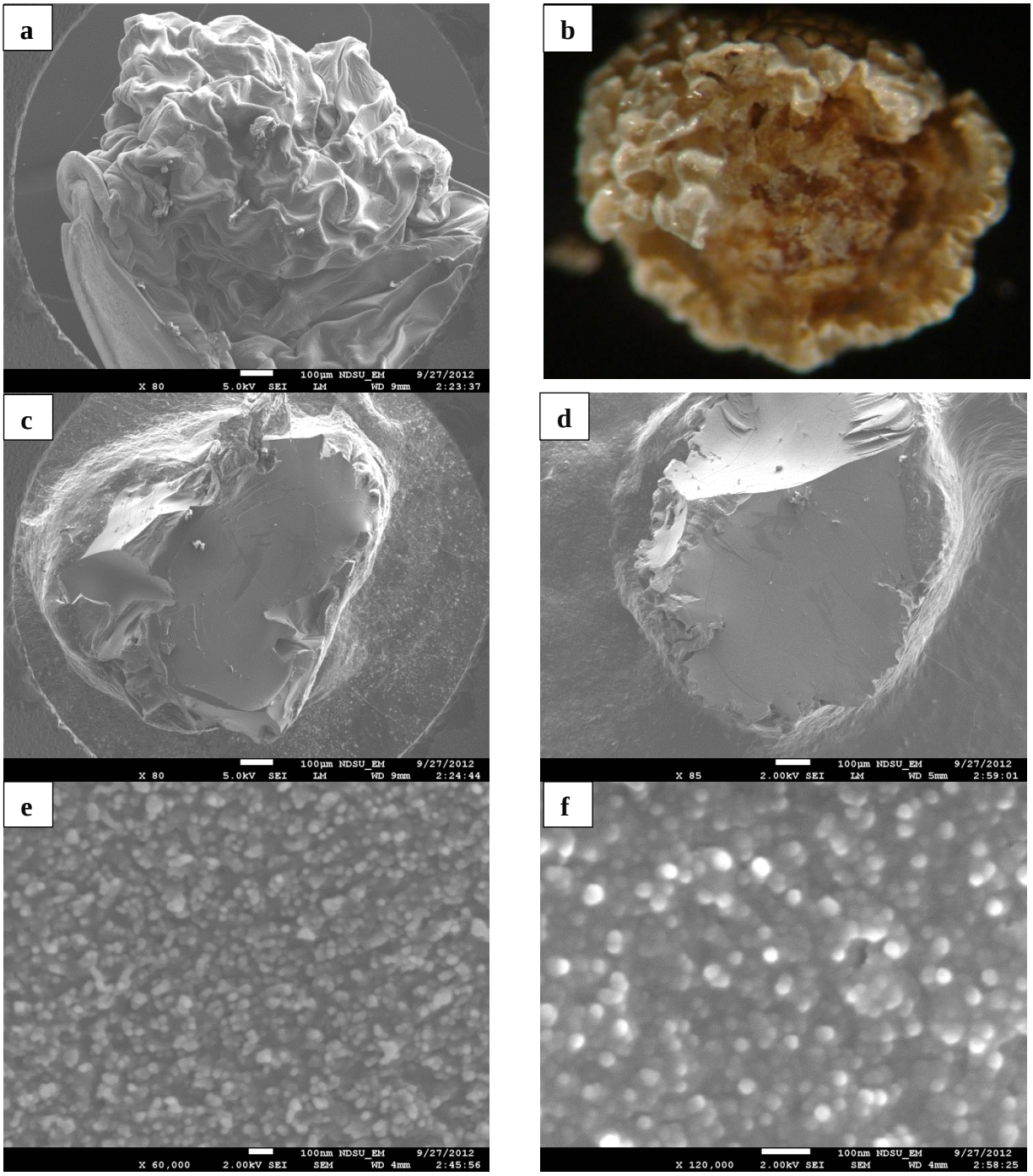

Figure 3.5: (a) SEM image of the surface of a fresh dry FCA bead, **(b)** light microscope image of an used FCA bead, **(c** and **e)** SEM image of the cross-section of the center of a fresh dry FCA bead, **(d** and **f)** SEM image of the cross-section of the center of an used dry FCA bead

EDS analysis of fresh (Fig. 3.6a) and the used beads (Fig 3.6b) revealed a consistent carbon weight % and similar iron weight % except for one point in the fresh beads which

indicates heterogeneous distribution of iron inside the beads. Chloride (~ 30%) present in the fresh beads was not observed in the used beads. It is suspected that the nanoparticles are some form of iron but further investigations are needed to completely characterize the particles.

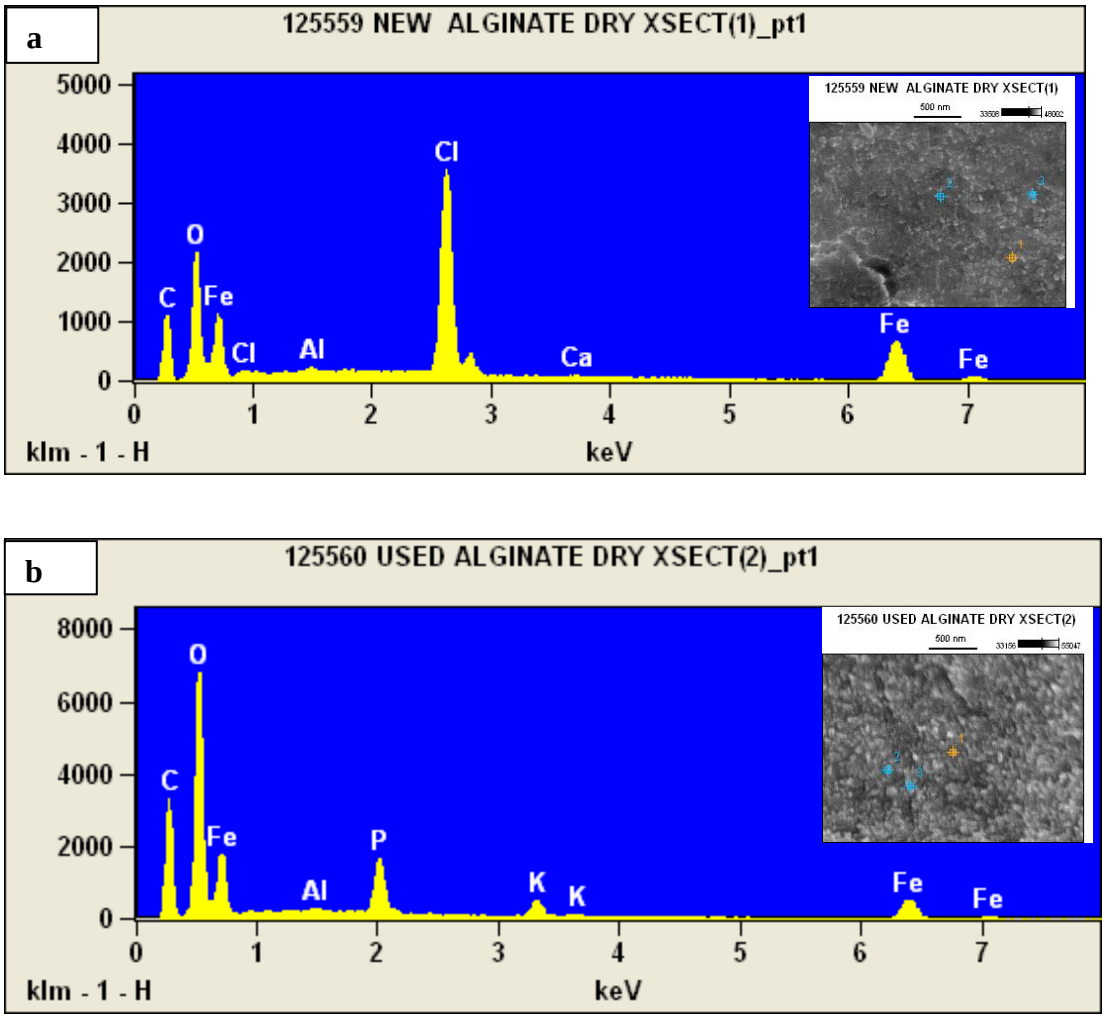

Figure 3.6: (a) EDS spectrum of one point of a freshFCA bead, and **(b)** EDS spectrum of one point of a used FCA bead

3.4.2. Batch Studies

3.4.2.1. Kinetic studies

Batch experiments were conducted to determine the kinetic parameters for PO_4^{3-} removal (C_0 = 5 and 100 mg PO_4^{3-}-P/L) with FCA beads. Zero, first, and second order reaction equations were fitted to determine the type of reaction and reaction rate constants (Fig. 3.7). The second

order reaction model fitted better for both the concentrations and observed reaction rates were found to be 0.771 and 2×10^{-4} per h for 5 and 100 mg PO_4^{3-}-P/L, respectively. Even though complete removal of PO_4^{3-} was observed within ~12 h (Fig 3.8, the curve achieved a plateau after that), a contact time of 24 h was chosen to conduct the rest of the FCA experiments to ensure completion of the reactions

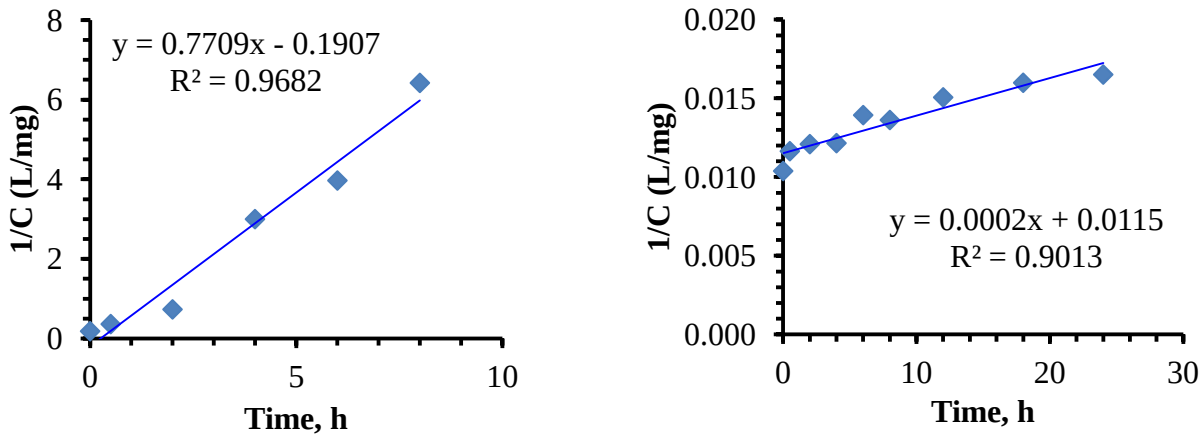

Figure 3.7: Second order reaction rate equations fitted the best for 5 and 100 mg PO_4^{3-}-P/L removal by FCA beads

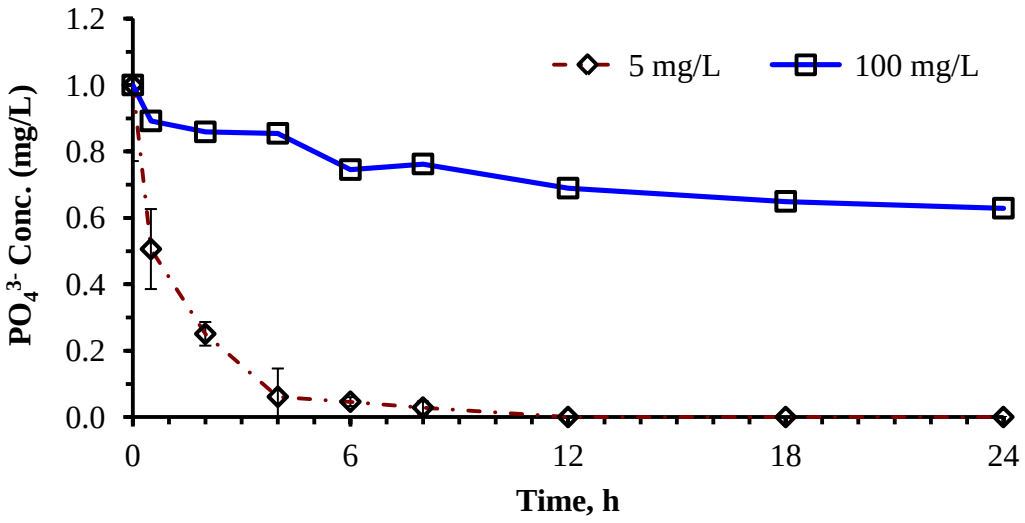

Figure 3.8: Phosphate removal over time using FCA beads, C_0= 5 and 100 mg PO_4^{3-}-P/L

3.4.2.2. Comparison Between bare NZVI, FCA, and NCC

Removal of PO_4^{3-} using FCA, CCA, and NCC beads was compared (Fig. 3.9) in this study while work on bare NZVI has been reported elsewhere (Almeelbi and Bezbaruah, 2012). Bare NZVI particles have high PO_4^{3-} removal rate (96-100 % phosphate in 30 min, Almeelbi and Bezbaruah 2012) but the spent NZVI particles are difficult to be recovered from the environment after PO_4^{3-} sorption has taken place. There are concerns about ecotoxicity of NZVI (El-Temsah and Joner, 2012; Kirschling et al., 2010, Phenrat et al., 2009). Entrapment of NZVI in alginate (NCC beads) allows for better post-use collection of NZVI. NCC beads had a relatively low removal rate and could completely remove PO_4^{3-} after ~24 h. However, FCA beads removed PO_4^{3-} faster and achieved 100% removal at ~12 h. It is important to note that CC beads (with no form of iron) could sorb PO_4^{3-} to a great extent 88% but was saturated after ~8 h. The presence of iron increased the removal efficiency in case of NCC and FCA beads (Table 3.1).

Table 3.1: Reaction rate constants calculated based on the obtained results

	C_o	**C_e**	**Equilibrium time**	**Zero Order**		**First Order**		**Second Order**	
	---mg/L---		h	K_{obs} *	R^2	K_{obs} **	R^2	K_{obs} ***	R
FCA	5	0	12	0.5402	0.6728	0.4369	0.931	0.7709	0.9682
CC	5	0.72	8	0.1344	0.4115	0.0741	0.5791	0.0578	0.7914
NCC	5	0	24	0.1987	0.4295	0.1349	0.7766	0.1633	0.9868
Bare NZVI#	5	0	2	4.06	0.3487	2.3633	0.4044	3.3441	0.5443

* mg/L/min; ** per min; *** L/mg/min; # Based on data presented in Almeelbi and Bezbaruah (2012).

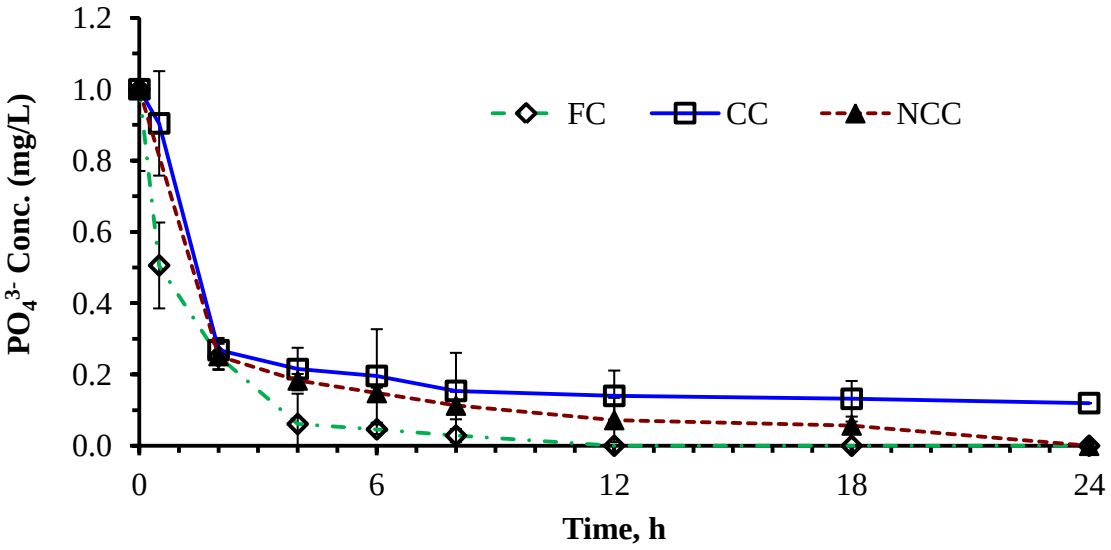

Figure 3.9: Phosphate removal using FCA, CCA, and NCC beads, C_0= 5 mg PO_4^{3-}-P/L

3.4.2.3. Effect of interfering ions

Effect of the presence of Cl^-, HCO_3^-, SO_4^{2-}, NO_3^- and NOM on PO_4^{3-} (C_0 = 5 mg PO_4^{3-}-P/L) removal efficiency of FCA beads was examined. No interference in the removal of PO_4^{3-} was observed because of the presence of these ions (Table 3.2). The ions used in this interference study are usually present in wastewater, surface water, and groundwater. Lee et al., (2011) reported a 78% reduction in PO_4^{3-} removal by slag microspheres in the presence of HCO_3^-.The addition of SO_4^{2-} was reported to decrease the PO_4^{3-} removal efficiency by ~60% in a polymer-based nanosized hydrated ferric oxides system (Pan et al., 2009), and the efficiency reduction was 24.5 % when layered double hydroxides were used (Das et al., 2006). SO_4^{2-} and Cl^- were found have a negative impact on PO_4^{3-}reomval from lake water using high gradient magnetic separation (Vicente et al., 2011). In the presence of NO_3^-, PO_4^{3-} removal decreased by 29.2% while using layered double hydroxides (Das et al., 2006) and by 6.27% while using NZVI (Almeelbi and Bezbaruah, 2012). NOMs are present in surface waters, and known to interfere with PO_4^{3-} removal in adsorption processes (Guan et al., 2006, Vicente et al., 2008). However,

no effect of NOM on PO_4^{3-} removal was observed in this study. Similar findings were reported earlier with bare NZVI (Almeelbi and Bezbaruah, 2012). The lack of interference by the dominant ions and NOM makes an FCA bead system a potential candidate for field application for PO_4^{3-} removal.

Table 3.2: Phosphate removal percentages in the presence of different concentration of interfering ions, C0=5 mg/L, contact time= 24 h

Ion	Concentration, mg/L	% Phosphate Removal
SO_4^{2-}	50	100
	100	100
	1000	99.3
NO_3^-	10	100
	50	99.3
	100	99.7
HCO_3^-	5	100
	10	99
	50	99.5
Cl^-	50	100
	100	98
	1000	99.7
NOM	5	100
	10	100
	50	100

3.4.2.4. Isotherm studies

A set of experiments were conducted to understand the isotherm behavior of the FCA beads during PO_4^{3-} removal. One batch of FCA beads was used in each batch reactor and PO_4^{3-} in the bulk solution was analyzed after 24 h to calculate the sorption capacity of FCA beads (Eq. 3.1). Initial concentration of phosphate was varied from 5 to 100 mg/L.

$$q = \frac{(C_0 - C_e) \times V}{m} \tag{3.1}$$

Where q is the unit mass (mg) of PO_4^{3-}-P per g of dry FCA bead, C_0 and C_e are the initial and equilibrium concentrations of PO_4^{3-}-P in mg/L, V is the volume of PO_4^{3-} solution in mL and m is mass of dry FCA beads in g.

Freundlich isotherm was found to most closely fit with experimental data (R^2 = 0.9078, Fig. 3.10). Maximum adsorption capacity was found to be 14.77 mg/g of dry FCA beads. Others (Chitrakar et al., 2006; Ogata et al., 2011) have reported that Freundlich describes sorption behavior better when dual sobents (alginate and iron in this study) are present. Freundlich isotherm model has been used to describe PO_4^{3-} adsorption behavior onto sulfate-coated zeolite, hydrotalcite, and activated alumina while the adsorption behaviors of the same materials without coating were described better by Langmuir isotherm model (Choi et al., 2012).

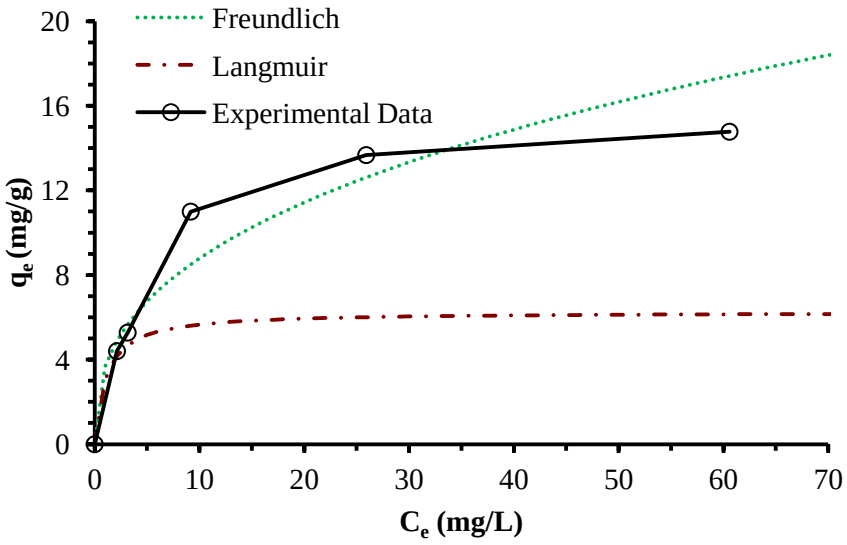

Figure 3.10: Freundlich and Langmuir isotherms models for the PO_4^{3-} removal by FCA beads

3.4.2.5. Effect of pH

The effect of pH on phosphate removal (C_0 = 5 mg PO_4^{3-}-P /L) by FCA was investigated at pH of 4, 7, 8 and 9, and the results were compared with those obtained from similar tests with

bare NZVI (Fig. 3.11). Changing the pH did not affect removal of PO_4^{3-} by FCA beads, and 100% removal was achieved in all pH values. However, PO_4^{3-} removal by bare NZVI was reported decreased with increasing pH as theorized by Almeelbi and Bezbaruah, 2012. The most marked decrease was observed between pH 8 and 9. Removal efficiency of PO_4^{3-} decreased from 84% at pH 8 to 49% at pH 9. It should be noted that the point of zero charge (PZC) for bare NZVI was ~7.7 (Giasuddin et al., 2007). That pH did not affect the PO_4^{3-} removal efficiency of FCA has important practical implications. The pH in eutrophic lakes ranges from 7.5 to 8.5 (Michaud, 1991) and FCA can possibly be used for phosphate removal in eutrophic lakes.

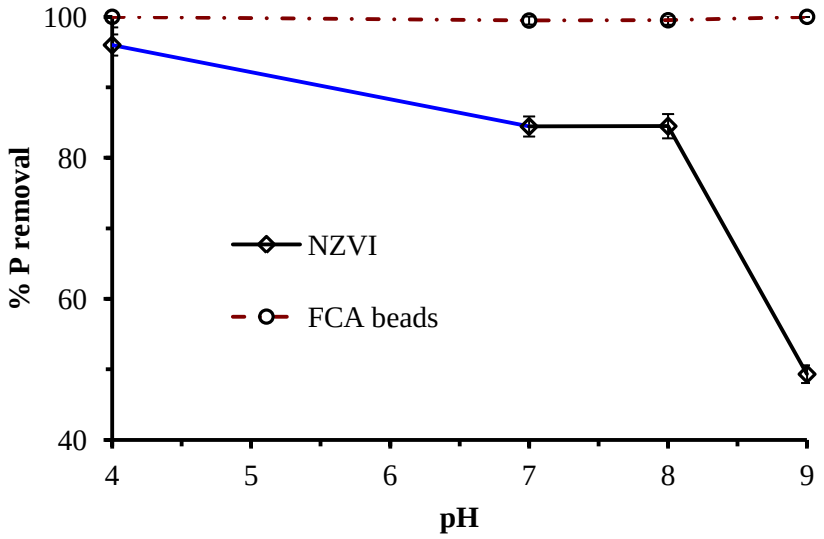

Figure 3.11: PO_4^{3-} removal using FCA beads and NZVI at pH 4, 7, and 9 (C_0 = 5 mg PO_4^{3-}-P/L, Run time = 30 min)

3.4.3. Column studies

Breakthrough behavior in FCA bead columns was studied with 15 and 30 mg PO_4^{3-}-P/L and a flow rate of ~0.1 mL/min. (Fig. 3.12). For the higher concentration (30 mg PO_4^{3-}-P /L), the breakthrough (C_e = 0.05 C_0) was achieved after 2 bed volumes when removal dramatically decreased from 99 to 57%. In the case of the lower concentration (15 mg PO_4^{3-}-P/L) removal

decreased gradually in the first 3 bed volumes (only ~5% decrease). The adsorption capacity increased from 0.97 to 1.81 mg/g of dry beads when initial PO_4^{3-}-P concentration was increased from 15 to 30 mg PO_4^{3-}-P/L which is much lower than the adsorption capacity obtained in batch study (14.77 mg/g of dry FCA beads).

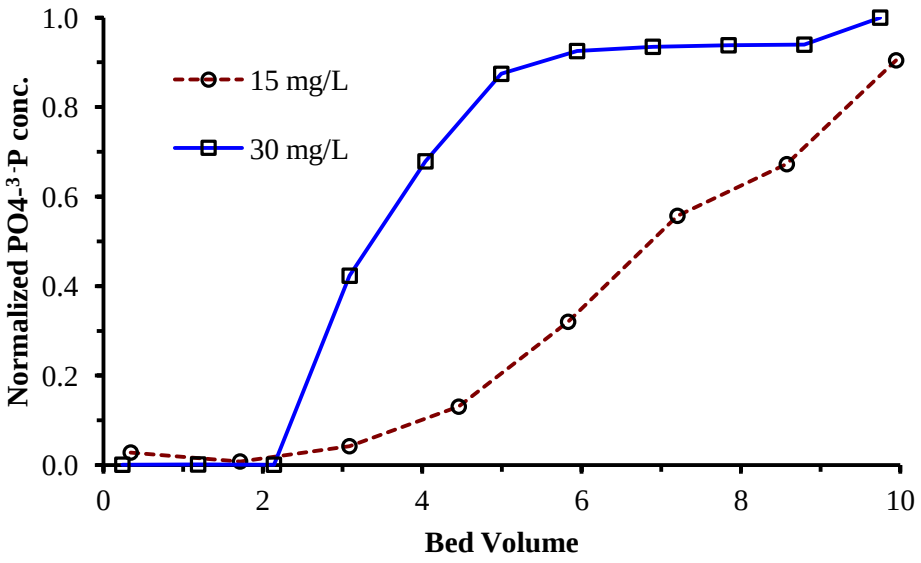

Figure 3.12: FCA bead column study results (C_0= 15 and 30 mg PO_4^{3-}-P/L)

3.5. Conclusions

Ferrous iron cross-linked alginate (FCA) beads were successfully synthesized and utilized for phosphate removal. Complete (100%) removal of aqueous phosphate was achieved after 12 h. The comparison between the three types of alginate based sorptive media (viz., Fe-cross-linked alginate/FCA, Ca-cross-linked alginate/CCA, and NZVI entrapped in Ca-cross-linked alginate/NCC) revealed that FCA media/beads works much better for phosphate removal. Further, there was no interference by Cl^-, HCO_3^-, SO_4^{2-}, NO_3^- and NOM in phosphate removal with FCA beads. Freundlich isotherm could best describe the phosphate sorption behavior of FCA beads. It was inferred (see Fig 3.8) that presence of iron in alginate beads increased the

phosphate removal capacity of the beads. Additional research is needed to find out the techno-economic feasibility of using FCA beads for phosphate removal.

3.6. References

Almeelbi T, Bezbaruah AN (2012) Aqueous phosphate removal using nanoscale zero-valent iron. Journal of Nanoparticle Research, 14(7), 1-14

Ashley K, Cordell D, Mavinic D (2011) A brief history of phosphorus: From the philosopher's stone to nutrient recovery and reuse. Chemosphere 84 (6):737-746.

Bezbaruah AN, Krajangpan S, Chisholm BJ, Khan E, Bermudez JJE (2009) Entrapment of iron nanoparticles in calcium alginate beads for groundwater remediation applications. Journal of Hazardous Materials 166 (2-3):1339-1343.

Bezbaruah AN, Shanbhogue SS, Simsek S, Khan EE (2011) Encapsulation of iron nanoparticles in alginate biopolymer for trichloroethylene remediation Journal of Nanoparticle Research 13:6673–6681.

Chitrakar R, Tezuka S, Sonoda A, Sakane K, Ooi K, Hirotsu T (2006) Phosphate adsorption on synthetic goethite and akaganeite. Journal of Colloid and Interface Science 298 (2):602-608.

Choi JW, Lee SY. Lee SH. Kim JE. Park KY. Kim DJ. Hong SW (2012) Comparison of Surface-Modified Adsorbents for Phosphate Removal in Water. Water Air and Soil Pollution. 223 (6), 2881-2890.

Cordary A (2008) Phosphorus removal characteristics on biogenic ferrous iron oxides. Washington State University, USA, USA

de Vicente I, Merino-Martos A, Guerrero F, Amores V, de Vicente J (2011) Chemical interferences when using high gradient magnetic separation for phosphate removal: Consequences for lake restoration. Journal of Hazardous Materials. 192 (3): 995-1001

de-Bashan LE, Bashan Y (2004) Recent advances in removing phosphorus from wastewater and its future use as fertilizer (1997-2003). Water Research 38 (19):4222-4246.

Dong YC, Dong WJ, Cao YN, Han ZB, Ding ZZ (2011) Preparation and catalytic activity of Fe alginate gel beads for oxidative degradation of azo dyes under visible light irradiation. Catalysis Today 175 (1):346-355.

Eaton AD, Franson MAH, Association AWW, Federation WE (2005) Standard methods for the examination of water and wastewate. 21st edn. American Public Health Association,

El-Temsah YS, Joner EJ, (2012) Ecotoxicological effects on earthworms of fresh and aged nano-sized zero-valent iron (nZVI) in soil. Chemosphere. 89, 76–82.

Fernandez J, Dhananjeyan MR, Kiwi J, Senuma Y, Hilborn J (2000) Evidence for Fenton photoassisted processes mediated by encapsulated Fe ions at biocompatible pH values. Journal of Physical Chemistry B 104 (22):5298-5301. doi:10.1021/jp9943777

Giasuddin ABM, Kanel SR, Choi H (2007) Adsorption of humic acid onto nanoscale zerovalent iron and its effect on arsenic removal. Environ Sci Technol 41:2022-2027.

Goebel TS, McInnes KJ, Senseman SA, Lascano RJ, Marchand LS, Davis TA (2011) Modifying polymer flocculants for the removal of inorganic phosphate from water. Tetrahedron Letters 52 (41):5241-5244.

Gouider M, Mlaik N, Feki M, Sayadi S (2011) Integrated Physicochemical and Biological Treatment Process for Fluoride and Phosphorus Removal from Fertilizer Plant Wastewater. Water Environ Res 83 (8):731-738.

Guan XH, Shang C, Chen GH (2006) Competitive adsorption of organic matter with phosphate on aluminum hydroxide. Journal of Colloid and Interface Science 296 (1):51-58.

Hussain S, Aziz HA, Isa MH, Ahmad A, Van Leeuwen J, Zou L, Beecham S, Umar M (2011) Orthophosphate removal from domestic wastewater using limestone and granular activated carbon. Desalination 271 (1-3):265-272.

Karageorgiou K, Paschalis M, Anastassakis GN (2007) Removal of phosphate species from solution by adsorption onto calcite used as natural adsorbent. Journal of Hazardous Materials 139 (3):447-452.

Kirschling TL, Gregory, KB, Minkley EG, Lowry GV, Tilton RD (2010) Impact of nanoscale zero valent iron on geochemistry and microbial populations in trichloroethylene contaminated aquifer materials. Environ. Sci. Technol. 44, 3474–3480.

Kroll E, Winnik FM, Ziolo RF (1996) In situ preparation of nanocrystalline gamma-Fe2O3 in iron(II) cross-linked alginate gels. Chemistry of Materials 8 (8):1594-1596

Mezenner NY, Bensmaili A (2009) Kinetics and thermodynamic study of phosphate adsorption on iron hydroxide-eggshell waste. Chemical Engineering Journal 147 (2-3):87-96.

Mishra SP, Das M, Dash UN (2010) Review on adverse effects of water contaminants like arsenic, fluoride and phosphate and their remediation. J Sci Ind Res 69 (4):249-253

Ogata T, Morisada S, Oinuma Y, Seida Y, Nakano Y (2011) Preparation of adsorbent for phosphate recovery from aqueous solutions based on condensed tannin gel. Journal of Hazardous Materials 192 (2):698-703.

Pan BJ, Wu J, Pan BC, Lv L, Zhang WM, Xiao LL, Wang XS, Tao XC, Zheng SR (2009) Development of polymer-based nanosized hydrated ferric oxides (HFOs) for enhanced phosphate removal from waste effluents. Water Research 43 (17):4421-4429.

Phenrat, T, Long, TC, Lowry, GV, Veronesi, B (2009). Partial oxidation (‘‘aging’’) and surface modification decrease the toxicity of nanosized zerovalent iron. Environ. Sci. Technol. 43, 195–200.

Sreeram KJ, Shrivastava HY, Nair BU (2004) Studies on the nature of interaction of iron(III) with alginates. Biochimica Et Biophysica Acta-General Subjects 1670 (2):121-125.

CHAPTER 4. IRON NANOPARTICLE-SORBED PHOSPHATE: BIOAVAILABILITY AND IMPACT ON *SPINACIA OLERACEA* AND *SELENASTRUM CAPRICORNUTUM* GROWTH

4.1. Abstract

In this study, nanoscale zero-valent iron (NZVI) particles have been used for phosphate recovery from aqueous solutions. The bioavailability of the sorbed phosphate onto NZVI particles was determined by supplying these particles to Spinach (*Spinacia oleracea*) and algae (*Selenastrum capricornutum*) grown in hydroponic solution. Spent NZVI (particles after phosphate adsoption) were added to the algae growth media as the only source of P and Fe. The concentration of algae increased by 5.7 times when the only source of phosphate was spent NZVI as compared to algae grown in standard all-nutrient media (including phosphate). Again, removing PO_4^{3-} from the growth media decreased the algae concentration 3 fold when compared to algae grown in all-nutrient media. In the spinach study, plant biomass increased in the presence of spent NZVI (where nanoparticles the only source of phosphate) by 4 time than the plant treated with all-nutrient solution. Iron and phosphorus uptakes by plants were determine in the presence of spent NZVI as the only source of P and Fe. Results indicated 20, 11, and 7 times more Fe content in the roots, stems, and leaves of the plant treated with spent NZVI, respectively, as compared to the controls. Amount of P in the biomass also found to be significantly higher in the plants treated with spent NZVI.

Keywords: Iron nanoparticles, Phosphate removal, Phosphate recovery, Adsorption, *Spinacia oleracea*, *Selenastrum capricornutum*, Bioavailability, Eutrophication

4.2. Introduction

Phosphorus (P) is a vital macronutrient for plants. Plants and other organisms mostly uptake dissolved aqueous orthophosphate, and incorporate it into their tissues (Shen et al., 2011). Dissolved organic phosphate (DOP) cannot be used by plants in the organic form. DOP is transformed into orthophosphate due to enzymatic hydrolysis, and is available for plants (Walker, 2012).

Phosphorus is an essential element for food production and there is no substitute for P (Cordell et al 2011). The amount of P in plants ranges from 0.05% to 0.30% of total dry weight. Although P is abundant in the most types of soils, only a tiny fraction is available for plants uptake (Vanec 2011). Low-phosphorus availability for plants has been tackled by addition of phosphate fertilizers to the soil. However, the amount of bioavailability of phosphate is reduced due to chemical immobilization of some of it in soil matrix (Shen et al., 2011). The extensive application of P fertilizers leads to a P buildup in the soil which in turn increases the potential for P loss to surface waters through surface or subsurface run-off. Increase in phosphate concentration in waterbodies leads to eutrophication.

Undesired loss of P and resulting non-point source pollution is only one aspect of the bigger problem. The major issue is the impact of excessive use of fertilizers on global food security given the fact that phosphorus is a nonrenewable resource. Phosphorous fertilizers are produced predominantly from ores from select mines in Morocco, Western Saharan region, and China (Cordell et al., 2009). Phosphorus bearing ore production rate is predicted to decline starting around 2035 (Cordell et al., 2011) the use of P fertilizers will be increasing under the current agriculture practices (Gilbert, 2009). The possible short supply of P fertilizers is a major concern for global food security. While there is no way of increasing the amount of natural

phosphorous supply, the spotlight has been shifted to sustainable practices related to P fertilizers including efficient recover and reuse of phosphates.

Almeelbi and Bezbaruah (2012) reported up to 100 removal rates of phosphate using nanoscale zero-valent iron (NZVI) particles and found them to be more efficient than larger size particles. Others have used iron oxide nanoparticles to remove (70-90%) phosphate (Jianbo et al., 2013; Martin et al., 2009; Pan et al., 2009; Zach-Maor et al., 2011). Phosphate removal by NZVI and iron oxide nanoparticles is known to be a sorptive process and the sorbed phosphate remains in the nanoparticles. It was hypothesized in this research that the sorbed phosphate would be bioavailable to plants.

Selenastrum capricornutum is a group of common green algae (Chlorophyceae) found in most fresh waters. It is readily available from suppliers and can be easily cultured, and, hence, has been widely used in the laboratory for growth inhibition and standard toxicity studies (Abouwaly et al., 1991; Brown and Button, 1979; Scherfig and Dixon, 1979; Errécalde and Campbell 2000; Francko, 1989; ISO 8692, 1989, Hall and Golding, 1998; Gutierrez-Wing et al., 2012). Higher plants like *Allium cepa* (onion bulbs) *Lolium perenne* (ryegrass), *Cucurbita pepo* (zucchini), *Cucurbita mixta* (pumpkin), and others in hydroponic systems have been used by others for growth studies (Ghodake et al , 2011; Lin and Xing, 2008; Stampoulis et al., 2009; Wang et al., 2011).

The objective of this research was to examine bioavailability of phosphate from spent NZVI (used for phosphate removal) using *Selenastrum capricornutum* and *Spinacia oleracea* (Spinach).

4.3. Materials and Methods

4.3.1. Chemicals

Chemicals (Table 4.1) were used as received unless and otherwise specified.

4.3.2. Synthesis and preparation of iron nanoparticles

NZVI Synthesis: NZVI particles were synthesized using sodium borohydride reduction method (Eq. 1, Huang and Ehrman 2007; Almeelbi and Bezbaruah, 2012).

$$2FeCl_3 + 6NaBH_4 + 18H_2O \rightarrow 2Fe^0 + 21H_2 + 6B(OH)_3 + 6NaCl \quad (4.1)$$

Ferric chloride hydrate (1.35 g) was dissolved in 40 mL of deoxygenated de-ionized (DI) water (solution A), and 0.95 g of sodium borohydride was dissolved in 10 mL of deoxygenated DI water in a separate beaker (solution B). Then solution A was added drop wise to solution B under vigorous stirring conditions (using a magnetic stirrer). The resultant black precipitates (NZVI) were centrifuged and washed with copious amount of deoxygenated DI water and methanol (Almeelbi and Bezbaruah, 2012) to remove the undesired chemicals. The washed NZVI were dried in vacuum oven under nitrogen environment and then were ground using a mortar and pestle.

Phosphate adsorption: NZVI (20 mg) was added to phosphate solution (50 mL of 100 mg PO_4^{3-}-P /L) in multiple 50 mL polypropylene plastic vials fitted plastic caps (reactors). The concentration of 100 mg/L for phosphate was decided based adsorption capacity studies (Appendix 4.A). The reactors were rotated end-over-end at 28 rpm in a custom-made shaker for 24 h and then content was centrifuged at 4000 rpm. The supernatant was collected for phosphate analysis. Ascorbic acid method (Eaton et al., 2005) was used for phosphate analysis. The precipitated iron particles were dried in vacuum oven under nitrogen environment and ground

using mortar and pestle. Others have reported that phosphate gets sorbed on NZVI (Almeelbi and Bezbaruah, 2012). The dried particles were characterized using X-ray photoelectron spectroscopy (XPS) and Energy Dispersive X-Ray Spectrometer (EDS). The dried particles were used in algae and plants growth studies.

Table 4.1: List of chemicals used in this study

Chemical Formula	Chemical Name	Supplier	Grade/Purity
NaOH	Sodium Hydroxide	BDH	ACS
$Ca(NO_3)_2 \cdot 4H_2O$	Calcium Nitrate Tetrahydrate	BDH	ACS
KNO_3	Potassium nitrate	Alfa Aesar	99%
KH_2PO_4	Potassium Phosphate Monobasic	BDH	ACS
$MgSO_4$	Magnesium Sulfate	Aldrich	+97%
K_2SiO_3	Potassium Silicate	Alfa Aesar	>99%
$FeCl_3 \cdot 6H_2O$	Iron(III) Chloride Hexahydrate	Mallinckrodt	ACS
$MnSO_4 \cdot 4H_2O$	Manganese Sulfate	Alfa Aesar	99%
$CuSO_4$	Copper(II) Sulfate	Alfa Aesar	99%
$ZnSO_4$	Zinc Sulfate Heptahydrate	Alfa Aesar	ACS
H_3BO_3	Boric Acid	Alfa Aesar	ACS
$Na_2MoO_4 \cdot 2H_2O$	Sodium Molybdate Dihydrate	J.T. Baker	ACS
HNO_3	Nitric Acid	BDH	ACS
$NaNO_3$	Sodium Nitrate	Fluka	>99%
$CaCl_2 \cdot 2H_2O$	Calcium Chloride Dihydrate	BDH	ACS
K_2HPO_4	Potassium Phosphate Dibasic	BDH	ACS
NaCl	Sodium Chloride	EMD	ACS

4.3.3. Algae studies

All glassware were washed with phosphate-free detergent and rinsed thoroughly with tap water, soaked in acid bath (10% HCl) overnight, rinsed with deionized (DI) water, and autoclaved for ~20 minute before use.

Cultivation of Algae: *S. capricornutum* (UTEX 1648) was obtained from the University of Texas Culture Collection (Austin, TX, USA) (UTEX, 2012). Erlenmeyer flask of 500 mL (nursery reactors) was used to culture the algal in liquid Bristol medium (Table 2). The culture was aerated and illuminated with cool-white fluorescent light on a 12-h light and 12-h dark cycle at room temperature (22±2.0^{o}C). The light intensity was 3.17 log Lum m^{-2} (HOBO U12-012 temp/RH/light external data logger, Onset Computer Corporation, Bourne, MA, USA).

Exponential growth phase was maintained as per the supplier's instructions through repetitive subculturing with freshly prepared medium every 4 days.

Growth Studies: Glass bottles (500 mL) were used as reactors, and 400 mL of different growth media and 5 mL of algae seed (*S. capricornutum*) obtained from the laboratory culture (see 'Cultivation of Algae' above) were added to the reactor. The algae were incubated for 28 days in the reactors illuminated with cool-white fluorescent light. During the incubation period, the reactors were manually shaken and aerated for 10 min once every day to maintain aerobic conditions. Five different growth nutrient solutions were used and algae growth was measured at the end of the test period. Each experiment was repeated three times. The five nutrient solutions used were: (1) Only DI water, (2) Bristol medium (Table 4. 2, no virgin NZVI added), (3) Bristol medium with virgin NZVI, (4) Bristol medium without PO_4^{3-} (no NZVI), and (5) Bristol medium without PO_4^{3-} but with spent NZVI. The only DI water (nutrient solution 1) was used to check whether residual nutrients from the laboratory algae culture were affecting algae growth. Additional nutrients (from the stock solution) were and nanoparticles are added once every week. Samples (10 mL) were collected from each reactor for biomass analysis after 28 days and analysis were preformed immediately.

4.3.4. Spinach studies

Germination and Plant Preparation: Spinach (Tyee spinach, *Spinacia oleracea*, Lake Valley Seed Company, Bolder, CO) seed was purchased from a local outlet. Seeds were washed then soaked in DI water over night. The seeds were then placed on moist filters paper in petri-dishes and kept in the dark at room temperature until germination. The germinated seeds were planted on sand in a glass tray. Nutrients solution (Table 4.3) was added to the growth media

(sand) everyday and the plants were illuminated with cool-white fluorescent light (12-h light and 12-h dark). The light intensity was 3.17 log Lum m^{-2}.

Table 4.2: Composition of Bristol media used for algae growth (Source: UTEX, 2012)

Salt	Stock Solution g/400mL DI H_2O	Volume used mL/L	Molar Conc. used mM
$NaNO_3$	10	10	2.94
$CaCl_2 \cdot 2H_2O$	1	10	0.17
$MgSO_4 \cdot 7H_2O$	3	10	0.3
K_2HPO_4	3	10	0.43
KH_2PO_4	7	10	1.29
NaCl	1	10	0.43

Table 4.3: Composition of hydroponic growth nutrient solution (USU, 2012)

Salt	Stock solution Conc. mM	Starter	Pre-anthesis	Post-anthesis
		---------- mL/10 L ----------		
$Ca(NO_3)$	1000	10	10	5
$K(NO_3)$	1000	10	40	20
KH_2PO_4	500	10	10	10
$MgSO_4$	500	10	10	5
K_2SiO_3	100	10	10	0
$FeCl_3$	50	2	0.5	0.5
$MnSO_4$	60	0.5	1	0.5
$CuSO_4$	2 0	1.5	1	1
$ZnSO_4$	20	3	1.5	1.5
H_3BO_3	40	0.5	0.25	0.1
Na_2MoO_4	1	1	0.5	0.5
HNO_3	1000	0.5	0.5	0.5

Growth Studies: After 5 days (during the early stage of stem and leaf formation) the seedlings were removed from the sand media, roots were thoroughly washed with DI water, and transplanted into hydroponic reactors (Figure 4.1 and 4.2). Plastic containers (2 L nutrient solution) were used for hydroponic culture. Three plants were placed into a foam disk float with the shoots supported above with non-absorbent cotton and roots below the disk (Jacob et al., 2013). The floats with the plants were then placed in the reactors. The arrangement of putting the plants in the floats ensured continuous root contact with the nutrient solution. The nutrient solution was aerated constantly with air throughout the experiment and the solution was replaced

every 4 days. Light was provided in 14-h light 10-h dark cycles with cool white bulbs with a light intensity of 3.17 log Lum m^{-2}. Three different treatments were run to study the effects of spent iron nanoparticles (NZVI that sorbed PO_4^{3-}) on plants. Treatment 1 was 0.15 g The amount of nanoparticles was decided based on the concentration of sorbed PO_4^{3-} on the particles. Spent iron (0.15 g) was used in the reactor. Equivalent amount of PO_4^{3-} in the nutrients solution was added each time. In another container (treatment 2 or control 1) all nutrients was used (Table 4.3). The last treatment was all nutrient except PO_4^{3-} and Fe^{3+} (Control 2). Each treatment was run in triplicate. The assignments of the reactor's place and plants were randomized. First the containers were numbered and each place was assigned a number randomly. Then plants were picked from sand washed thoroughly with DI-water then places randomly in a container until the last plant was places in the last container.

4.3.5. Analytical procedures

Algae measurement: Algae samples were collected and algae biomass was estimated by measuring chlorophyll *a* (Chl *a*) concentration using a pigment extraction method (Globbelaar et al., 1984; Lorenzen, 1967). Ten milliliters of algal culture was filtered using a Whatman GF/F glass fiber filters (pore size 0.5 to 0.7 µm, 47 mm diameter). Pigment (chlorophyll) extraction was done by soaking the filter (with algal biomass retained on them) in 5 mL of 95% ethanol and keeping it in the dark for 20 h. The solvent was then filtered through a GF/F a glass fiber filter. Absorbance of the extracted sample (solvent with the pigment dissolved) was measured on a DR 5000 UV spectrophotometer using a 1-cm path length cuvette at 665 nm and 750 nm. The sample was then treated with 1N HCl and absorbance was measured again at 665 nm and 750 nm. . The following equation was used to calculate Chl *a* concentration (Globbelaar et al., 1984; Lorenzen, 1967):

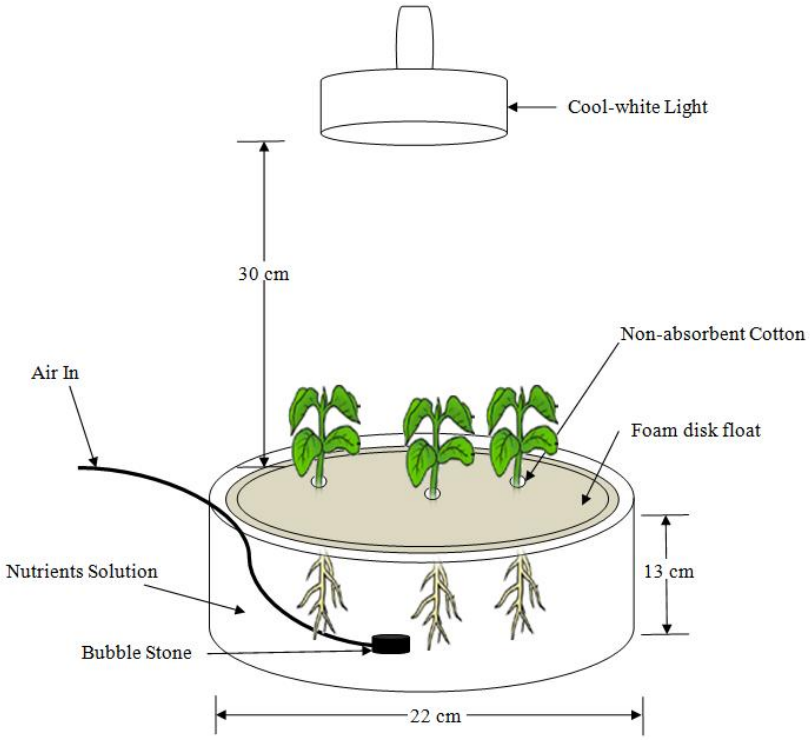

Figure 4.1: Schematic of hydroponic system setup

Figure 4.2: Experimental set-up for the hydroponic system for spinach studies.

$$\text{Chl a (mg/m}^3 \text{ or µg/L)} = \frac{26.7 \times (E_{665\,o} - E_{665\,a}) \text{ x V}}{V_f \times L} \quad (4.2)$$

Where,

V = volume of ethanol used for extraction (mL)
V_f = water filtered (L)
L = path length of cuvette (cm)
$E_{665\,o}$ = turbidity-corrected absorption at 665nm before acidification ($A_{665o} - A_{750o}$)
$E_{665\,a}$ = turbidity-corrected absorption at 665nm after acidification ($A_{665a} - A_{750\,a}$)

To ensure reproducibility and data reliability this experiments was ran in triplicate at different times and concentration of Chl *a* was measured in triplicate for each treatment.

Plant measurement: Plants were harvested after 28 days of hydroponic growth. The harvested plants were washed with DI water, and the height of shoots and roots were recorded. Roots were washed with 10 mM $CaCl_2$ solution to remove NZVI physically attached onto the surface (Jacob et al., 2013). Roots, stem and leafs were separated and then dried at 80^{o}C for 48 h before measuring the weight (Bezbaruah and Zhang, 2009). The similar parts (e.g., roots) of plants from each reactor (3 plants each) were combined together and the combined weight has been reported and further analyses were done assuming such combined mass as one entity.

Iron measurement: The dry plant tissue (roots, stems, shoots) were ground and digested in a CEM Mars Xpress microwave digester using. Concentrated nitric acid (HNO_3, 3 mL) was added to the ground plant tissue or standard reference material (NCS DC 73350 leaves of poplar, China National Analysis Center of Iron and Steel) in a 55 ml PFA venting vessel. Weight of plant tissue was measure before digestion. Samples were divided into three groups based on their weight and reference samples were prepared accordingly. DI waster (3 mL) was added after 20 min of pre-digestion then the samples were digested at 200 °C for 15 minutes at 1600 W 100% power (for 28 vessels) after 10 minutes ramp time. The digests were analyzed for Fe and P with a

Spectro Genesis ICP-OES with Smart Analyzer Vision software (v. 3.013.0752), crossflow nebulizer (three replicate measurements, 21 seconds integration time). Analysis of control standard was done after every 10 samples and checked whether it was within acceptable limits (10%).

Statistical Analysis: Analysis of variances (ANOVA) and Bonferroni Simultaneous Tests were used to analyze the result using Minitab 16 software.

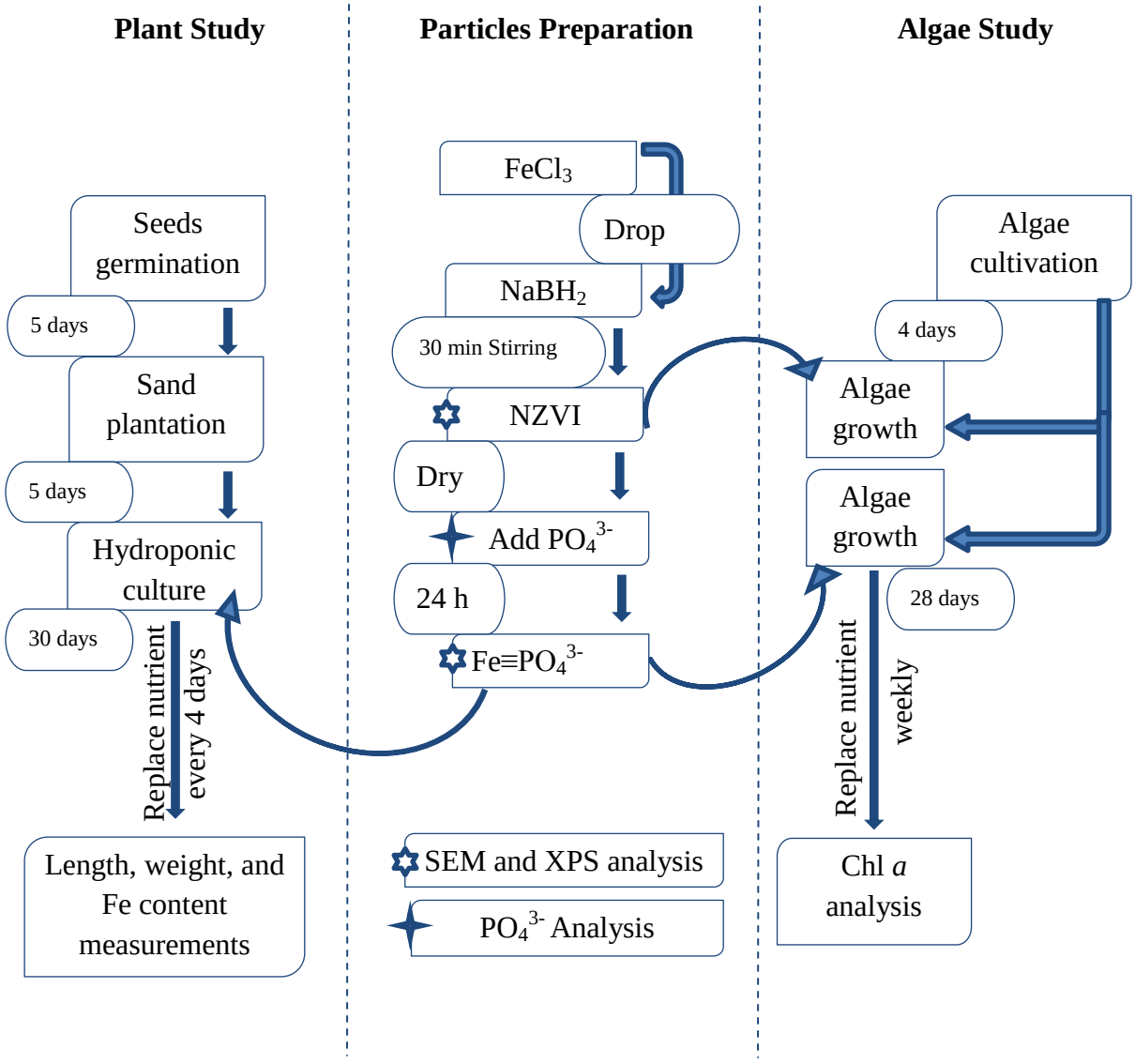

Figure 4.3: Schematic of the experimental design

4.4. Results and Discussion

4.4.1. Particles characterization

Average particles size of virgin NZVI was found to be 16.24±4.05 nm (Almeelbi and Bezbaruah, 2012). NZVI particles were synthesized and analyzed using XPS and EDS to confirm the presence of the phosphate (Figs. 4.4 and 4.5). High Resolution X-ray Photoelectron Spectroscopy (HR-XPS) was performed on a Surface Science SSX-100 spectrometer with an Al anode (Kα X-rays at 1486.66 eV) operated at 10 kV and 20 mA. Samples were mounted on the sample stage using conductive carbon sticky tape and transferred to the analysis chamber (with a pressure below 1×10^{-8} torr).

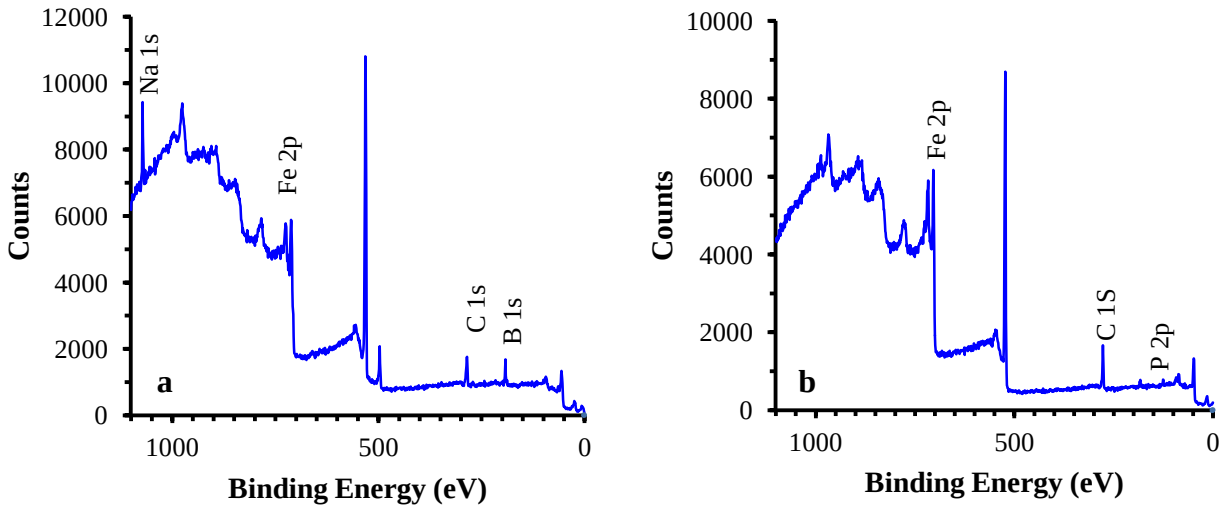

Figure 4.4: XPS spectra of **(a)** virgin NZVI, **(b)** spent NZVI, after PO43- adsorption

From XPS spectrum of the new NZVI (Fig. 4.4 a), peaks at 711 and 725 eV represent the binding energies of $2p_{3/2}$, and $2p_{1/2}$, respectively which can be assigned to the metallic Fe^0 and the oxide layer on the metal core. In addition, O 1s peak at 531 and adventitious carbon on the sample peak at 285 eV BE. Peaks at 1071 and 192 eV BE from Na 1s and B 1s, respectively, indicate considerable concentrations of Na and B from residual $NaBH_4$. This finding is in

agreement with others (Jabeen et al 2011; Li and Zhang, 2006; Martin *et al.*, 2008). The new peak at 133 eV (Fig. 4.4 b) is attributed to the presence of phosphate adsorbed onto the surface of the spent NZVI particles (Jianbo et al 2013; Zach-Maor, 2011). The HR-XPS spectra of Fe 2p (Fig. 4.5) shows a small shoulder at around 707 eV for virgin NZVI only which can be assigned to $2p_{3/2}$ peaks of Fe^0. Since the nanoparticle surface is covered with an oxidized iron layer (Krajangpan et al., 2012), only small amount of Fe^0 is exposed to XPS (5−50 Å in depth) (Li and Zhang, 2006).

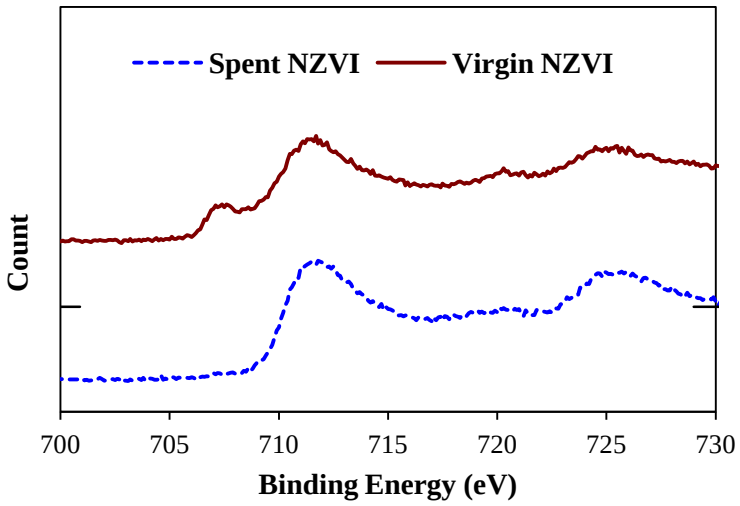

Figure 4.5: HR-XPS survey on the Fe 2p for virgin NZVI and spent NZVI.

Elemental composition of virgin spent NZVI was determined using scanning electron microscopy with energy dispersive spectroscopy (SEM/EDS, JEOL JSM-6300, JEOL Ltd.). The percentage of oxygen in the virgin NZVI was 12.10%. The amount of oxygen in the spent NZVI varied between 13.02 and 25.15% due to oxidation and phosphate sorption. Cao et al (2008) reported 8.21% oxygen in fresh NZVI which increased to 26.14% after an hour of purging with air. Krajangpan et al (2012) also reported 15.66% of oxygen in NZVI. While there was no phosphorus in the virgin NZVI, the percentage was found to be 7.95, 2.10, and 1.67% at three different parts in the spent sample (Table 4.4 and Fig. 4.6b). The highest percentage of P (7.95%)

was at the part number 1 which was a relatively large particle (circled in Fig. 4.6b). The isotherm experiments also determined adsorption capacity of NZVI as 63 mg PO_4^{3-}P/ g NZVI (i.e., 6.3%) (Appendix Fig.A.6). The presence of a very low amount (0.51%, Table 4.4 and Fig. 4.6) of sodium was observed in the virgin NZVI but was not present in the spent NZVI. Sodium was possibly left as the residual from sodium borohydride ($NaBH_4$) used in the NZVI synthesis process.

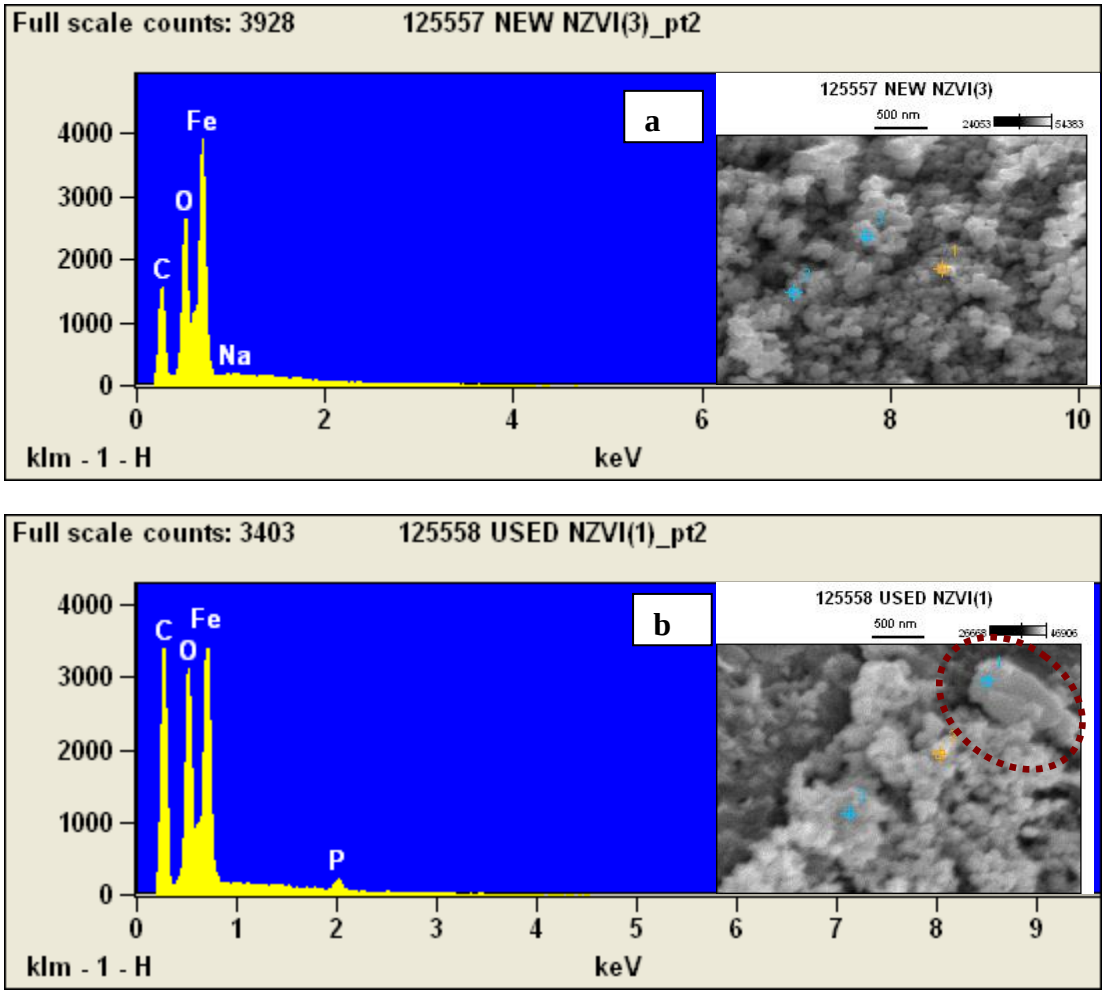

Figure 4.6: EDS spectrum of (**a**) Virgin NZVI, (**b**) Spent NZVI

Table 4.4: Weight percentage of elements present in virgin and spent NZVI.

Particles Type	Part Number*	% Weight			
		O	Fe	Na	P
Virgin NZVI	1	12.10	87.39	0.51	0.00
	2	10.37	89.32	0.31	0.00
	3	10.90	88.70	0.39	0.00
Spent NZVI	1	25.15	66.90	0.00	7.95
	2	13.13	84.77	0.00	2.10
	3	13.02	85.31	0.00	1.67

***** The part numbers used for analysis are identified in the SEM images (Figs. 5a and 5b)

4.4.2. Algae growth

The concentration of chlorophyll *a* (Chl *a*) is an indicator of algae health and a measure of growth. Chl a increased substantially when virgin NZVI and PO_4^{3-} sorbed NZVI used as compared to other treatments (Table 5 and Fig. 6). Bonferroni test (α=0.05) identified two groups of experimental data based on the statistically significant differences. The first group included results from algae treated with DI water, all nutrients, and all nutrients expect PO_4^3, and the second group was treated with virgin and spent NZVI particles. The algae batches treated with DI water provided the baseline data for comparison. There was slight increase in the concentration of Chl *a* when all nutrients expect PO_4^{3-} were added as the growth media (from 21 to 107 µg/L). The increase was very similar to what was seen in the DI water batch (from 21 to 108 µg/L). It should be noted all treatments (including DI water batch) had some initial growth nutrients as the seed algae was grown in Bristol media (Table 4.2), and the nutrients got transferred to each batch when 5 mL of seed was taken from the nursery reactor. The presence of the PO_4^{3-} the Chl *a* concentration increased 1.8 times as compared to the batch without PO_4^{3-}. The results from the second batch showed significant difference with the first group. The algae batch treated with all nutrients and virgin NZVI showed an increase of algae concentration from 21 to 1673 µg/L. When spent NZVI particles (with PO_4^{3-} sorbed onto them as the PO_4^{3-} source) were used the algae growth was even more profuse (from 21 to 2003 µg Chl *a*/L). It is very

evident that the presence of iron nanoparticles significantly increased the growth of algae. The growth of algae was profuse when spent NZVI apparently supplied the PO_4^{3-} needed for algae growth and the final algae concentration was 5.7 times more that the batch with all nutrients (no NZVI).

The presence of nanoparticles definitely played a major role in algae growth as has been evident from the comparison of data obtained from the two groups. However, it is difficult to postulate a reason for that. Bioavailability of iron from NZVI may be another possible reason for enhanced algae growth. It is worth mentioning that the Bristol media do not contain iron as a nutrient for algal growth. Kadar et al., (2012) have reported a normal growth of three different types of marine algae (*Pavlova lutheri*, *Isochrysis galbana* and *Tetraselmis suecica*) in the presence of NZVI. In particular *Tetraselmis suecica* showed 30% higher growth rate in the presence of NZVI. Another study (Liu et al., 2008) has also indicated that iron content in the growth media affected the algae growth of marine micro-algae (*Chlorella vulgaris*). However, Ruangsomboon, (2012) reported no significant effect of iron on green algae (*Botryococcus braunii*) biomass using $FeSO_4$ as source of iron. In this study, the comparison between the two batches in the second group indicates that PO_4^{3-} sorbed onto NZVI was possibly bioavailable for algal growth. Phosphate plays a major role in algae growth as could be observed from the Chl *a* growth in batches 1-B and 1-C (Table 4.5). The final concentration of Chl *a* without PO_4^{3-} (108 µg Chl *a*/L in 1-C) was ~3 times less than Chl *a* concentration when the nutrient solution contained PO_4^{3-} (300 µg Chl *a*/L in 1-B). Others have also reported PO_4^{3-} as a limiting nutrient for algal growth (Meeuwig, 1996). Fried et al., (2012) reported a positive effect of PO_4^{3-} on algae growth. Based on this logic it is reasonable to say that PO_4^{3-} sorbed in NZVI was bioavailable to algae and that is why similar growths were onbseved in batches 2-A and 2-B (Table 4.5).

Table 4.5: Concentrations of chlorophyll *a* at 0 and 28 days of algae growth

Batch	Growth Medium	Chlorophyll *a* concentration (µg/L)	
		0 d	28 d
1-A	DI-Water	20.80±1.83	81.58±22.84
1-B	All Nutrients	20.80±1.83	300.38±14.59
1-C	All nutrients (No PO_4^{3-})	20.80±1.83	107.54±45.73
2-A	All nutrients (No- PO_4^{3-}) + Spent NZVI	20.80±1.83	2002.50±981.45
2-B	All nutrient + Virgin NZVI	20.80±1.83	1673.20±270.10

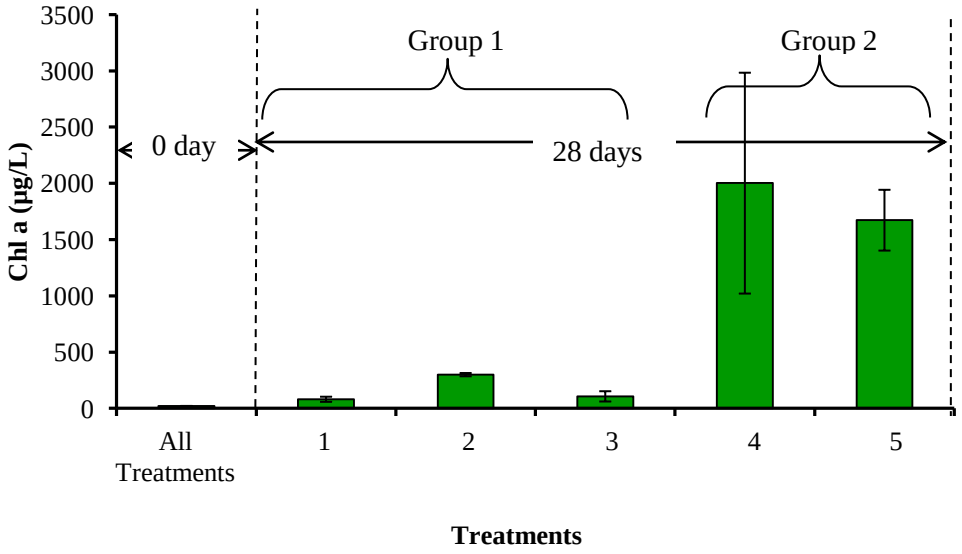

Figure 4.7: Chl a concentrations at 0 and 28 days. Treatments are as follow: (**1**) DI Water, (**2**) All Nutrients, (**3**) All nutrients (No PO_4^{3-}), (**4**) All nutrients (No PO_4^{3-}) + spent NZVI (with PO_4^{3-} sorbed onto NZVI), and (**5**) All nutrients + Virgin NZVI

4.4.3. Plant growth

Seeds germination started after 5 d and continued till 10 d. The percent of seed germination varied from 72 to 100%. Plant with similar germination time and growth were selected for the batch studies (Fig. 4.8).

Root and shoot lengths: Spinacia oleracea plants were harvested after 30 d of hydroponic growth. The length of shoots and roots were recorded immediately after harvesting (Table 4.6 and Fig. 4.9). In the plants treated with spent NZVI particles (with PO_4^{3-} sorbed onto them) the lengths of roots and shoots were 13.1±2.8 and 20.9±0.3 cm, respectively. The lengths of roots

and shoots in Control 1 (plants treated with all nutrients, Table 4.3) were 3.8±1.0 and 5.9±0.6 cm, respectively, while the corresponding values for Control 2 (all nutrient but no PO_4^{3-} and Fe) were 3.2±0.5 and 5.8±1.0 cm. Bonferroni test (α=0.05) put the data sets into two groups with data from spent NZVI in the first group and data from the two controls in the second group based on the statistically significant differences. Plants treated with only DI water showed no growth and died in 10 d.

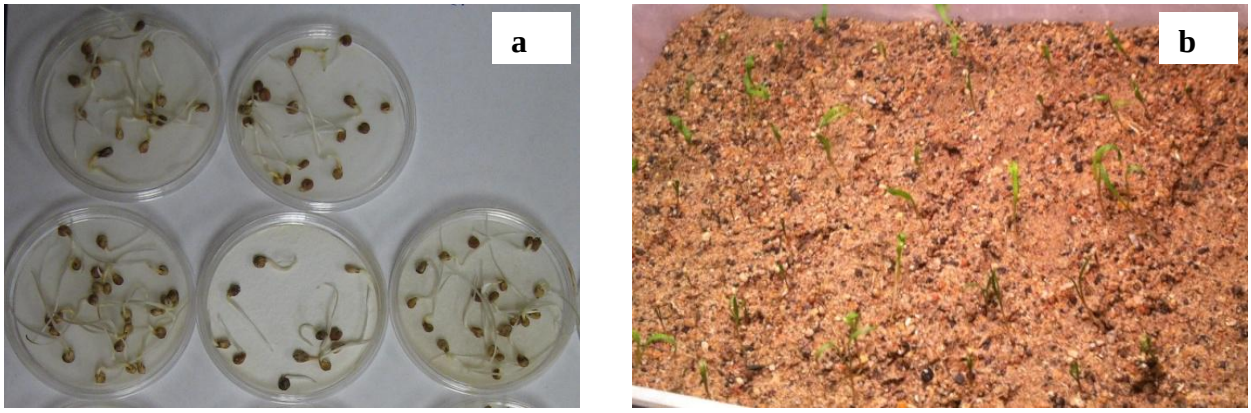

Figure 4.8: (**a**) Germinated seeds after 5 d. The percent of seed germination varied from 72 to 100%, and (**b**) Plant seedlings in sand bed

When the length of roots and shoots from the NZVI treated plants compared with those from Control 1 it was evident that the present of the spent NZVI had an major impact on plant growth. The roots and shoots of the plants treated with spent NZVI were ~3.5 longer than those from the plants in Control 1. This observation, however, does not help in concluding that PO_4^{3-} and Fe from NZVI was bioavailable given the fact that there are no significant differences in data obtained from Control 1 and Control 2. However, visual observation (Fig.4.10) indicate that plants supplied with PO_4^{3-} and Fe (Plate 3a and Plate 3c) were healthier and the leaves were vibrant green, while Control 2 (no PO_4^{3-} and Fe, Plate 3b) has weathered leaves and the stems were skinner. Ewa et al., (2012) reported plants (*Avena sativa L. Arab, Polar, and Szakal*) deprived of PO_4^{3-} showed a reduction in shoot growth with simultaneous root elongation. It is,

there, safe to conclude that plants treated with spent NZVI and Control 1 (all nutrients) had uptaken PO_4^{3-} and Fe.

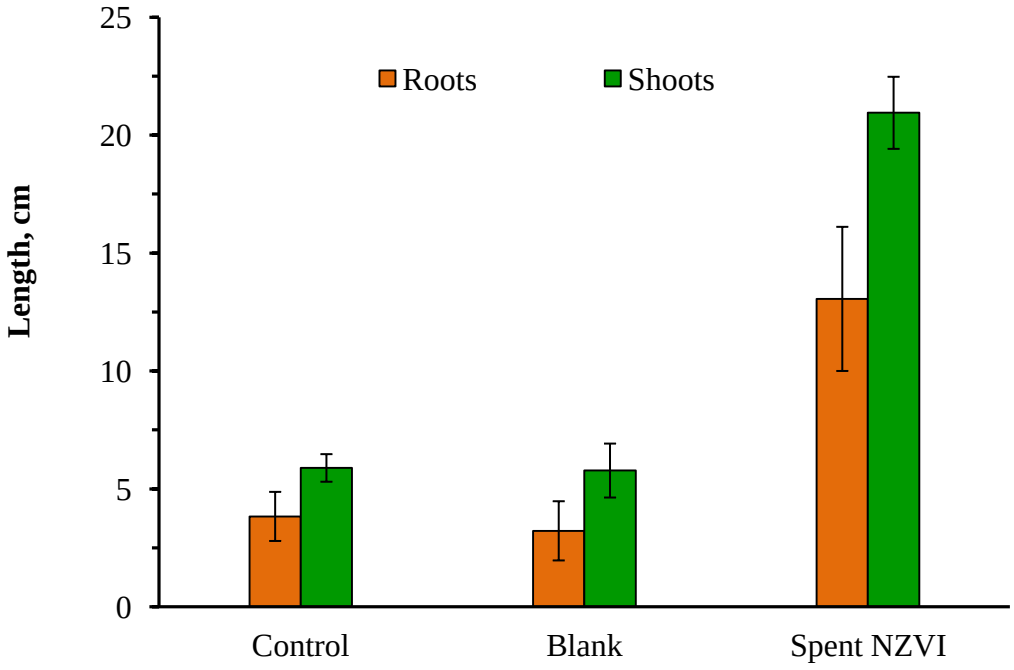

Figure 4.9: Length of roots and shoots after 30 d of hydroponic growth. Control 1: All nutrients, Blank: All nutrients but no PO_4^{3-} and Fe

Figure 4.10: Plants after 30 d of hydroponic treatment. Plant were supplied with (**a**) All nutrients, (**b**) All nutrients (but no PO_4^{3-} and Fe), and (**c**) All nutrients (but no PO_4^{3-} and Fe) + Spent NZVI

Plant biomass: Everage shoots and roots biomass of individual plants from each of the three groups of plants after 30 d was measured (Table 4.6 and Fig. 4.11). Plants grown in only DI-water died after 10 d and no measurement could be made.

Table 4.6: Length and weight of plants parts for each treatment

Treatment	**Length (cm)**		**Weight (mg)**	
	Roots	**Shoots**	**Roots**	**Shoots**
Blank*	----------Seedling died in 10 d----------			
Control 1**	3.8±1.04	5.89±0.59	3.8±0.3	36.7±5.6
Control 2***	3.22±0.54	5.78±0.96	2.5±0.6	16.9±5.2
PO_4^{3-} sorbed NZVI	13.06±2.76	20.94±0.35	15.3±7.0	81.7±2.8

* DI-Water, ** All nutrients ***All nutrients but (PO_4^{3-} and Fe)

In the plants treated with spent NZVI particles (with PO_4^{3-} sorbed onto them) the average biomass of roots and shoots (per plant) were 15.3±7.0 and 81.7±2.8 mg, respectively. The biomass of roots and shoots in Control 1 (plants treated with all nutrients, Table 4.3) were 3.8±0.3 and 36.7±5.6 mg, respectively, while the corresponding values for Control 2 (all nutrient but no PO_4^{3-} and Fe) were 2.5±0.6 and 16.9±5.2 mg. Bonferroni test (α=0.05) put the data sets into two groups with data from spent NZVI in the first group and data from the two controls in the second group based on the statistically significant differences. The treatment with nanoparticles had a significant effect on plant biomass. The plants treated with NZVI had ~4 times more root biomass that Control 1, and similarly had ~2.2 times higher shoot biomass. The most effect of nanoparticles was on roots weight with increase 3 times as compared to controls 1. Shoots also has increased by 1.22. Other researchers have reported both positive and negative impacts of different nanoparticles on plants (Table 4.7).

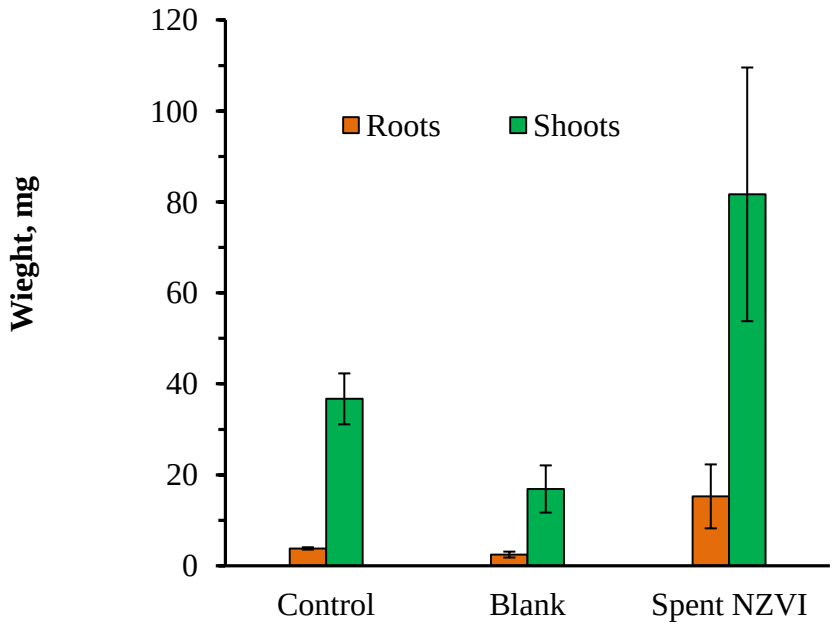

Figure 4.11: Weights of roots, stems, and leaves

Table 4.7: ANOVA analysis for Fe and P concentrations in plant parts.

Plant Part	Element	P- value mg/kg- dry weight	mg/biomass
Root	Fe	0.006	0.01
	P	0.066	0.033
Stem	Fe	0.080	0.052
	P	0.003	0.000
Leaf	Fe	0.042	0.017
	P	0.027	0.002

Significance level is ($P < 0.05$)

Iron and Phosphorus analysis: Iron and phosphorus contents in plant were analyzed. There was significant deferences in Fe and P concentrations between control and NZVI treatments in roots and leaves, however, in stems concentration of Fe was not significatnt (Fig. 4.12 and Table 1.7). Concentration of Fe in the stem increased by 1.9 times in the plants treated with spent NZVI (590.54±279.54) when compared to the control (205.34±57.72). Concentration of Fe was expressed in mg of Fe or P/kg of the dry weight.

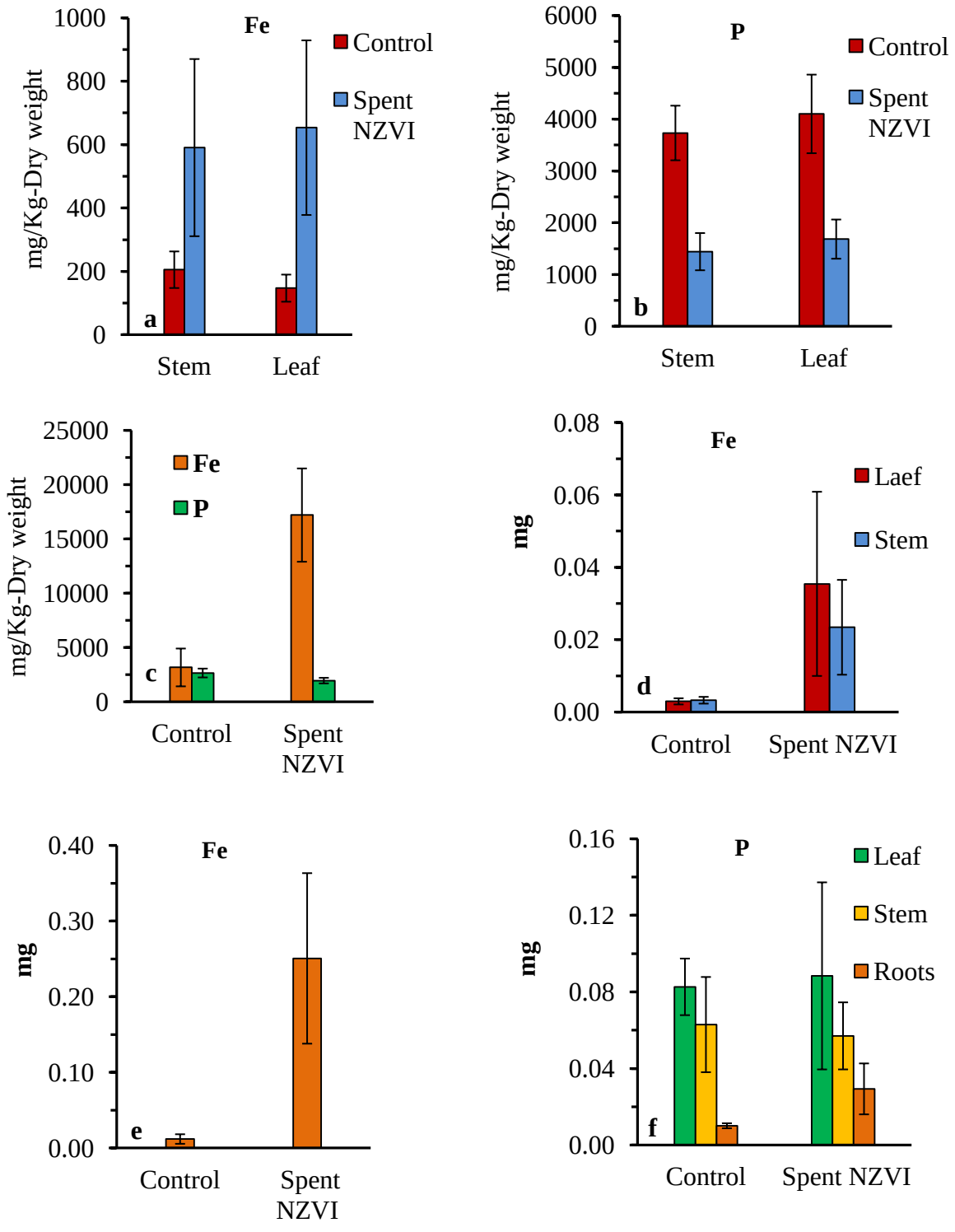

Figure 4.12: Fe and P analysis data in control and spent NZVI treatments, (**a**) Fe in stems and leaves, (**b**) P in stems and leaves, (**c**) Fe and P in roots, (**d**) Total Fe in stems and leaves, (**e**) Total Fe in roots, and (**f**) Total P in stems, leaves, and roots. Biomass was measured for each plant separately.

Table 4.8: Nanoparticle-plant interactions

Nanoparticle	Plant	Medium	Effects	Source
TiO_2	*Triticum* (Wheat)	Murashige and Skoog (MS)	Accumulation of nanoparticles in the roots, No major impact on seed germination and vegetation development	Camille et al., 2012
Multiwall carbon nanotubes	*Solanum lycopersicum* (Tomato)	MS	Increase in germination and growth rate	Khodakovskaya, et al 2009
CuO and ZnO	*Triticum* (Wheat)	Soil	Reduction on roots growth Bioaccumulation of NP were detected in the shoots	Christian et al., 2012
ZnO	*Lolium perenne* (ryegrass)	Hydroponic	Significant reduction of biomass, NPs aggregation in the roots, inhibition of the seedling growth	Lin and Xing, 2008
CoOx and ZnO	*Allium cepa* (Tnion)	Hydroponic	Roots inhibition by both, and roots damaged by ZnO accumulation	Gajanan et al., 2011
Al_2O_3, SiO_2, Fe_3O_4, and ZnO	*Arabidopsis thaliana* (mouseear cress)	MS	Phytotoxicity: ZnO > Fe_3O_4 > SiO_2 Al_2O_3 was found to be not Phytotoxic	Lee et al., 2010
NZVI	Linum usitatissimum (Flax), *Lolium perenne* (ryegrass) Hordeum vulgare (barley)	Soil and hydroponic	Complete inhibition of germination at 1-2 g NZVI/L	El-Temsah and Joner, 2010
Fe_3O_4	Cucurbita Maxima	Hydroponic and sand	NPs translocateed, and accumulated in the plant tissues. Level of uptake and accumulation in hydroponic was more than soil	Zhu et al., 2011
TiO_2 and ZnO	*Triticum* (Wheat)	Soil	NPs are found to reduce biomass. Zn was dissolved in the soil increasing Zn uptake by the plant	Du et al., 2011
Ag and Cu	*Cucurbita pepo* (zucchini)	hydroponic	Ag and Cu reduced biomass by 57and 90%, respectively	Stampoulis et al., 2009

In the case of P concentration there was higher concentration in all plant parts of the control but after calculating the amount of P present in the biomass of the plant there was more P in plants from spent NZVI treatment than those from controls. The results are strong evidence that the adsorbed PO_4^{3-} was bioavailable for plant uptake. In the roots total Fe uptake increased ~ 20 times from in control 0.012±0.006 to 0.251±0.011 mg in the presence of spent NZVI, respectively. In the stems and leaves, Fe increased by ~7 and 11 times in the presence of NZVI. The significant increase of Fe concentration in the plant tissues indicates that the Fe from NZVI was bioavailable as well.

4.5. Conclusions

In this study the bioavailability of phosphate and iron from PO_4^{3-} sorbed iron nanoparticles was examined using *Selenastrum capricornutum* (algae) and *Spinacia oleracea* (Spinach). NZVI was synthesized and used for phosphate removal from aqueous solution. The particles characterization using XPS and SEM/EDS confirmed the presence of the PO_4^{3-} on the surface of nanoparticles. Algae Growth increased significantly in the presence of the iron nanoparticles (virgin and spent NZVI). Algae growth when spent NZVI was the only source of PO_4^{3-} increased by 5.7 times more than the algae growth in stadard all-nutrient solution. It can be concluded that the PO_4^{3-} sorbed onto spent NZVI was bioavailable for algal growth. Spinach growth experiment also produced similar results where presence of spent NZVI enhanced the growth of the plants and increased the plant biomass by 4 times as compared to control where PO_4^{3-} was supplied from the all-nutrient hydroponic solution. Fe content significantly increased in all plant parts (roots, stems, and leaves) when NZVI was added. Roots of the plants exposed to spent NZVI had the heights concentration of Fe (increased ~20 times as compared to the control). Fe content also increased in the stem and leaves of the plant treated with spent NZVI by 7 and 11 times as

compared to the control, respectively. All parts of plants treated with spent NZVI also had higher content of P than the control plants. It is evident that Fe and P was bioavialable for plants when the only source of P and Fe was the spent nanoparticles. Furtrher research is needed to consolidate the finding and evaluate phosphate sorbed NZVI particles as fertilizer and Fe fortifier.

4.6. References

Abouwaly H, Abousetta MM, Nigg HN, Mallory LL (1991) Growth response of freshwater algae, Anabaena flos-aquae and Selenastrum capricornutum to Atrazine and Hexazinone Herbicides. Bull. Environ. Contam. Toxicol, 46(2): 223-229.

Almeelbi T, Bezbaruah AN (2012) Aqueous phosphate removal using nanoscale zero-valent iron. Journal of Nanoparticle Research, 14(7), 1-14

Bezbaruah AN, Zhang TC (2009) Ncorporation Of Oxygen Contribution by Plant Roots into Classical Dissolved Oxygen Deficit Model for A Subsurface Flow Treatment Wetland. Water Science and Technology, 59, 1179-1184

Brown EJ, Button DK (1979) Phosphate-limited growth kinetics of Selenastrum capricornutum (Chlorophyceae). Journal of Phycology, 15: 305-311.

Cao J Li X, Tavakoli J Zhang W (2008) Temperature programmed reduction for measurement of oxygen content in nanoscale zero-valent iron. Environmental Science & Technology, 42(10):3780-3785.

Christensen ER, Scherfig J, Dixon PS (1979) Effects of manganese, copper and lead on Selenastrum capricornutum and Chlorella stigmatophora. Water Res. 13: 79-92.

Dimkpa CO, McLean JE, Latta DE, Manangon E, Britt DW, Johnson WP, Boyanov MI, Anderson AJ (2012) CuO and ZnO nanoparticles: phytotoxicity, metal speciation, and induction of oxidative stress in sand-grown wheat. Journal of Nanoparticle Research, 14(9).

Du W, Sun Y, Ji R, Zhu J, Wu J, Guo H, (2011) TiO2 and ZnO nanoparticles negatively affect wheat growth and soil enzyme activities in agricultural soil. Journal of Environmental Monitoring,13(4):822-828

Eaton AD, Franson MAH, Association AWW, Federation WE (2005) Standard methods for the examination of water and wastewate. 21st ed. American Public Health Association, Washington, DC, USA

El-Temsah YS, Joner EJ (2012) Ecotoxicological effects on earthworms of fresh and aged nano-sized zero-valent iron (nZVI) in soil. Chemosphere, 89(1):76-82.

Errécalde O, Campbell PGC (2000) Cadmium and zinc bioavailability to Selenastrum capricornutum (Chlorophyceae): accidental metal uptake and toxicity in the presence of citrate. Journal of Phycology, 36: 473-483.

Francko DA (1989) Modulation of photosynthetic carbon assimilation in Selenastrum capricornutum (Chlorophyceae) by cAMP: an electrogenic mechanism. Journal of Phycology, 25: 305-313.

Ghodake G, Seo YD, Lee DS (2011) Hazardous phytotoxic nature of cobalt and zinc oxide nanoparticles assessed using Allium cepa. Journal of Hazardous Materials, 186(1), 952-955.

Ghodake G, Seo YD, Lee DS. 2011. Hazardous phytotoxic nature of cobalt and zinc oxide nanoparticles assessed using Allium cepa. Journal of Hazardous Materials, 186(1):952-955.

Gilbert, N. (2009). The disappearing nutrient. Nature, 461, 716–718.

Gutierrez-Wing MT, Benson BC, Rusch KA (2012) Impact of light quality and quantity on growth rate kinetics of Selenastrum capricornutum. Engineering in Life Sciences, 12(1), 79-88.

Hall JA, Golding LA (1998) Standard methods for whole effluent toxicity testing: development and application. Report no. MFE80205. NIWA report for the Ministry for the Environment, Wellington, New Zealand.

ISO 8692, (1989) Water Quality—Fresh Water Algal Growth Inhibition Test with Scendemus subspicatus and Selenastrumcapricornutum. International Organization of Standardization, Geneva, Switzerland.

Jabeen H, Chandra V, Jung S, Lee J, Kim K, Bin Kim S (2011) Enhanced Cr(VI) removal using iron nanoparticle decorated graphene. Nanoscale, 3(9):3583-3585.

Jacob DL, Borchardt JD, Navaratnam L, Marinus LO, Bezbaruah AN (2013) Uptake and translocation of Ti from nanoparticles in crops and wetland plants. International Journal of Phytoremediation, 15:2,142-153

Jianbo Lǔ, Huijuan Liu, Ruiping Liu, Xu Zhao, Liping Sun, Jiuhui Qu, (2013) Adsorptive removal of phosphate by a nanostructured Fe–Al–Mn trimetal oxide adsorbent. Powder Technology, 233,146-154

Khodakovskaya M, Dervishi E, Mahmood M, Xu Y, Li ZR, Watanabe F, Biris AS (2009) Carbon Nanotubes Are Able To Penetrate Plant Seed Coat and Dramatically Affect Seed Germination and Plant Growth. Acs Nano, 3(10):3221-3227.

Larue C, Laurette J, Herlin-Boime N, Khodja H, Fayard B, Flank AM, Brisset F, Carriere M (2012) Accumulation, translocation and impact of TiO2 nanoparticles in wheat (Triticum aestivum spp.): Influence of diameter and crystal phase. Science of the Total Environment, 431:197-208.

Lee C, Mahendra S, Zodrow K, Li D, Tsai Y, Braam J, Alvarez P (2010) Developmental phytotoxicity of metal oxide nanoparticles to arabidopsis thaliana. Environmental Toxicology and Chemistry, 29(3):669-675.

Li X, Zhang W (2006) Iron nanoparticles: the core-shell structure and unique properties for Ni(II) sequestration. Langmuir, 22(10):4638-4642.

Lin DH, Xing BS (2008) Root uptake and phytotoxicity of ZnO nanoparticles. Environmental Science & Technology, 42(15), 5580-5585.

Lin DH, Xing BS (2008) Root uptake and phytotoxicity of ZnO nanoparticles. Environmental Science & Technology 42(15):5580-5585.

MacDonald GK, Bennett EM, Potter PA, Ramankutty N (2011) Agronomic phosphorus imbalances across the world's croplands. Proc. Natl. Acad. Sci. U.S.A., 108, 3086−3091.

Martin J, Herzing A, Yan W, Li X, Koel B, Kiely C, Zhang W (2008) Determination of the oxide layer thickness in core-shell zerovalent iron nanoparticles. Langmuir, 24(8):4329-4334.

Martin B, Parsons S, and Jefferson B (2009) Removal and recovery of phosphate from municipal wastewaters using a polymeric anion exchanger bound with hydrated ferric oxide nanoparticles. Water Science and Technology, 60: 2637-2645.

Pan B, Wu J, Pan B, Lv L, Zhang W, Xiao L, Wang X, Tao X, Zheng S (2009) Development of polymer-based nanosized hydrated ferric oxides (HFOs) for enhanced phosphate removal from waste effluents. Water Research, 43: 4421-4429.

Stampoulis D, Sinha SK, White JC (2009) Assay-Dependent Phytotoxicity of Nanoparticles to Plants. Environmental Science & Technology, 43(24), 9473-9479.

Stampoulis D, Sinha SK, White JC (2009) Assay-Dependent Phytotoxicity of Nanoparticles to Plants. Environmental Science & Technology, 43(24):9473-9479.

Stutter MI, Shand CA, George TS, Blackwell SA, Bol R, MacKay RL, Richardson AE, Condron LM, Turner BL, and Haygarth PM (2012) Recovering Phosphorus from Soil: A Root Solution? Environmental Science & Technology, 46: 1977-1978.

UTEX (2012), UTEX The culture collection of algae: Web Interface. Retrieved on October 4, 2012. http://www.sbs.utexas.edu/utex/

USU (2012), Hydroponic solutions recipes: Web Interface. Retrieve on October, 21, 2012. http://www.usu.edu/cpl/PDF/solution_recipes.pdf

Wang HH, Kou XM, Pei ZG, Xiao JQ, Shan XQ, Xing BS (2011) Physiological effects of magnetite (Fe3O4) nanoparticles on perennial ryegrass (Lolium perenne L.) and pumpkin (Cucurbita mixta) plants. Nanotoxicology, 5(1), 30-42.

Zach-Maor A, Semiat R, Shemer H (2011). Adsorption-desorption mechanism of phosphate by immobilized nano-sized magnetite layer: Interface and bulk interactions. Journal of Colloid and Interface Science 363(2):608-614.

Kadar E, Rooks P, Lakey C, White D (2012) The effect of engineered iron nanoparticles on growth and metabolic status of marine microalgae cultures. Science of The Total Environment, 439(15) 8-17, ISSN 0048-9697.

Liu Z, Wang G, Zhou B (2008) Effect of iron on growth and lipid accumulation in Chlorella vulgaris. Bioresource Technology, 99(11):4717-4722.

Ruangsomboon S (2012) Effect of light, nutrient, cultivation time and salinity on lipid production of newly isolated strain of the green microalga, Botryococcus braunii KMITL 2. Bioresource Technology, 109:261-265.

Singh A, Nigam P, Murphy J (2011) Mechanism and challenges in commercialisation of algal biofuels. Bioresource Technology, 102(1):26-34.

Fried S, Mackie B, Nothwehr E (2012). Nitrate and phosphate levels positively affect the growth of algae species found in Perry Pond. Tillers, 4, 21-24.

Żebrowska E, Bujnowska E, Ciereszko I (2012). Differential responses of oat cultivars to phosphate deprivation: plant growth and acid phosphatase activities. Acta Physiologiae Plantarum, 1-10.

CHAPTER 5. BARE NZVI AND IRON CROSS-LINKED ALGINATE BEADS: APPLICATIONS FOR PHOSPHATE REMOVAL FROM ACTUAL WASTEWATERS

5.1. Abstract

Applications of nanosacle zero-valent iron (NZVI) and iron corss-linked alginate (FCA) beads were explored in this study for phosphate removal from actual wastewaters. Wastewater treatment plant effluent (WTPE) and animal feedlot effluent/runoff (AFLE) samples were used in the phosphate removal studies. While FCA beads removed 97% of the PO_4^{3-} in 2 h from WTPE, NZVI removed 84%. However, the difference was not statistically significant. Fast removal rate was observed with FCA used to remove phosphate from AFLE (~77% removal at the end of 15 min). The FCA beads continued to remove phosphate fater than NZVI till ~ 60 min. Results have indicated that FCA beads were more efficient (85%) as compared to NZVI particles (57%) in the first hour. The overall PO_4^{3-} removal by FCA beads reduced from 85% in 1 h to 75% at 24 h. This removal rate has possible application in the field with hiegh flowrate systems.

Keywords: Nanoscale zero-valent iron, iron cross-linked alginate, municipal wastewater, feedlot runoff, phosphate removal

5.2. Introduction

Excessive discharge of phosphorus (P) in surface water causes deterioration of water quality. Nutrient (P) richness in surface water bodies results in eutrophication of the water bodies. Eutroiphication has significant economic impacts on local communities.

Two of the major sources of phosphate in surface water are wastewater effluent (point-source) and animal feedlot runoff (nonpoint-source). The estimated contributions of P sources to municipal wastewater from human wastes, laundry detergents, and other cleaners are 0.6, 0.3, and 0.1 kg P/capita/year, respectiveluy (Sengupta et al 2011). Municipal wastewater contains adequate amount (5 -15 mg/L) of P (Blackall et al., 2002). Even though the contribution of laundry detergents in inceasing P in wastewater successfully reduced nowadays, P concentration in WWT effluent would reduce be only to 4–5 mg/L P (USGS, 1999). This effluent with high concentration of P finds its way to lakes and surface waters. Various studies have indicated that concentrations of P above 0.02 mg/L accelerate eutrophication of water bodies (Sharpley et al., 2003; Seviour et al., 2003).

The objective of this study is to examine the phosphate removal efficiency of NZVI and FCA beads from actual wastewater plant effluent and animal feedlot runoff.

5.3. Materials and Methods

5.3.1. Chemicals

Iron (II) chloride tetrahydrate ($FeCl_2 \cdot 4H_2O$, reagent grade, J.T. Baker), calcium chloride ($CaCl_2$, ACS grade, BDH), monopotassium phosphate (KH_2PO_4, 99% pure, EMD), sodium alginate (production grade, Pfaltz & Bauer), potassium nitrate (KNO_3, 99%, Alfa Aesar), sodium hydroxide (NaOH, ACS Grade, BDH), sodium borohydride ($NaBH_4$, 98%, Aldrich), methanol (production grade, BDH) were used as received unless and otherwise specified.

5.3.2. NZVI synthesis

NZVI was prepared as described by (Almeelbi, 2012). Briefly, $FeCl_3$ solution was dropped into sodium borohydride solution and stirred for 30 min. The black resultant black precipitate (NZVI) was separated, washed by methanol and water using a centrifuge. The washed (NZVI) particles were dried using a vacuum oven under N_2 environment overnight and then ground using a mortar and pestle. The fine black powder was stored in a 20 mL vial for later use. Particles were not stored more than two weeks. The detailed method of NZVI has been reported by Almeelbi and Bezbaruah (2012).

5.3.3. Beads synthesis

A minor modification has been made to the procedure of FCA beads synthesis described in Chapter 3. Alginate solution (5 mL of 2% w/v) was dropped into $FeCl_2$ solution (35 mL of 2% w/v) in a 50 mL polypropylene plastic vial using a pump with very small tube track to reduce the loss of alginate. Moreover, the first batch was sacrificed to ensure eliminate any effect of alginate volume reduction due to alginate that might have remained within the tubings. Rest of the produre was same as described uin Chapter 3. Beads were kept in the $FeCl_2$ solution for at least 6 h with vial was capped. The beads were prepared for the experiments as described earlier (Chapter 3).

5.3.4. Samples collection and storage

Municipal Wastewater Treatment Plant (WTPE) Effluent: Samples were obtained from the City of Moorhead Wastewater Treatment Plant (Moorhead, MN, USA). Moorhead follows a pure oxygen activated sludge treatment scheme. The secondary treated wastewater is subjected to tertiary treatment that involved nitrogen removal and

additional polishing for organics and suspended solids. Tertiary treated wastewater samples from the effluent sampling point in outlet leading to the Red River outfall were collected in plastic containers (~8L). The WTPE was filtered through a 1.2 μm pore-size Whatman glass microfiber filter (GF/C) before use in the experiments or stored in the refrigerator at 4^{o}C for later use. Stored samples were used within a month.

Animal Feedlot Effluent (AFE): Samples were collected from a privately owned cattle feedlot at Sargent County, North Dakota, USA. Unfiltered samples were used immediately or stored in a plastic container (~8L) in the refrigerator at 4^{o}C for later use. Stored samples were used within a month.

5.3.5. Batch studies

WTPE and AFLE samples were used in PO_4^{3-} removal studies with NZVI and FCA beads as the sorbents. One batch of FCA beads (0.121g dry weight) or 0.02 g NZVI were added to 50 mL of wastewater in multiple polypropylene plastic vials fitted plastic caps (reactors). The reactors were rotated end-over-end at 28 rpm in a custom-made shaker to reduce mass transfer resistance. A set of sacrificial reactors was withdrawn at specific time interval. The phosphate concentration in the bulk solution was measured and reported as average (with standard deviations) of readings from three replicate studies.

5.3.6. Phosphate analysis

Ascorbic acid method (Eaton et al., 2005) was used for phosphate analysis. This method depends on the direct reaction of orthophosphare with molybdate anions to form a yellow-colored phosphomolybdate complex. Ascorbic acid reduces phosphomolybdic

to form molybdenum blue species that has a broad absorbance range in between 700 nm to 900 nm. The color was measured in a UV-vis spectrophotometer (HACH, DR 5000) at wavelength of 880 nm. A five-point calibration was done routinely.

5.3.7. Quality control

All experiments were done in triplicates during this research and the average values are reported along with the standard deviations. Blanks with only wastewater/runoff (without NZVI/FCA beads) were run along with the NZVI and FCA bead experiments. The analytical instruments and tools were calibrated before the day's measurements. One-way ANOVA tests were performed to compare the variance between data sets as needed. Minitab 16 software (Minitab, USA) was used for all statistical analyses.

5.4. Results and Discussion

5.4.1. Beads characterization

FCA bead characterization has been reported in Chapter 3. Beads were approximately spherical in shape with average diameters of 3.09±0.16 mm and each batch of dry FCA beads weighted 0.121±0.002 g. SEM analysis of the beads were done after drying the beads for 24 h in a vacuum oven under nitrogen environment. Iron nanoparticles was observed inside the dried the beads (Fig. 5.1), and the nanoparticles had an average size of 74.45±35.60 nm (n = 97).

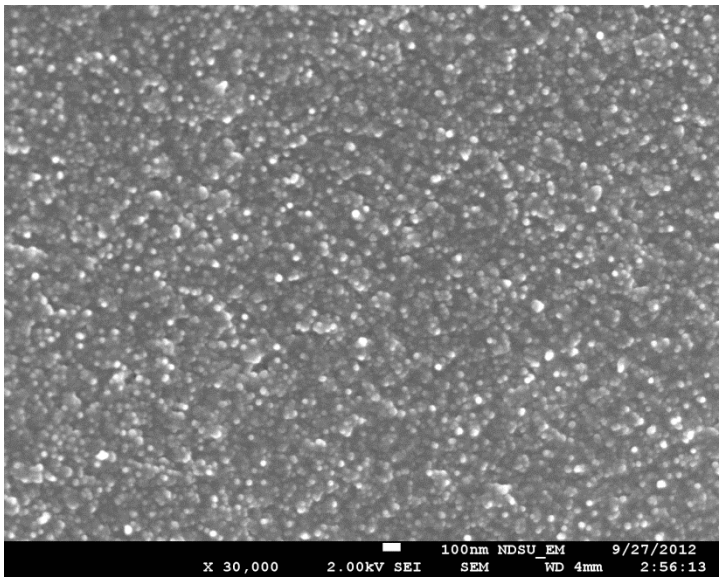

Figure 5.1: SEM image a fresh dry FCA beads

5.4.2. NZVI characterization

Almeelbi and Bezbaruah (2012) have used TEM to determine the size of NZVI and reported the particle size as 16.24±4.05 nm (n = 109). Characterization the particles morphology by SEM/EDS and XPS has been reported in Chapter 3.

5.4.3. Phosphate removal from WTPE

In batch studies conducted using NZVI and FCA beads for PO_4^{3-} removal from WTPE, FCA beads removed 97% of the PO_4^{3-} in 2 h while NZVI removed only 84% (Fig. 5.2). NZVI was faster in removing PO_4^{3-} as compared FCA in the first 15 min, and removed 80% PO_4^{3-} while FCA beads removed only 63%. NZVI continued to perform better till ~30 min beyond which FCA removed PO_4^{3-} at better rate than NZVI. However, ANOVA analysis indicates that there is no significant difference between the PO_4^{3-} removal efficiencies by NZVI and FCA beads after 2 h ($p = 0.629$). The finding is important from field application perspective. While it may be difficult to use and then

recover NZVI particles (average diameter ~16 nm) in wastewater treatment plant or similar set-ups, the FCA beads whch are much larger (average diameter ~3 mm) will be easily recoverable. Further, there are still a number of unknowns about the toxicity of NZVI. Saleh et al., (2008) found that coated NZVI can remain mobile in aqueous media even after 8 months of application and may be toxic to humans. There are also other reports on toxicity of NZVI (Keller, 2012; Li, 2010; Phenrat, 2009; Xiu, 2010) that call for caution in wide scale application of the bare or unmodified nanoparticles.

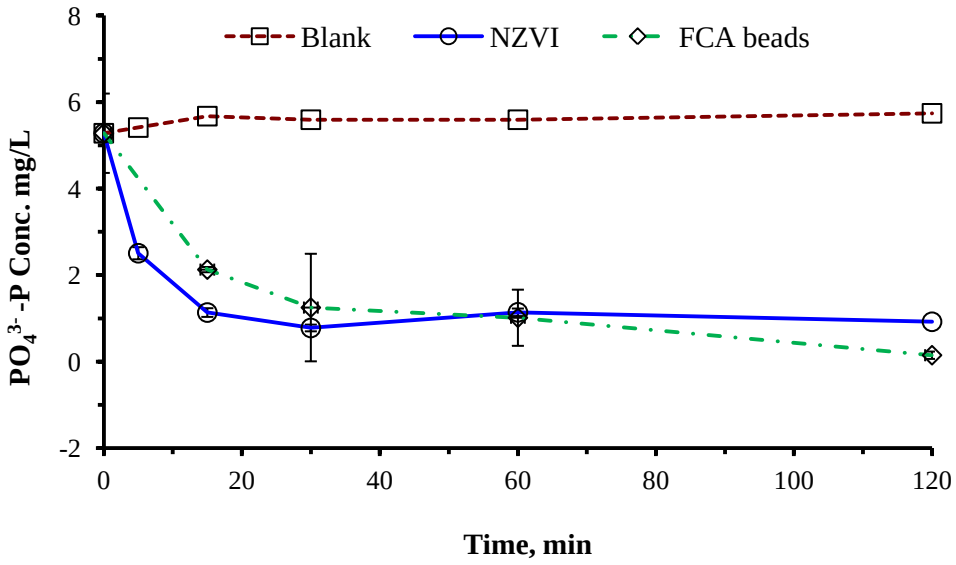

Figure 5.2: Removal of PO_4^{3-} from WTPE using bare NZVI and FCA beads

5.4.4. Phosphate removal from AFLE

Batch study results have indicated that FCA beads were more efficient (85%) as compared to NZVI particles (57%) in the first hour (Fig. 5.3) of reaction in removing PO_4^{3-} from animal feedlot effluent (AFLE). Statistical analysis indicate that the results from these two sets of experiments are significantly different (one-way ANOVA, p = 0.00). Data points could not be collected exactly at 2 h for all the samples due to management issues and, therefore, have not been compared.

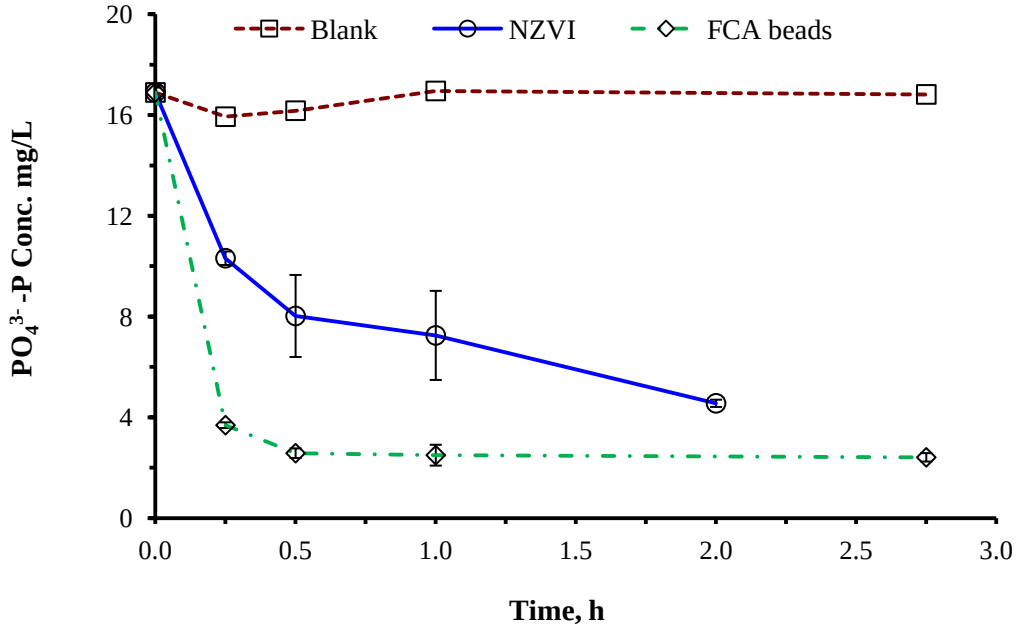

Figure 5.3: PO_4^{3-} removal from animal AFLE using NZVI and FCA beads

The batch studies with the AFLE were continued till 24 h and it was observed that the overall PO_4^{3-} removal by FCA beads reduced from 85% in 1 h to 75% at 24 h. There is no immediate explanation for this behavior of the beads till further research is conducted. However, a possible reason may have to do with the presence of orthophosphate in the particulate form. AFLE was used as received (without any filtration) for PO_4^{3-} removal using NZVI and FCA beads. A layer of visible black particles were observed on the beads at the end of the reaction which may be the particulate PO_4^{3-} and they might have contributed to the increase in PO_4^{3-} concentration. Further studies may be needed to understand this behavior of the beads. It is, however, clear that FCA beads can be used to remove phosphate from AFLE. PO_4^{3-} removal was ~77% at the end of 15 min (Table 5.1). The short contact time needed for PO_4^{3-} removal is expected to have major ramifications as FCA beads can possibly be used in high flow system (e.g., pumped system).

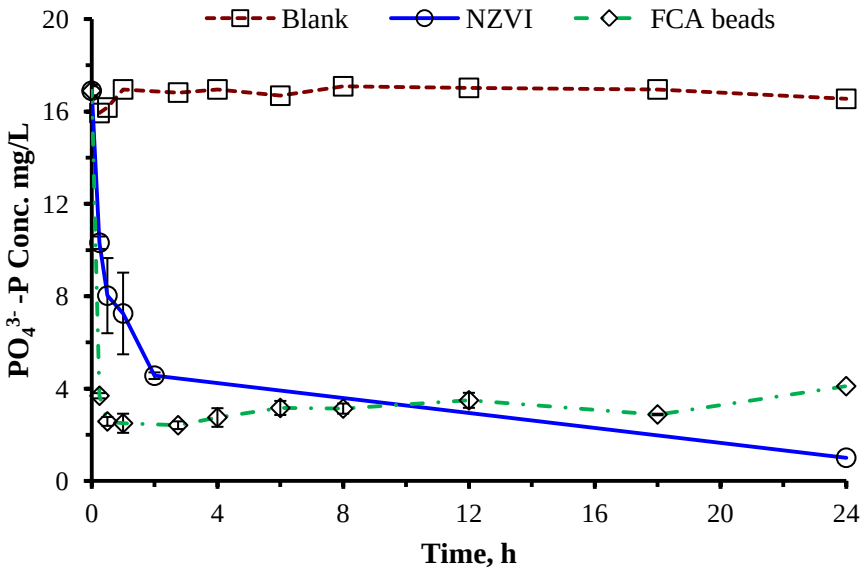

Figure 5.4: PO_4^{3-} removal from AFLE using NZVI and FCA beads over a 24 h period

Table 5.1: PO_4^{3-} removal from AFLE using NZVI and FCA beads

Time, h	% PO_4^{3-} Removal	
	FCA	NZVI
0.25	76.85	35.23
0.50	84.07	50.39
1.00	85.27	57.22
2.75	85.66	72.91
4.00	83.80	-
6.00	81.05	-
8.00	81.67	-
12.00	79.50	-
18.00	83.03	-
24.00	75.21	94.06

Data at 4, 6, 8, 12, and 18 h were not collected for NZVI studies

5.5. Conclusions

NZVI and FCA beads successfully removed PO_4^{3-} from both municipal wastewater (WTPE) and animal feedlot effluent (AFLE). The fact that FCA beads could remove 63% and 77% PO_4^{3-} from WTPE and AFLE, respectively, within the first 15 min

provides a huge advantage for their application in high flow systems. NZVI particles were also effective in removing PO_4^{3-} from waters. However, FCA beads performed better with AFLE. More experiments need to be conducted to determine the possibility of PO_4^{3-} recovery from FCA beads.

5.6. References

Almeelbi T, Bezbaruah AN (2012) Aqueous phosphate removal using nanoscale zero-valent iron. Journal of Nanoparticle Research, 14(7), 1-14

Saleh N, KimHJ, Phenrat T, Matyjaszewski K. Tilton R D. Lowry GV. (2008) Ionic strength and composition affect the mobility of surface-modified Fe^0 nanoparticles in water-saturated sand columns. Environ. Sci. Technol, 42, 3349-3355.

Li ZQ, Greden K, Alvarez PJJ, Gregory KB, Lowry GV (2010) Adsorbed Polymer and NOM Limits Adhesion and Toxicity of Nano Scale Zerovalent Iron to E. coli. Environ Sci Technol 44:3462-3467. doi:10.1021/es9031198

Phenrat T, Long TC, Lowry GV, Veronesi B (2009) Partial oxidation ("aging") and surface modification decrease the toxicity of nanosized zerovalent iron. Environ. Sci. Technol., 43: (1), 195–200.

Xiu ZM, Gregory KB, Lowry GV, Alvarez PJ (2010). Effect of Bare and Coated Nanoscale Zerovalent Iron on tceA and vcrA Gene Expression in Dehalococcoides spp. Environmental science & technology, 44(19), 7647-7651.

Keller AA, Garner K, Miller RJ, Lenihan HS (2012) Toxicity of Nano-Zero Valent Iron to Freshwater and Marine Organisms. PLoS ONE 7(8) e43983

Blackall LL, Crocetti G, Saunders AM, Bond PL (2002) A review and update of the microbiology of enhanced biological phosphorus removal in wastewater treatment plants. Antonie Van Leeuwenhoek International Journal of General and Molecular Microbiology 81(1-4):681-691.

USGS (1999) Phosphorus in a Ground-Water Contaminant Plume Discharging to Ashumet Pond, Cape Cod, Massachusetts, Northborough, MA.

Sharpley AN, Daniel T, Sims T, Lemunyon J, Stevens R, Parry R (2003)Agricultural Phosphorus and Eutrophication (second ed.) United States Department of Agriculture, Agricultural Research Service

Seviour RJ, McIlroy S (2008) The microbiology of phosphorus removal in activated sludge processes - the current state of play. Journal of Microbiology 46(2):115

CHAPTER 6. CONCLUSIONS AND FUTURE DIRECTIONS

6.1. Conclusions

NZVI was successfully synthesized in the laboratory and HRTEM analysis revealed average of particles size of 16.24±4.05 nm (n = 109). Batch studies conducted to examine the effectiveness of NZVI for phosphate removal and recovery (C_0=1, 5, 10 mg PO_4^{3-}-P/L) revealed that PO_4^{3-}removal of 88-95% was achieved in the first 10 min, and 96-100% PO_4^{3-}removal was achieved in 30 min. Increasing the initial NZVI concentration from 80 to 560 mg/L increased the removal of phosphate by ~78% (C_0 = 5 mg/L) and the effect of initial NZVI concentration on phosphate removal followed a linear trend (R^2 = 0.9539). Ionic strength and changing temperature showed little interference with phosphate removal. While nitrate marginally improved phosphate removal, presence of sulfate and natural organic matters has statistically significant negative impacts on the removal efficiencies. There was no change in phosphate removal efficiency in the presence of high concentrations of humic acid. The sorbed phosphate onto NZVI was successfully recovered (~78%). The phosphate recovery process was found to be pH dependent with maximum recovery achieved at pH 12.

NZVI has potential applications in wastewater treatment plants for phosphate removal, where phosphate removal is otherwise not very efficient. The fact that NZVI removed 88-95% of the phosphate the first 10 min gives the nanoparticles an advantage over other sorbents. A commercially viable treatment system with low detention time and minimal infrastructure can be designed using NZVI. Recovery of phosphate from NZVI

at pH 12 may not be a practical proposition from economic and hazard perspectives. More research is needed to phosphate recovery from spent NZVI..

Phosphate removal by by NZVI entrapped in calcium alginate beads were compared with the novel ferrous iron cross-linked alginate beads. Complete (100%) removal of aqueous phosphate was achieved after 12 h with the new Fe cross-linked alginate beads. The comparison between the two types of alginate based sorptive media and control (viz., Fe-cross-linked/FCA, alginate entrapped NZVI/NCC, and Ca-cross-linked/CCA) revealed that FCA media/beads works much better for phosphate removal. Further, there was no interference by Cl^-, HCO_3^-, SO_4^{2-}, NO_3^- and NOM in phosphate removal with FCA beads. Phosphate sorption behavior of FCA beads is best described with Freundlich isotherm. The presence of iron in alginate increased the phosphate removal capacity of the beads. FCA beads performed better than NZVI under higher pH conditions. Removal up to 100% was achieved for a wide range of pH (4-9) which gives the FCA beads another advantage for the field application where pH ranges between 7 and 9 depending upon the water source. SEM imaging of the new and used beads revealed the presence of nanoparticles inside the bead.

NZVI and FCA beads successfully removed PO_4^{3-} from both municipal wastewater effluent (WTPE) and animal feedlot effluent (AFLE). FCA beads could remove 63% and 77% PO_4^{3-} from WTPE and AFLE, respectively, within the first 15 min and that provides a huge advantage for FCA for possible application in high flow systems. More experiments need to be performed to determine the possibility of PO_4^{3-} recovery from the spent FCA beads.

6.2. Future direction

- Test PO_4^{3-} removal using FCA beads from eutrophic lake waters.
- Test PO_4^{3-} removal by FCA beads in high flow through systems.
- Study bioavailability of PO_4^{3-} and Fe available in used FCA beads.
- Study bioavailability of other nutrients sorbed by NZVI (e.g., Se).
- Dried FCA beads for PO_4^{3-} removal.
- Study the mechanism of PO_4^{3-} removal by FCA beads.
- Additional characterization of the FCA beads.

APPENDIX

SPRINGER LICENSE
TERMS AND CONDITIONS

Oct 07, 2012

This is a License Agreement between Talal Almeelbi ("You") and Springer ("Springer") provided by Copyright Clearance Center ("CCC"). The license consists of your order details, the terms and conditions provided by Springer, and the payment terms and conditions.

All payments must be made in full to CCC. For payment instructions, please see information listed at the bottom of this form.

License Number	2997171095483
License date	Sep 27, 2012
Licensed content publisher	Springer
Licensed content publication	Journal of Nanoparticle Research
Licensed content title	Aqueous phosphate removal using nanoscale zero-valent iron
Licensed content author	Talal Almeelbi
Licensed content date	Jan 1, 2012
Volume number	14
Issue number	7
Type of Use	Thesis/Dissertation
Portion	Full text
Number of copies	1
Author of this Springer article	Yes and you are the sole author of the new work
Order reference number	
Title of your thesis / dissertation	Phosphate Removal and Recovery using Iron Nanoparticles and Iron Cross-linked Alginate
Expected completion date	Nov 2012
Estimated size(pages)	180
Total	0.00 USD

Figure A.1: Publisher permission for Almeelbi and Bezbaruah, 2012

Table A.1: Phosphate removal by NZVI/L from bulk solutions with 5 mg/L initial phosphate concentrations

Time		**5 ppm**		
	Data set	Adsorption capacity mg Phosphate-P/g of NZVI		
60.00		Adsorb Capacity	Average	STDEV
	I	12.50	12.00	0.87
	II	12.50		
	III	10.99		
30.00	I	12.50	11.81	1.20
	II	12.50		
	III	10.42		
15.00	I	12.50	11.62	1.53
	II	9.85		
	III	12.50		
10.00	I	12.50	11.52	1.70
	II	12.50		
	III	9.56		

Table A.2: Phosphate removal by NZVI/L from bulk solutions with 10 mg/L initial phosphate concentrations

Time		**10 ppm**		
	Data set	Adsorption capacity mg Phosphate-P/g of NZVI		
60.00		Adsorb Capacity	Average	STDEV
	I	24.39	24.38	0.04
	II	24.34		
	III	24.42		
30.00	I	23.66	24.09	0.38
	II	24.22		
	III	24.38		
15.00	I	23.59	23.72	0.17
	II	23.66		
	III	23.90		
10.00	I	23.70	23.62	0.11
	II	23.49		
	III	23.66		

Table A.3: Effect of initial NZVI concentration on phosphate removal.
Initial PO_4^{3-}P = 5 mg/L

NZVI	Removal %	Stdv
0	0	0
40	27.75836	3.276542
160	27.25811	7.719856
240	48.22925	10.53162
320	65.17985	4.422103
400	97.23285	4.792843
480	95.11395	0.926586
560	100	0

Table A.4: Phosphate removal using FCA beads C_0= 100 mg PO_4^{3-}-P mg/L

	PO43- Conc mg/L				Normalized Conc.				
Time	A	b	c	Average	a	b	c	average	STDEV
0	96.334			96.334	1.000			1.000	0.000
0.5	85.384	89.164	83.168	85.905	0.886	0.926	0.863	0.892	0.031
2	81.864	85.775	80.560	82.733	0.850	0.890	0.836	0.859	0.028
4	84.471	80.951	81.473	82.298	0.877	0.840	0.846	0.854	0.020
6	73.570	71.973	69.806	71.783	0.764	0.747	0.725	0.745	0.020
8	72.772	72.772	74.711	73.418	0.755	0.755	0.776	0.762	0.012
12	66.197	66.197	66.832	66.409	0.687	0.687	0.694	0.689	0.004
18	60.371	63.867	63.443	62.560	0.627	0.663	0.659	0.649	0.020
24	58.571	62.490	60.689	60.583	0.608	0.649	0.630	0.629	0.020

Table A.5: Phosphate removal using FCA beads C_0= 5 mg PO_4^{3-}-P mg/L

Time	**a**	**b**	**c**	**Average**	**SD**	**Removal**
0	5.571948	5.203922	5.624523	5.466797733	0.2291694	1
0.5	2.791131	2.633405	2.869993	2.764842987	0.1204646	0.505752
2	1.403452	1.371906	1.332475	1.369277727	0.0355611	0.250472
4	0.236285	0.370351	0.39401	0.333548913	0.0850596	0.061014
6	0.259944	0.236285	0.259944	0.25205756	0.0136594	0.046107
8	0.136493	0.173296	0.157523	0.155770858	0.0184638	0.028494
12	0	0	0	0	0	0
18	0	0	0	0	0	0
24	0	0	0	0	0	0

Table A.6: Fruendlich and Langmuir isotherm, corresponding to figure 3.9

C0	Ce	C-sorbed	Qe	lnQe	lnCe	Qe	Ce/Qe
12.78	2.13	10.65	4.40	1.48	0.76	4.40	0.48
15.92	3.15	12.77	5.28	1.66	1.15	5.28	0.60
35.78	9.17	26.61	11.00	2.40	2.22	11.00	0.83
59.00	25.92	33.08	13.67	2.62	3.25	13.67	1.90
96.33	60.58	35.75	14.77	2.69	4.10	14.77	4.10

Table A.7: Column study corresponding to Figure 3.10

Sample	Time	Time min	ppm	Norm Conc	Flow rate mL/min	Volume	BV	C
ID						0.000		mg of P
C1-1	3	180	0.395	0.028	0.101	18.180	0.673333	0.2727
C1-2	15	900	0.115	0.008	0.101	90.900	3.366667	1.3635
C1-3	27	1620	0.593	0.042	0.101	163.620	6.06	2.4543
C1-4	39	2340	1.828	0.131	0.101	236.340	8.753333	3.5451
C1-5	51	3060	4.480	0.320	0.101	309.060	11.44667	4.6359
C1-6	63	3780	7.791	0.557	0.101	381.780	14.14	5.7267
C1-7	75	4500	9.406	0.673	0.101	454.500	16.83333	6.8175
C1-8	87	5220	12.651	0.905	0.101	527.220	19.52667	7.9083
C1-9	99	5940	13.178	0.942	0.101	599.940	22.22	8.9991
C1-10	111	6660	13.705	0.980	0.101	672.660	24.91333	10.0899
C1-11	123	7380	13.985	1.000	0.101	745.380	27.60667	11.1807
C2-1	3	180	0.033	0.001	0.07	12.600	0.466667	0.378
C2-2	15	900	0.049	0.002	0.07	63.000	2.333333	1.89
C2-3	27	1620	0.033	0.001	0.07	113.400	4.2	3.402
C2-4	39	2340	13.159	0.423	0.07	163.800	6.066667	4.914
C2-5	51	3060	21.101	0.679	0.07	214.200	7.933333	6.426
C2-6	63	3780	27.179	0.874	0.07	264.600	9.8	7.938
C2-7	75	4500	28.761	0.925	0.07	315.000	11.66667	9.45
C2-8	87	5220	29.057	0.935	0.07	365.400	13.53333	10.962
C2-9	99	5940	29.164	0.938	0.07	415.800	15.4	12.474
C2-10	111	6660	29.206	0.940	0.07	466.200	17.26667	13.986
C2-11	123	7380	31.083	1.000	0.07	516.600	19.13333	15.498

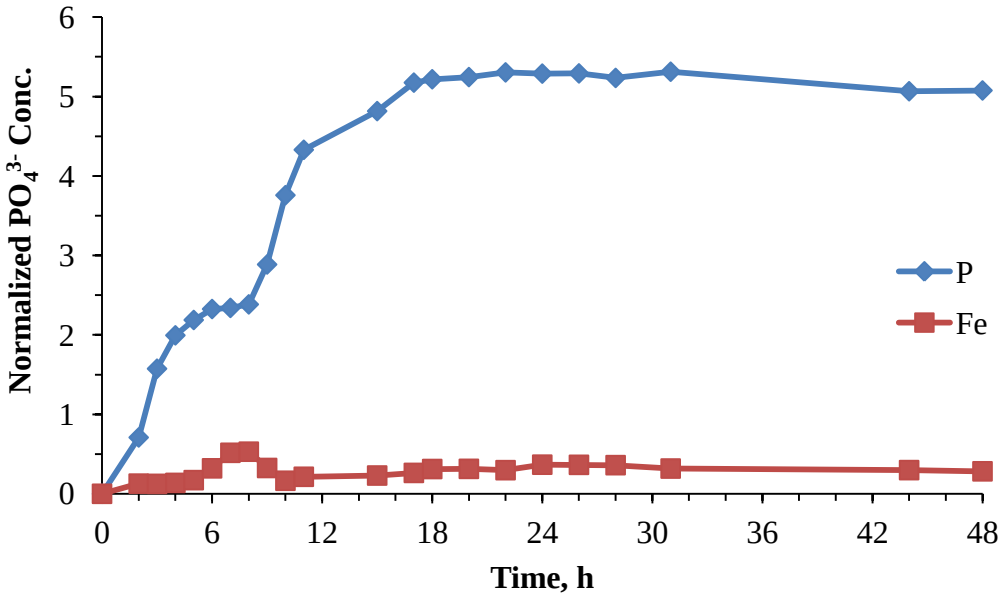

Figure A.2: Bare NZVI column study in sand medium

Flow rate = 0.8 mL/min
Column Volume = 53mL
Inner diameter = 1.5 cm
Length= 30 cm
PO_4^{3-} -P C_0 = 5 mg/L

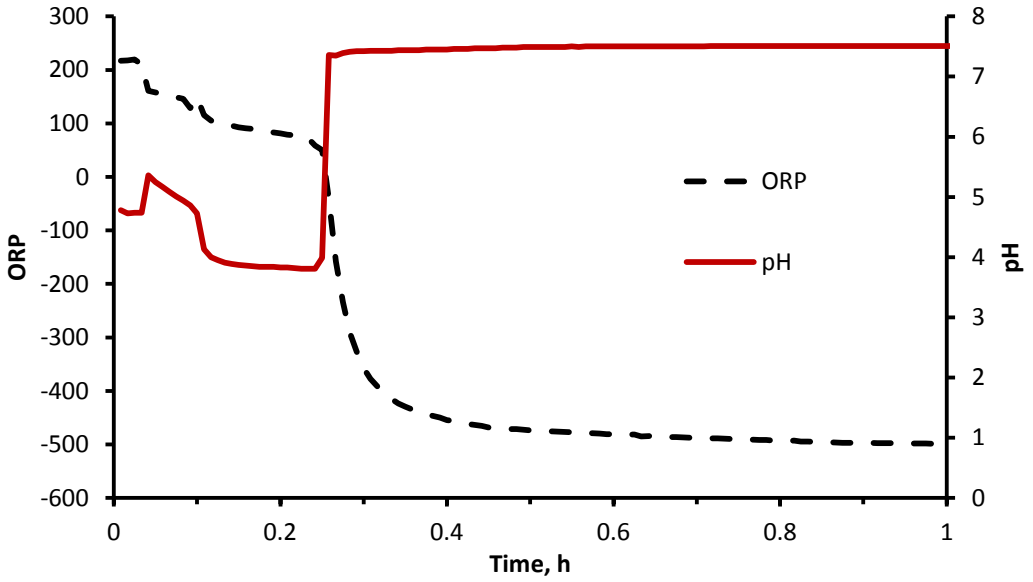

Figure A.3: pH vs ORP curve for phosphate removal by NZVI, C0= 5 mg/L

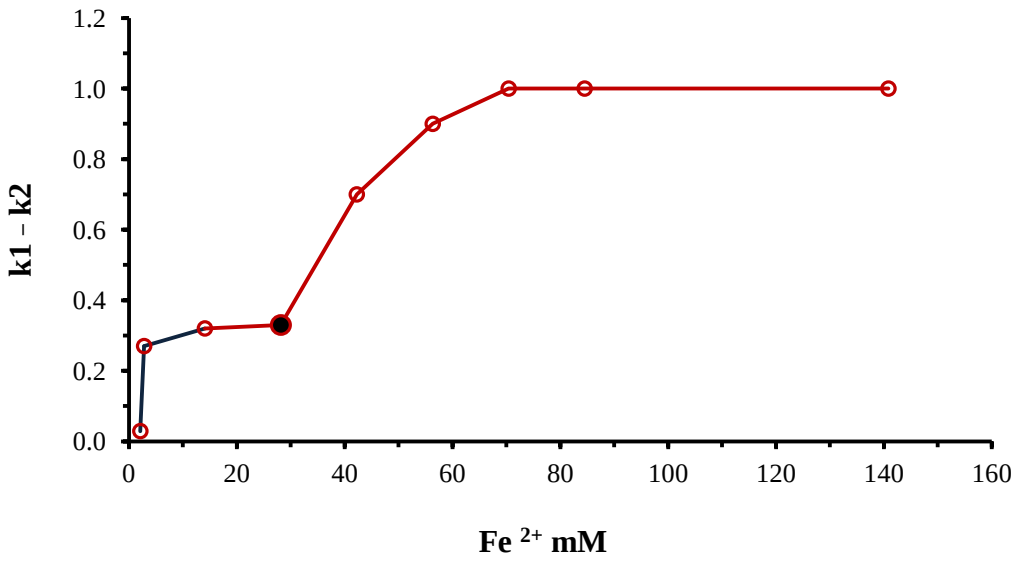

Figure A.4: Conductivity study for FCA beads synthesis

k1: Conductivity before adding alginate to the solution
k2: Conductivity after adding alginate to the solution
Concentrations used in the experiments: [Fe^{2+}]= 28 mom, [Alginate unit]= 50 mom
~Molar ratio = 1:2

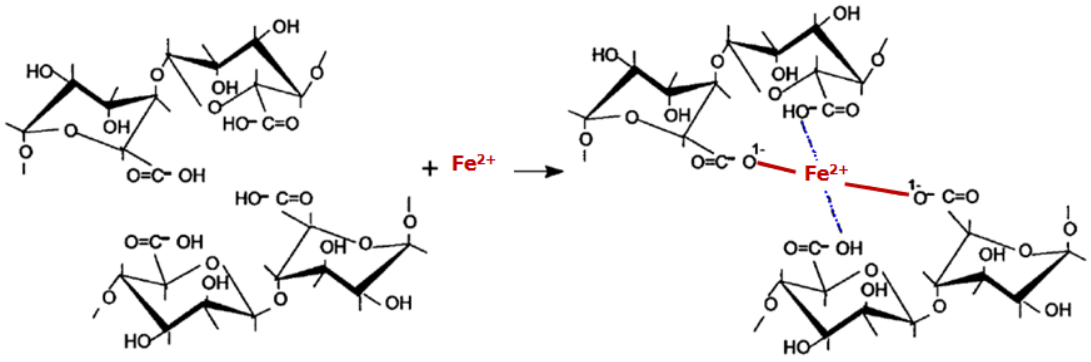

Figure A.5: Formation and chemical structure of Fe (II) alginate coordination polymer

Based on the molar ratio of alginate to Fe (II) of 1: 2 (from the conductivity study), the above structure can be predicted where the iron ion coordinates with carboxyl group on the L-guluronic acid (G units). Other forms of hydrogen bonds between the iron ion and other hydroxyl groups might take place as well.

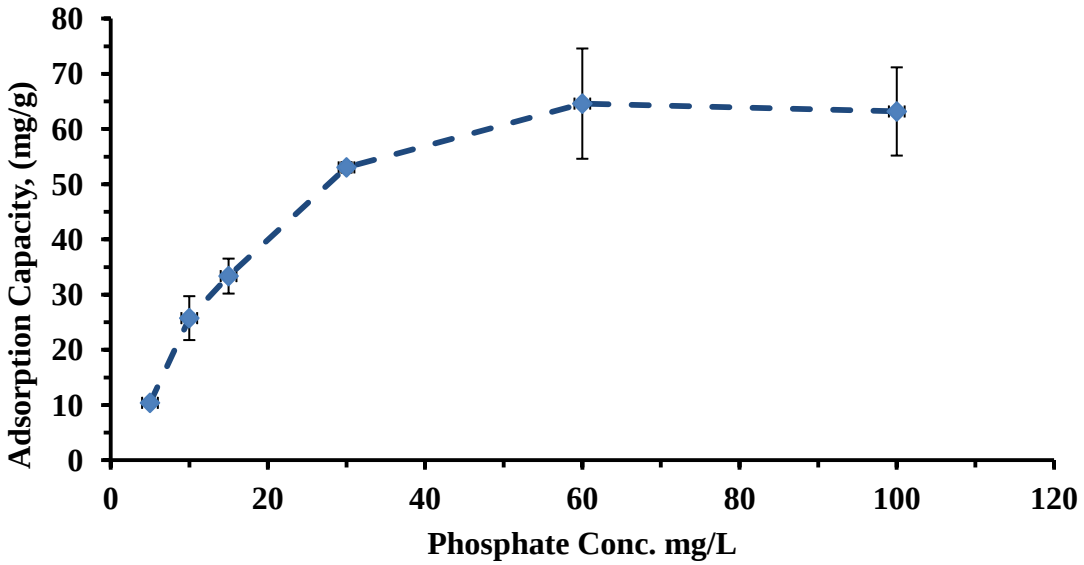

Figure A.6: Adsorption capacity of phosphate adsorption by NZVI

Table A.8: Plants length measurements

Treatment	Plant	Total length	Root Length
1	I	9	3
	II	11	4.5
	III	5	1.5
2	I	17	11
	II	11	3.5
	III	6.5	0.5
3	I	11	5.5
	II	10.5	4.5
	III	11	5
4	I	18	8
	II	11	4
	III	Plant dead	Plant dead
5	I	Plant dead	Plant dead
	II	15	4.5
	III	14	4
6	I	15	5
	II	12	3.2
	III	8	2.5
7	I	46	26
	II	40	20
	III	32	13
8	I	32	10
	II	55	35
	III	43	20
9	I	36	9
	II	40	18
	III	35	16
10	I	6.5	1
	II	10	4
	III	11	3.5
11	I	8	3
	II	5	1
	III	10	5
12	I	10	2.5
	II	12	4
	III	6	2.5
13	I	39	17
	II	40	18
	III	30	12
14	I	32	12
	II	33	12
	III	39	16
15	I	29	8
	II	32	9
	III	32	13.5

Table A.9: Plants weight

	Weight (g)			
Treatment	Leaf	Stem	Roots	total
1	0.0592	0.0605	0.0113	0.131
2	0.0656	0.0543	0.0108	0.1307
3	0.0569	0.0338	0.0123	0.103
4	0.0361	0.0484	0.0141	0.0986
5	0.0361	0.053	0.013	0.1021
6	0.0666	0.0483	0.012	0.1269
7	0.1538	0.1301	0.0344	0.3183
8	0.1841	0.144	0.0463	0.3744
9	0.0994	0.113	0.0222	0.2346
10	0.0337	0.0178	0.0052	0.0567
11	0.0203	0.0144	0.0081	0.0428
12	0.0436	0.0222	0.0089	0.0747
13	0.1889	0.1236	0.0566	0.3691
14	0.114	0.1571	0.0215	0.2926
15	0.0683	0.0831	0.0593	0.2107

Table A.10: Plants tissue ICP analysis raw data

Treatment		Fe		P		Se	
		Average	STDEV	Average	STDEV	Average	STDEV
	Roots	3167.970	1741.987	2653.674	407.501	*	*
	Stem	205.342	57.715	3733.219	527.125	*	*
1	Leaf	147.130	42.779	4101.511	758.703	*	*
	Roots	4839.244	1878.509	2564.629	913.257	102.656	*
	Stem	69.757	NA	3756.372	NA	145.730	*
2	Leaf	103.699	27.206	4035.783	557.249	274.287	68.301
	Roots	7214.168	4039.056	6765.511	1051.899	80.481	24.540
	Stem	126.886	53.657	5935.990	434.192	*	*
3	Leaf	542.791	101.550	6268.751	158.424	8.923	2.378
	Roots	17202.919	4297.736	1953.036	257.467	*	*
	Stem	590.539	279.538	1441.796	359.265	*	*
5	Leaf	653.498	275.420	1684.243	378.415	*	*

* Under detection limit

Table A.11: Amount of Fe and P in plant biomass

mg Fe/kg Biomass			mg P		
Leaf	Stem	Roots	Leaf	Stem	Roots
0.003855	0.002798	0.0182633	0.098205	0.087387	0.01161
0.002891	0.004349	0.0118248	0.080906	0.063745	0.009387
0.002159	0.00267	0.0056193	0.06881	0.037682	0.009312
0.001854	NA	0.0199355	0.074678	NA	0.025215
0.002372	NA	0.0425618	0.061997	NA	0.015052
0.00171	0.001123	0.0205681	0.100684	0.060478	0.007207
0.031568	0.00609	0.0368118	0.326438	0.243966	NA
0.026192	0.003252	0.1742044	0.373478	0.276006	0.115894
0.019409	0.006497	0.0528703	0.210489	0.242279	0.044561
0.053411	0.011164	0.3674385	0.1229	0.074515	0.040571
0.017432	0.037231	0.142525	0.053833	0.05711	0.014669
	0.021874	0.2420629	NA	0.039506	0.032848